# ACOUSTIC DETERMINATION OF PHASE BOUNDARIES AND CRITICAL POINTS OF GASES: $CO_2$, $CO_2$-$C_2H_6$ MIXTURE, AND $C_2H_6$

By

CHADIN DEJSUPA

A DISSERTATION PRESENTED TO THE GRADUATE SCHOOL
OF THE UNIVERSITY OF FLORIDA IN PARTIAL FULFILLMENT
OF THE REQUIREMENTS FOR THE DEGREE OF
DOCTOR OF PHILOSOPHY

UNIVERSITY OF FLORIDA

1991

To my mother and father
who eternally love me -
and to my sister - Narisa,
my brothers - Bordin and Pubordee

# ACKNOWLEDGEMENTS

The author expresses his sincere gratitude to his advisor, professor Samuel O. Colgate for his indispensable intellectual and moral support, and especially when bottlenecks were encountered. It has been privilege working with such an outstanding teacher and chemist. His dedication to excellence and clarity of thought and lucid insights will perpetually serve as an example.

This work would also have been impossible without the expertise of Drs. A. Sivaraman, Kenneth C. McGill, and V. Evan House of the acoustic research group which made colossal barriers become insignificant. Thanks also to Joseph Shalosky for his marvelous machining dexterity. Special thanks are extended to professors David Micha and Martin Vala and to Paul Campbell for their valuable moral support and to all of peers of the author in this institution, particularly Casey Rentz and Michael Clay for their truly meaningful friendships.

Last but not least the author wishes to warmly thank all of his teachers who shared their knowledge and understanding with him.

## TABLE OF CONTENTS

ACKNOWLEDGEMENTS . . . . . . . . . . . . . . . . . . . . . iii

LIST OF TABLES . . . . . . . . . . . . . . . . . . . . . vi

LIST OF FIGURES . . . . . . . . . . . . . . . . . . . . viii

ABSTRACT . . . . . . . . . . . . . . . . . . . . . . . . xiii

CHAPTER 1 INTRODUCTION . . . . . . . . . . . . . . 1

CHAPTER 2 THEORETICAL BACKGROUND . . . . . . . . . . 6
- Acoustics . . . . . . . . . . . . . . . . . 6
  - Angular Part . . . . . . . . . . . . 7
  - Radial Part . . . . . . . . . . . . . 8
- Overall Solutions . . . . . . . . . . . . 11
- Searching for Resonance Frequencies . . 13

CHAPTER 3 APPLICATION OF SPEED OF SOUND TO LOCATE CRITICAL POINTS . . . . . . . . . . . . 19
- Phase Behavior of Fluids and Fluid Mixtures . . . . . . . . . . . . . . 19
- Determinations of Critical Point . . . . 24
- Isotherm Approach . . . . . . . . . . . . 24
- Isobar Approach . . . . . . . . . . . . . 25
- Isochore Approach . . . . . . . . . . . . 28
- Speed of Sound as a Probe for the Critical Point . . . . . . . . . . 30

CHAPTER 4 EXPERIMENT . . . . . . . . . . . . . . . . . 32
- Instruments . . . . . . . . . . . . . . . . 32
- Resonance Frequency Measurements . . . . 51

CHAPTER 5 RESULTS AND DISCUSSIONS . . . . . . . . . 60
- Carbon Dioxide . . . . . . . . . . . . . . 60
- A Mixture of Carbon Dioxide and Ethane . 70
- Ethane . . . . . . . . . . . . . . . . . . 90
- Analysis of Ethane Data . . . . . . . . 105
  - Observation 1 . . . . . . . . . . . 106
  - Observation 2 . . . . . . . . . . . 107
  - Observation 3 . . . . . . . . . . . 107
  - Observation 4 . . . . . . . . . . . 112
- Curve Fitting . . . . . . . . . . . . . 112

Three Dimensional Phase Diagram . . . 116

CHAPTER 6 CONCLUSION . . . . . . . . . . . . . . 120

APPENDIX A CHARGING PRESSURE CALCULATIONS . . . . 126

APPENDIX B QUANTITATIVE ANALYSIS OF GAS MIXTURE . 128

APPENDIX C SIMPLEX . . . . . . . . . . . . . . 136

APPENDIX D LABORATORY STANDARD PRESSURE GAUGE . . 147

APPENDIX E COMPUTER PROGRAMS . . . . . . . . . . 163

REFERENCES . . . . . . . . . . . . . . . . . . . . . 194

BIOGRAPHICAL SKETCH . . . . . . . . . . . . . . . . . 203

# LIST OF TABLES

Table 2.1. The values of the roots $\xi_{\ell,n}$ in ascending order of magnitude. . . . . . . . . . . . . . . . . . 18

Table 4.1. Summary of electronic hardware. . . . . . . 48

Table 4.2. Gas Specifications. . . . . . . . . . . . . 51

Table 4.3. Charging Pressure of gas systems. . . . . . 51

Table 5.1. Comparison of Dewpoint Pressures of Carbon Dioxide. . . . . . . . . . . . . . . . . . . . . 67

Table 5.2. Values of critical point parameters from the literature. . . . . . . . . . . . . . . . . . . . 68

Table 5.3. Angles between pressure-temperature lines before and after phase boundary of supercritical density fluid of carbon dioxide and ethane. . . . 79

Table 5.4. Experimental results for construction of phase diagrams of a mixture of carbon dioxide and ethane. . . . . . . . . . . . . . . . . . . . . 81

Table 5.5. Comparison of Dewpoint Pressures of $CO_2$ + $C_2H_6$ Mixture ($X_{CO2}$ = 0.7425). . . . . . . . . . . . . . 89

Table 5.6. Sixth order polynomial fit statistics of GRAPHER program applied to experimental data points in figure 5.25. . . . . . . . . . . . . . . . . 93

Table 5.7. Summary of results for ethane measurements. 98

Table 5.8. Comparison of Bubble-Point Pressures of Ethane. . . . . . . . . . . . . . . . . . . . . 101

Table 5.9. Comparison of experimental vapor pressures and those calculated with an equation of state of ethane proposed by Sychev.(110) . . . . . . . . . 102

Table 5.10. Chronological collection of critical point parameters of ethane. . . . . . . . . . . . . . . 103

Table 5.11. Coefficients Obtained by Simplex Optimization Method. . . . . . . . . . . . . . . . 115

Table 6.1. Comparison of Critical Temperatures and Pressures. . . . . . . . . . . . . . . . . . . . 123

Table B.1. Data for calibration curve of ethane. . . 134

Table D.1. Experimental Test of Dead Weight Pressure Gauge. . . . . . . . . . . . . . . . . . . . 158

## LIST OF FIGURES

Figure 2.1. The first six orders of the spherical Bessel function. Points where slope equals zero yield eigen values, $\xi_{1,n}$. . . . . . . . . . . . . . . . . 12

Figure 3.1. Figure 3.1. The p-$\tilde{v}$-T behavior of pure fluid. In the center is sketched the surface p = p($\tilde{v}$,T). [From Hirschfelder Joseph O., Curtiss Charles F., and Bird R. Byron. Molecular Theory of Gases and Liquids. Copyright © 1954 by John Wiley & Sons, Inc. Reprinted by permission of John Wiley & Sons, Inc.]. . . . . . . . . . . . . . . . . . . . 21

Figure 3.2 Pressure-Temperature-Mole fraction relationship of system of carbon dioxide and ethane. . . . . . . . . . . . . . . . . . . . . . 23

Figure 3.3. Pressure-temperature projection of the system carbon dioxide-ethane in the critical region. Lines $Z_AK_A$ and $Z_BK_B$ are vapor pressure curves of pure carbon dioxide and of pure ethane respectively. . . . . . . . . . . . . . . . . . . . 23

Figure 3.4. Schematic diagram of pressure and volume relationship of carbon dioxide with several isotherms in a broad region. . . . . . . . . . . . 25

Figure 3.5. Pressure and density relationship of carbon dioxide with several isotherms around critical point(47) . . . . . . . . . . . . . . . . . . . . . 26

Figure 3.6. Schematic diagram of graphical determination of critical temperature of carbon dioxide. . . . . 26

Figure 3.7. Schematic diagram of critical point determination from measurements of the liquid density $\rho_l$ and the vapor density $\rho_g$ according to the method of Cailletet and Mathias. . . . . . . . . . 27

Figure 3.8. Schematic diagram of isochoric method of critical point determination. . . . . . . . . . . . 28

Figure 4.1. Observed sonic speed versus temperature for a North Sea natural gas mixture.(Reference 53) . . . . 33

Figure 4.2. A side view of the spherical resonator equipped with the transducers. . . . . . . . . . . 35

Figure 4.3. The spherical resonator. . . . . . . . . . 36

Figure 4.4. The transducer (cross-sectional view). . . 38

Figure 4.5. The mixing control unit. . . . . . . . . . 40

Figure 4.6. The Instrumental Setup. . . . . . . . . . . 43

Figure 4.7. The experimental setup for $CO_2$ and $CO_2$-$C_2H_6$ mixture. . . . . . . . . . . . . . . . . . . . . 44

Figure 4.8. The first experimental setup for $C_2H_6$. . . 45

Figure 4.9. The second experimental setup of $C_2H_6$. . . 46

Figure 4.10. Series of scanning routine. . . . . . . . 55

Figure 4.11. Two experimental approaches of resonance frequency determination: the maximum amplitude approach and the voltage phase change approach. . 58

Figure 4.12. Flow chart of experimental scheme and data processing. The broken-line boxes represent the experimental systems of interest. The thick-line boxes represent the computer programs. . . . . . . 59

Figure 5.1. Relationship between resonance frequency and temperature of carbon dioxide for an isochore near its critical density . . . . . . . . . . . . . . . 61

Figure 5.2. Relationship between first radial mode resonance frequency and temperature of carbon dioxide for an isochore near the critical density. . . . . . . . . . . . . . . . . . . . . 62

Figure 5.3. Relationship between the speed of sound and temperature of carbon dioxide for an isochore near the critical density. . . . . . . . . . . . . . . 62

Figure 5.4. First derivative of resonance frequency versus temperature. . . . . . . . . . . . . . . . 64

Figure 5.5. Enlarged temperature scale of figure 5.4 showing the critical temperature to be at 304.215 K. . . . . . . . . . . . . . . . . . . . . . . . 64

Figure 5.6. Pressure and temperature behavior of carbon dioxide for isochore near the critical density. . 66

Figure 5.7. Experimental vapor pressure curve compared with the NIST model. . . . . . . . . . . . . . . . . 66

Figure 5.8. Typical behavior of resonance frequency versus temperature of the carbon dioxide-ethane mixture at a supercritical density. . . . . . . . 72

Figure 5.9. Typical behavior of resonance frequency versus temperature of the carbon dioxide-ethane mixture at a subcritical density. . . . . . . . . 73

Figure 5.10. Typical behavior of resonance frequency versus temperature of the carbon dioxide-ethane mixture near critical density. . . . . . . . . . . 74

Figure 5.11. Typical experimental results of near-critical density gas of the carbon dioxide-ethane mixture. Curve 1 shows a forced cooling run. Curve 2 shows a forced warming run. Curve 3 is a slow naturally warming run. . . . . . . . . . . . . . . 76

Figure 5.12. Other resonance frequency (top curve) results in same critical temperature as first radial resonance frequency (bottom curve.) . . . . 77

Figure 5.13. A sequence of supercritical pressure versus temperature isochores of the carbon dioxide-ethane mixture. . . . . . . . . . . . . . . . . . . . . 78

Figure 5.14. Relationship between the angles θ and the charging pressures of the carbon dioxide-ethane mixture. . . . . . . . . . . . . . . . . . . . . 80

Figure 5.15. Relationship between the starting pressures and the temperatures of phase change of the carbon dioxide-ethane mixture. . . . . . . . . . . . . . 85

Figure 5.16. Relationship between the starting pressures and the speed of sound at a phase change of the carbon dioxide-ethane mixture. . . . . . . . . . . 86

Figure 5.17. Coexistence curve of the carbon dioxide-ethane mixture near azeotrope composition. . . . . 86

Figure 5.18. The sonic speed versus temperature of the carbon dioxide-ethane mixture for an isochore near critical density. . . . . . . . . . . . . . . . . 87

Figure 5.19. Pressure and temperature behavior of the carbon dioxide-ethane mixture charged near its critical density. . . . . . . . . . . . . . . . . . 87

Figure 5.20. Pressure and temperature relationship of a set of several isochores of the carbon dioxide-ethane mixture. . . . . . . . . . . . . . . . . . 88

Figure 5.21. Resonance frequency (1s mode) and temperature relationship of ethane near the critical density. . . . . . . . . . . . . . . . . . 91

Figure 5.22. Resonance frequency (1s mode) and pressure relationship of ethane near the critical density. 91

Figure 5.23. Pressure and temperature relationship of 1s mode resonance frequency of ethane near the critical density. . . . . . . . . . . . . . . . . . 92

Figure 5.24. Speed of sound and temperature of 1s mode resonance frequency of ethane near the critical density. . . . . . . . . . . . . . . . . . . . . . 92

Figure 5.25. Phase diagram of pure ethane showing temperature of phase changes as a function of starting pressure. . . . . . . . . . . . . . . . . 94

Figure 5.26. Phase diagram of ethane showing pressure and temperature behavior of 23 different isochores. . . . . . . . . . . . . . . . . . . . . 95

Figure 5.27. Trajectory plot of temperature, pressure, and sonic speed of ethane at different densities. The one nearest the critical density reaches the lowest sonic speed. . . . . . . . . . . . . . . . 96

Figure 5.28. Resonance frequency and temperature relationship revealing some phenomena observed in the experiment on pure ethane. . . . . . . . . . 106

Figure 5.29. Movement of tracked peak and its neighbor below the critical temperature. These curves are numbered in the proper time sequence but many curves showing only one strong peak have been omitted. . . . . . . . . . . . . . . . . . . . . 108

Figure 5.29. Continued movement of tracked peak and its neighbor below the critical temperature. . . . . 109

Figure 5.30. Possible routes of movement of two neighbor peaks (peak one and peak two) below the critical temperature. . . . . . . . . . . . . . . . . . . 110

Figure 5.31. Experimental curve of ethane showing dynamic behavior of speed of sound near critical point. . . . . . . . . . . . . . . . . . . . . 113

Figure 5.32. Comparison of experimental data for the ethane and curve generated by renormalization group theory equation. . . . . . . . . . . . . . . . . 114

Figure 5.33. Three dimensional phase diagram of a mixture of carbon dioxide and ethane. . . . . . 118

Figure 5.34. Three dimensional phase diagram of ethane. . . . . . . . . . . . . . . . . . . . 119

Figure B.1. Block diagram of the gravimetric method. 129

Figure B.2. The hexagon reaction vessel for a gravimetric analysis. . . . . . . . . . . . . . 130

Figure B.3. The high pressure gas sampling container. 131

Figure B.4. Calibration curve of ethane for gas chromatography. . . . . . . . . . . . . . . . . 135

Figure D.1. Conventional dead weight pressure gauge: A = piston; B = cylinder; C = steel U tube; D = oil injector; N, N' = indicator contact needles. . . 148

Figure D.2. The present deadweight pressure gauge. . 149

Figure D.3. The arrangement of the deadweight pressure gauge. . . . . . . . . . . . . . . . . . . . . 150

Figure D.4. An electroformed nickel bellow pressure sensor. . . . . . . . . . . . . . . . . . . . 160

Figure D.5. The calibration curve for dead weight pressure gauge. . . . . . . . . . . . . . . . . 162

Abstract of Dissertation Presented to the Graduate School
of the University of Florida in Partial Fulfillment of the
Requirements for the Degree of Doctor of Philosophy

# ACOUSTIC DETERMINATION OF PHASE BOUNDARIES AND CRITICAL POINTS OF GASES: $CO_2$, $CO_2$-$C_2H_6$ MIXTURE, AND $C_2H_6$

By

Chadin Dejsupa

December 1991

Chairperson: Samuel O. Colgate
Major Department: Chemistry

The acoustic resonance technique developed in this laboratory is a remarkable tool for the determination of the thermophysical properties of materials. The measured frequencies of radially symmetric modes of vibration are simply related to the sonic speed in fluids enclosed in the spherical cavity. To minimize experimental perturbations a relative measurement against argon gas used as a standard reference was employed. The sonic speed in turn is utilized as a sensitive probe for detecting phase boundaries and critical points of substances. Location of the boundary is revealed by a discontinuity in the variation of sonic speed with temperature for a sample confined isochorically in the resonator. The corresponding temperature at which this discontinuity occurs was taken as a phase boundary temperature. This indicator is very pronounced, especially when the system is near the critical condition for which strong local density fluctuations disperse sound and cause the sonic speed to dip sharply toward zero. This research reports on such studies for two pure gases $CO_2$, and $C_2H_6$ and one mixture of these two. For each system, data on resonance frequency, amplitude and pressure as a function of temperature were collected under computer control for a series of different loading densities around the critical value. Portions of the phase diagrams revealed by the measurements were recorded in tabular and graphical formats.

# CHAPTER 1
# INTRODUCTION

Natural gas and gasoline are primarily mixtures of the lighter hydrocarbons with varying amounts of nonhydrocarbons such as water, carbon dioxide, and hydrogen disulfide. Heavier fossil fuel mixtures such as crude oil consist of a myriad of higher boiling hydrocarbons and various compounds containing sulfur, nitrogen, and oxygen. In designing production, processing, transport, and handling systems for these materials reliable knowledge of their physical properties is crucial. For example, in the important activities of enhanced petroleum recovery by carbon dioxide injection into a resevoir[1] and transport of natural gas mixtures containing carbon dioxide, precise knowledge of the equilibrium phase behaviors of the systems is important. Additionally, the need exists for knowledge of critical point parameters, hydrate formation conditions, density, enthalpy, dew points, bubble points, etc. Information of these kinds about select pure components and mixtures is further needed to support the development of semiempirical equations of state and other correlations useful for predicting the behavior of a wide range of systems. For this reason, much research has been done in both the measurement (experimental method) and prediction (theoretical method) of hydrocarbon fluid properties. The great variety of chemical systems of practical interest, combined with the experimental difficulties and time investment involved with direct measurements, is a powerful driving force behind the development of useful correlations.

---

[1] Under the right condition of pressure, temperature, and oil composition, carbon dioxide will mix with the crude in the reservoir to form a single phase liquid which is much lighter than the original oil and consequently easier to bring to the surface.

Numerous empirical equations of state have been developed over the years. The pioneering work of van der Waals focused attention on the possible causes for nonideal gas behavior. Although his efforts remain historically instructive, his equation of state(1) is little used today having been superseded by a succession of others ranging in complexity from those of Benedict, Webb and Rubin,(2) Redlich and Kwong,(3) and Peng and Robinson(4) to much more sophisticated ones containing forty or more coefficients such as the AGA8 equation,(5) for example. Also a number of semi-theoretical and theoretical equations based on molecular models have been devised (see for examples references 6-11.) They were invented to rectify for non-ideality both pure and multicomponent gases and, in general, they work remarkably well for predictions of gas properties in the noncritical region. They generally fail, however, to describe the unique behavior of fluids in the critical region, but progress toward overcoming this shortcoming is being made on some fronts.(12-15) Thus far all models developed to work in the critical region require knowledge of the critical parameters; therefore the prediction abilities of these models rely partly on the accuracy of these parameters which in turn must be obtained experimentally. This is typically done only for pure components, and the critical behavior of mixtures is deduced using various combining schemes. The chance for introducing uncertainty increases then as the complexity of the mixture and is generally substantial for most mixtures of importance to the gas industry. One popular combining scheme uses Kay's mixing rules(16): $P_{pc}=\Sigma Y_i P_{ci}$ and $T_{pc}=\Sigma Y_i T_{ci}$ where $P_{pc}$ and $T_{pc}$ are the so-called pseudocritical pressure and temperature, respectively, for the mixture, and $Y_i$, $P_{ci}$, $T_{ci}$ is the mole fraction, pressure, and temperature, respectively, of component i in the mixture. Alternatively, pseudocritical parameters may be obtained from a correlation based on a collection of natural gas data(17,18). The values for a specific mixture in general depend on the combining scheme used to predict them.

The importance of accurate values of the critical point parameters of both pure and mixed fluids is established. Good values for many pure components are available, but very few mixtures have received careful experimental study. The higher the number of system components the fewer the number of tabulated values are generally available. This scarcity is partly due to the difficulty in location of the critical point in mixtures by conventional methods. The most widely used method is based on direct observation of the appearance and disappearance of a meniscus, indicating a boundary line between gas and liquid phases when a system enters the critical condition.(19) This method relies on the visual acuity of the operator, and clearly has some subjectivity.

Acoustic determination of thermodynamic properties such as heat capacity, virial coefficients, vapor pressure, etc. by spherical resonator techniques has been very successful in the past, especially in this research group.(20-26) This success stems mainly from the unusual sensitivity of the cavity resonator. Resonance frequencies can be readily measured to precisions of one part in $10^6$ or better compared to one part in $10^4$ or $10^5$ for pressure, temperature, volume density etc. The acoustic resonator also benefits thermodynamic measurements by operating at low frequencies. At high frequencies the speed of sound is affected by irreversibilities resulting principally from the delay of energy flow into and out of internal energy modes, particularly vibrational modes.(27)

This work is a first attempt to bring the superiority of the spherical acoustic resonance technique to bear on development of a new approach to critical point determination. Experiments were performed according to logical scientific approach. To start with, verification of this new technique was made using a gas system for which the critical point parameters are well-established. That gas was pure carbon dioxide, which has the richest history of prior critical behavior studies. Choosing this gas is beneficial not only because of its well-known values of critical point parameters but also for its recognized importance in the fuel industry as a near-critical-state solvent in enhanced oil recovery and as a supercritical extractant. Next, the complexity of the gas system was increased by selecting a binary component gas mixture ($CO_2$-$C_2H_6$) for study. The lessons learned in working with these first two systems were applied to a follow-up study of the other component of the mixture, ethane, to further confirm the reliability of the technique. Chapter two will briefly review some relevant equations of acoustics and explain how to identify individual resonance frequencies, which are the key parameters leading to values of the speed of sound. Chapter three will review some aspects of the phase behavior of both pure and mixed gases. The critical point determination will subsequently be discussed, starting from a background on conventional approaches to the newly proposed approach, which utilizes speed of sound as a critical point indicator. Chapter four explains comprehensively the experimental procedures used in this work. Chapter five contains results including discussions and observations. The final chapter is a conclusion.

# CHAPTER 2
# THEORETICAL BACKGROUND

## Acoustics

This derivation follows that given by references 28, 29, 30, and 31. The propagation of pressure waves in a lossless fluid at rest satisfy the general wave equation(28)

$$\nabla^2\phi = \frac{1}{C^2}\frac{\partial^2\phi}{\partial t^2} \qquad (2.1)$$

where $\nabla^2$ = Laplacian operator, $\phi$ is the velocity potential and C is the wave velocity (speed of sound).
Assuming that $\phi = \phi_o e^{i\omega t}$ equation (2.1) becomes

$$\nabla^2\phi + \frac{\omega^2}{C^2}\phi = 0 \qquad (2.2)$$

or

$$\nabla^2\phi + k^2\phi = 0 \qquad (2.3)$$

where $k = \omega/C$ = wave number. If we consider only the time-independent wave, equation (2.3) becomes

$$\nabla^2\phi_0 + k^2\phi_0 = 0 \qquad (2.4)$$

If the variables are separable $\phi_o$ may be written as $\phi_o = f(r)g(\theta)h(\varphi)$, and equation (2.4) becomes:[29]

$$\left.\begin{aligned} r^2\frac{d^2f}{dr^2} + 2r\frac{df}{dr} + (k^2r^2-M^2)f = 0 \\ \frac{1}{\sin\theta}\frac{d}{d\theta}\left(\sin\theta\frac{dg}{d\theta}\right) + \left(M^2 - \frac{q^2}{\sin^2\theta}\right)g = 0 \\ \frac{d^2h}{d\varphi^2} + q^2h = 0. \end{aligned}\right\} \tag{2.5}$$

where $M^2$ and $q^2$ are separation constants. The first of these three equations gives the radial part and the other two the angular part of the solution.

Angular Part

The last equation in equations (2.5) is a linear homogeneous second-order differential equation. Its solutions are h = sine($q\varphi$) and cosine($q\varphi$). In order that h be single-valued $[h(r,\theta,\varphi+2\pi) = h(r,\theta,\varphi)]$ values of q must be integers, i.e. $q = 0, \pm1, \pm2, \ldots.$ Denoting this integer by m the second of equations (2.5) becomes

$$\frac{1}{\sin\theta}\frac{d}{d\theta}\left(\sin\theta\frac{dg}{d\theta}\right) + \left(M^2 - \frac{m^2}{\sin^2\theta}\right)g = 0. \tag{2.6}$$

This equation has finite solutions for $\theta = 0$ & $\pi$ when

$M^2 = \ell(\ell+1)$ ; $\ell = 0,1,2,\ldots$

Then

$$\frac{1}{\sin\theta}\frac{d}{d\theta}\left(\sin\theta\frac{dg}{d\theta}\right) + \left(\ell(\ell+1) - \frac{m^2}{\sin^2\theta}\right)g = 0. \tag{2.7}$$

The general solution of this equation is

$$\Theta = A_\ell P_\ell^m(\cos\theta) + B_\ell Q_\ell^m(\cos\theta). \qquad (2.8)$$

where $P_\ell^m(\cos\theta)$ = The associated Legendre polynomial of the first kind of degree $\ell$ and order m

$Q_\ell^m(\cos\theta)$ = The associated Legendre polynomial of the second kind of degree $\ell$ and order m.

Since $Q_\ell^m(\cos\theta)$ becomes infinite at $\theta = 0$ & $\pi$, it does not apply to this physical situation(28). Consequently,

$$\Theta = A_\ell P_\ell^m(\cos\theta)$$

$$\text{where} \quad P_\ell^m(\cos\theta) = (\sin\theta)^{m/2}\frac{d^m P_\ell(\cos\theta)}{d(\cos\theta)^m} \qquad (2.9)$$

if m = 0, $P_\ell^0(\cos\theta)$ is the Legendre polynomial.

Finally, the general solution of the angular part can be written as follows:

$$Y_\ell^m(\theta,\varphi) = P_\ell^m(\cos\theta)_{\sin}^{\cos}(m\varphi). \qquad (2.10)$$

These are the spherical harmonics of the first kind.

## Radial Part

Equation 2.5a is:

$$r^2\frac{d^2f}{dr^2} + 2r\frac{df}{dr} + (k^2r^2 - M^2)f = 0. \qquad (2.11)$$

Using the above result for the angular part:

$M^2 = \ell(\ell+1)$ ; $\ell = 0,1,2,\ldots$ equation (2.11) becomes

$$r^2\frac{d^2f}{dr^2} + 2r\frac{df}{dr} + (k^2r^2 - \ell(\ell+1))f = 0. \qquad (2.12)$$

Dividing both sides by $k^2r^2$ gives

$$\frac{1}{k^2}\frac{d^2f}{dr^2} + \frac{2}{k^2r}\frac{df}{dr} + \left(1 - \frac{\ell(\ell+1)}{k^2r^2}\right)f = 0 \qquad (2.13)$$

Changing the form of the function from $f(r)$ to $F(Z)$ where $Z = kr$ and rearranging yields:

$$\frac{d^2F(Z)}{dZ^2} + \frac{2}{Z}\frac{dF(Z)}{dZ} + \left(1 - \frac{\ell(\ell+1)}{Z}\right)F(Z) = 0. \qquad (2.14)$$

Particular solutions are the spherical Bessel function of three kinds:

First kind,

$$F(z) = j_\ell(z) = \sqrt{\frac{\pi}{2z}}\, J_{(\ell+\frac{1}{2})}(Z). \qquad (2.15)$$

Second kind,

$$F(z) = y_\ell(z) = \sqrt{\frac{\pi}{2z}}\, Y_{(\ell+\frac{1}{2})}(Z). \qquad (2.16)$$

Third kind,

$$\begin{aligned} F(z) &= h_\ell^{(1)}(z) = j_\ell(z) + iy_\ell(z) = \sqrt{\frac{\pi}{2z}}\, H^{(1)}_{(\ell+\frac{1}{2})}(Z) \\ F(z) &= h_\ell^{(2)}(z) = j_\ell(z) - iy_\ell(z) = \sqrt{\frac{\pi}{2z}}\, H^{(2)}_{(\ell+\frac{1}{2})}(Z) \end{aligned} \qquad (2.17)$$

where $J(Z)$, $Y(Z)$, and $H(Z)$ is Bessel function of the first, second, and third kind, respectively.

With, for example,

$$\begin{aligned} j_0(z) &= \frac{\sin(z)}{z} \\ j_1(z) &= \frac{[\sin(z) - z\cdot\cos(z)]}{z^2} \\ y_0 &= -\frac{\cos(z)}{z} \\ y_1 &= -\frac{[\cos(z) + z\cdot\sin(z)]}{z^2}. \end{aligned} \qquad (2.18)$$

For higher orders of 1 the solutions may be obtained from the following recurrence relation:

$$f_{(\ell+1)}(z) = \frac{1}{z}(2\ell + 1)f_{\ell}(z) - f_{(\ell-1)}. \qquad (2.19)$$

The general solution may be written as a linear combination of the first and second kind solutions as follows:

$$F(kr) = Aj_{\ell}(kr) + By_{\ell}(kr). \qquad (2.20)$$

F, however, must be finite at r=0. Spherical Bessel functions of the second kind do not satisfy this constraint, so the equation (2.20) becomes

$$F(kr) = Aj_{\ell}(kr). \qquad (2.21)$$

A second condition imposes that the normal velocity must vanish at the rigid wall of the sphere, i.e.

$$\left(\frac{\partial F(kr)}{\partial r}\right)_{r=a} = 0. \qquad (2.22)$$

This is a transcendental equation whose roots give the normal frequencies of vibration, ξ. For example if

$$j_0(kr) = \frac{\sin(kr)}{kr}$$

$$\text{Then} \quad \left(\frac{dj_0(kr)}{dr}\right)_{r=a} = -\frac{\sin(ka)}{ka^2} + \frac{\cos(ka)}{a} = 0 \qquad (2.23)$$

$$\frac{\sin(ka)}{ka^2} = \frac{\cos(ka)}{a}$$

$$\text{Hence,} \quad \tan(ka) = ka = \xi_{\ell,n}.$$

For each value of $\ell$ there exists an infinite number of ξ values designated as $\xi_{\ell,n}$. The first few points corresponding to roots of equation (2.23) for the first six orders are shown in figure 2.1.

Overall Solutions

Combining the results of the radial and angular parts yields the solution of the time-independent monochromatic wave equation in the spherical polar coordinate system as

$$\phi_0(r,\theta,\varphi) = \sum_{n=0}^{\infty}\sum_{m=-\ell}^{+\ell}\sum_{\ell=0}^{\infty} j_\ell(k_{\ell,n}r)Y_\ell^m(\theta,\varphi). \qquad (2.24)$$

It is clear that in order to determine fully any particular mode of vibration, we must specify the values of three characteristic numbers: n, $\ell$, and m.

The roots of the radial part $\xi_{\ell,n}$ correspond to the frequency through the relation

$$\begin{aligned} \xi_{\ell,n} &= ka = \frac{\omega a}{C} = \frac{2\pi f_{\ell,n}a}{C} \\ f_{\ell,n} &= \frac{\xi_{\ell,n}C}{2\pi a} \end{aligned} \qquad (2.25)$$

where C = speed of sound

a = the radius of the spherical cavity

$f_{\ell,n}$ = resonance frequencies corresponding to $\xi_{\ell,n}$

$\xi$ = root of the spherical Bessel function of the first kind

= eigenvalues.

Lord Rayleigh(30) was the first to study this problem. In 1872 he solved for the lowest 23 eigenvalues (sometimes called natural frequencies). In 1952 H. G. Ferris(31) revised and extended the list to the lowest 84 eigenvalues as shown in

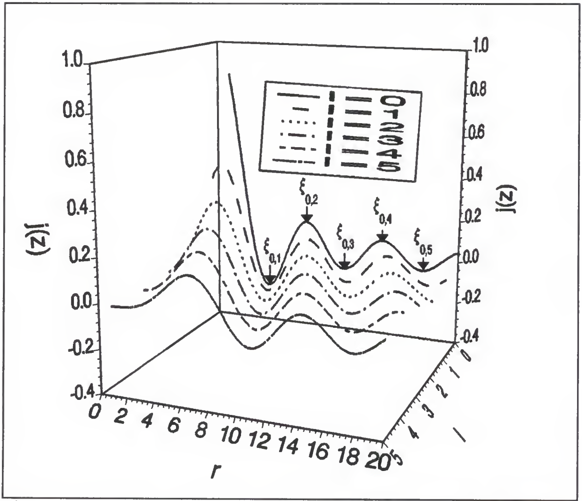

Figure 2.1. The first six orders of the spherical Bessel function. Points where slope equals zero yield eigen values, $\xi_{1,n}$.

table 2.1. Even more complete tabulations can be found in the literature(32).

## Searching for Resonance Frequencies

From the relationship $f_{\ell,n}=\frac{\xi_{\ell,n}C}{2\pi a}$ it is obvious that in order to find the resonance frequency corresponding to the normal mode of vibration of an eigenvalue, $\xi_{\ell,n}$, the speed of sound and the radius of the sphere must be known. The latter may be obtained precisely from geometric considerations on the resonator cavity. The former may be approximately calculated from an assumed equation of state. In this study we used the American Gas Association equation called AGA8(5). which requires as input only temperature, pressure, and composition. Using the predicted sonic speed together with the measured cavity radius and the tabulated eigenvalue, the corresponding resonance frequency $f_{1,n}$ may be approximately calculated and then experimentally searched by scanning frequency around that value. When excited at a resonance frequency the amplitude of the detected acoustic signal sharply increases. The series of resonance peaks arranged by frequency defines a zeroth order acoustic spectrum of resonances of gas enclosed in the spherical cavity.

Once a resonance frequency has been found, it can serve as an internal reference point to search for another, as follows:

$$
\begin{aligned}
f_{\ell,n} &= \xi_{\ell,n}\frac{C}{2\pi a} \\
\frac{f_{\ell,n}}{\xi_{\ell,n}} &= \frac{C}{2\pi a} \\
&= g \ .
\end{aligned}
\tag{2.26}
$$

If g is assumed to be a constant, this enables us to calculate a resonance frequency corresponding to each root $\xi_{\ell,n}$ from the following relationship:

$$
\begin{aligned}
\frac{(f_{\ell,n})_{ref}}{(\xi_{\ell,n})_{ref}} &= \frac{f_{ref}}{\nu_{ref}} \\
&= g \\
&= \frac{(f_{\ell,n})}{(\xi_{\ell,n})} \quad \text{at any other values of } (\ell,n).
\end{aligned}
\tag{2.27}
$$

Consequently,

$$
f_{\ell,n} = (\xi_{\ell,n})g. \tag{2.28}
$$

Note that this method also serves as a self check routine for the identity of the first reference frequency. If the observed frequency is not correctly identified, it is unlikely that we will find another resonance frequency in the expected region by using the above equation.

So far we have discussed a zeroth order perturbation relationship:

$$
f_{\ell,n} = \xi_{\ell,n}\frac{C}{2\pi a} \ . \tag{2.29}
$$

In reality there are higher perturbations to this relation. Moldover has suggested that these effects should be added to the above equation in the following manner(33,34):

$$f_{\ell,n} = \frac{(\xi_{\ell,n})(C)}{2\pi a} + \Delta f_s + \Delta f_{el} + \Delta f_t + \Delta f_{geom}\ldots \qquad (2.30)$$

The first correction term is due to the thermal boundary layer effect at the wall of the resonator. The second correction term is due to the finite elastic compliance of the sphere which is not infinitely rigid. The third term corrects for effects of the gas entrance and gas exit tubes which contribute departures from sphericity. The last term corrects for imperfection of the cavity geometry. For absolute measurements the exact treatment could be computationally and experimentally demanding.

These problems, however, can be greatly reduced by utilizing a relative measurement technique as follows: equation (2.30) may be written as

$$f_{\ell,n} = \frac{(\nu_{\ell,n})(C)}{2\pi a} \qquad (2.31)$$

where $\nu_{1,n}$ is an effective eigenvalue which depends on the unperturbed eigenvalue and all perturbations for the particular mode (1,n). If it is assumed to be independent of gas properties, then

$$\nu_{\ell,n} = \frac{(2\pi a)(f_{\ell,n})}{C}. \qquad (2.32)$$

Consequently, if we choose some system whose speed of sound is known or can be calculated precisely from a reliable equation of state, we will get a relationship:

or

$$2\pi a\left(\frac{f_{\ell,n}}{C}\right)_{Ar} = 2\pi a\left(\frac{f_{\ell,n}}{C}\right)_{I} \tag{2.33}$$

$$C_I = C_{Ar}\left(\frac{f_I}{f_{Ar}}\right)_{\ell,n} \tag{2.34}$$

where I refers to the system under investigation. The speed of sound of argon is calculated from the virial equation truncated after the third term as follows[35]:

$$C^2_{Ar} = \frac{\gamma RT}{\tilde{M}_{Ar}}\left[1+\frac{A_1(T)}{\tilde{V}}+\frac{A_2(T)}{\tilde{V}^2}\right] \tag{2.35}$$

where $\gamma$ = heat capacity ratio ($C_p/C_v$)

$\tilde{M}_{Ar}$ = Molecular mass of argon

R = Gas constant

T = Absolute Temperature

$\tilde{v}$ = molar volume

$A_1(T)$ = Second acoustic virial coefficient

$A_2(T)$ = Third acoustic virial coefficient.

The effective eigenvalue determined this way is not exact, but the effect on sonic speed measurements is small and of no consequence for the accurate determination of phase boundaries.

The practical advantages of spherical resonators is realized for the purely radial modes of vibration, which involve no tangential motion of the gas with respect to the resonator wall, i.e. no viscous drag effect. In addition, the radial mode resonance peaks typically have narrow half-width, (high Q value[2]). Furthermore, resonance frequencies of the radial modes are sensitive to imperfections of non-sphericity only to second order(36). Consequently, from all points of view the most accurate measurements of the speed of sound should be obtained by utilizing the radial modes of vibration. The first few radial modes are mostly used because of their associated low frequencies. A more complete account of these effects can be found in references 33 and 34.

---

[2] Q is usually defined as:

$$Q = \frac{\text{Center Frequency of Resonance}}{\text{Frequency Width - 3dB Points}}$$

Table 2.1. The values of the roots $\xi_{\ell,n}$ in ascending order of magnitude. D=degeneracy

| $\xi_{\ell,n}$ | n | l | D | NAME | $\xi_{\ell,n}$ | n | l | D | NAME |
|---|---|---|---|---|---|---|---|---|---|
| 2.08158 | 1 | 1 | 3 | 1p | 12.2794 | 6 | 2 | 13 | 2i |
| 3.34209 | 2 | 1 | 5 | 1d | 12.4046 | 1 | 4 | 3 | 4p |
| 4.49341 | 0 | 1 | 1 | 1s | 13.2024 | 11 | 1 | 23 | 1n |
| 4.51408 | 3 | 1 | 7 | 1f | 13.2956 | 4 | 3 | 9 | 3g |
| 5.64670 | 4 | 1 | 9 | 1g | 13.4721 | 7 | 2 | 15 | 2j |
| 5.94036 | 1 | 2 | 3 | 2o | 13.8463 | 2 | 4 | 5 | 4d |
| 6.75643 | 5 | 1 | 11 | 1h | 14.0663 | 0 | 4 | 1 | 4s |
| 7.28990 | 2 | 2 | 5 | 2d | 14.2580 | 12 | 1 | 25 | 1o |
| 7.72523 | 0 | 2 | 1 | 2s | 14.5906 | 5 | 3 | 11 | 3h |
| 7.85107 | 6 | 1 | 13 | 1i | 14.6513 | 8 | 2 | 17 | 2k |
| 8.58367 | 3 | 2 | 7 | 2f | 15.2446 | 3 | 4 | 7 | 4f |
| 8.93489 | 7 | 1 | 15 | 1j | 15.3108 | 13 | 1 | 27 | 1q |
| 9.20586 | 1 | 3 | 3 | 3p | 15.5793 | 1 | 5 | 3 | 5p |
| 9.84043 | 4 | 2 | 9 | 2g | 15.8193 | 9 | 2 | 19 | 2l |
| 10.0102 | 8 | 1 | 17 | 1k | 15.8633 | 6 | 3 | 13 | 3i |
| 10.6140 | 2 | 3 | 5 | 3d | 16.3604 | 14 | 1 | 29 | 1r |
| 10.9042 | 0 | 3 | 1 | 3p | 16.6094 | 4 | 4 | 9 | 4g |
| 11.0703 | 5 | 2 | 11 | 2h | 16.9776 | 10 | 2 | 21 | 2m |
| 11.0791 | 9 | 1 | 19 | 1l | 17.0431 | 2 | 5 | 5 | 5d |
| 11.9729 | 3 | 3 | 7 | 3f | 17.1176 | 7 | 3 | 15 | 3j |
| 12.1428 | 10 | 1 | 21 | 1m | 17.2207 | 0 | 5 | 1 | 5s |
| 17.4079 | 15 | 1 | 31 | 1t | 21.6667 | 3 | 6 | 7 | 6f |
| 17.9473 | 5 | 4 | 11 | 4h | 21.8401 | 8 | 4 | 17 | 4k |
| 18.1276 | 11 | 2 | 23 | 2h | 21.8997 | 1 | 7 | 3 | 7p |
| 18.3565 | 8 | 3 | 17 | 3k | 22.0000 | 11 | 3 | 23 | 3n |
| 18.4527 | 16 | 1 | 33 | 1u | 22.5781 | 6 | 5 | 13 | 5i |
| 18.4682 | 3 | 5 | 7 | 5f | 22.6165 | 20 | 1 | 41 | 1y |
| 18.7428 | 1 | 6 | 3 | 6p | 22.6625 | 15 | 2 | 31 | 2t |
| 19.2628 | 6 | 4 | 13 | 4i | 23.0829 | 4 | 6 | 9 | 6g |
| 19.2704 | 12 | 2 | 25 | 2o | 23.1067 | 9 | 4 | 19 | 4l |
| 19.4964 | 17 | 1 | 35 | 1v | 23.1950 | 12 | 3 | 25 | 3o |
| 19.5819 | 9 | 3 | 19 | 3f | 23.3906 | 2 | 7 | 5 | 7d |
| 19.8625 | 4 | 5 | 9 | 5g | 23.5194 | 0 | 7 | 1 | 7s |
| 20.2219 | 2 | 6 | 5 | 6d | 23.6534 | 21 | 1 | 43 | 1z |
| 20.3714 | 0 | 6 | 1 | 6s | 23.7832 | 16 | 2 | 33 | 2u |
| 20.4065 | 13 | 2 | 27 | 2q | 23.9069 | 7 | 5 | 15 | 5j |
| 20.5379 | 18 | 1 | 37 | 1w | 24.3608 | 10 | 4 | 21 | 4m |
| 20.5596 | 7 | 4 | 15 | 4j | 24.3824 | 13 | 3 | 27 | 3q |
| 20.7960 | 10 | 3 | 21 | 3m | 24.4749 | 5 | 6 | 11 | 6h |
| 21.2312 | 5 | 5 | 11 | 5h | 24.6899 | 22 | 1 | 45 | 1a |
| 21.5372 | 14 | 2 | 29 | 2r | 24.8503 | 3 | 7 | 7 | 7f |
| 21.5779 | 19 | 1 | 39 | 1x | 24.8995 | 17 | 2 | 35 | 2v |

# CHAPTER 3
# APPLICATION OF SPEED OF SOUND TO LOCATE CRITICAL POINTS

## Phase Behavior of Fluids and Fluid Mixtures

The critical point of a fluid, whether it be a pure substance or a mixture, is a property of considerable practical as well as theoretical importance. This is because the critical point identifies the temperature, pressure and density at which the liquid and gaseous phases have identical properties and is, therefore, a key point in the construction of the phase diagram. Also, a knowledge of critical temperature and critical pressure makes possible, through the principle of corresponding states and an appropriate equation of state, the prediction of the thermodynamic properties of the compound when these properties have not yet been experimentally determined. The need for information about phase behavior has substantially increased in recent years. For example, the petroleum industry has given much attention to the phase behavior of fluid mixtures at high pressures to support useful strategies to increase the yield of petroleum from oil wells. To have a clear picture of the phase behavior at high pressure and temperature of a fluid mixture, the critical point, the maximum pressure and the maximum temperature for the heterogeneous region must be known.

Evidence for the existence of a critical point was first presented in 1823 by de La Tour(37), who observed that a liquid when heated in a hermetically sealed glass tube is reduced to vapor in a volume from two to four times the original volume of the sample. However, it was not until the quantitative measurements of Andrews on carbon dioxide(38,39) in 1869 that the nature of the transition was understood. He was the first to coin the term "critical point" for the phenomenon associated with this liquid-vapor transition. For fluid mixtures the first reliable experimental investigation of the critical state began with the work of Kuenen(40,41) in 1897. Interest in the critical region in the period 1876-1914 was peaked by the experimental and theoretical studies of pressure-volume-temperature ($p$-$\tilde{v}$-$T$) relationship for both pure gases and gaseous mixtures of van der Waals and his associates at the Universities of Amsterdam and Leiden.

Figure 3.1 shows the $p$-$\tilde{v}$-$T$ relationship of the liquid and gas phases of a pure fluid. The upper-right projection shows several isotherms on a $p$-$\tilde{v}$ diagram, the upper-left projection is a $p$-$T$ plot showing several isochores and the bottom projection shows several isobars on a $T$-$\tilde{v}$ plot. The tongue-shaped region bounded by points A, D, C, E, B is the coexistence curve (or vapor pressure curve.) This curve may be considered as consisting of two curves: the bubble-point (the

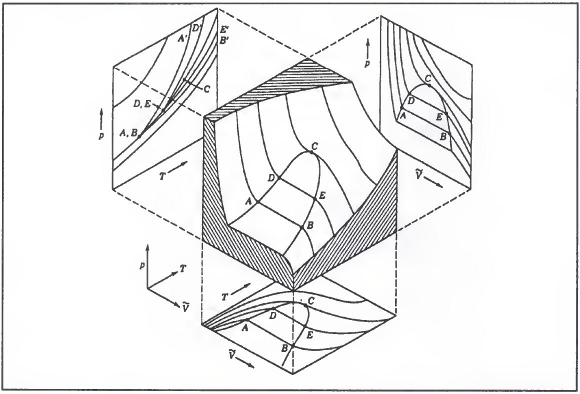

Figure 3.1. The p-$\tilde{v}$-T behavior of pure fluid. In the center is sketched the surface $p = p(\tilde{v},T)$. [From Hirschfelder Joseph O., Curtiss Charles F., and Bird R. Byron. Molecular Theory of Gases and Liquids. Copyright © 1954 by John Wiley & Sons, Inc. Reprinted by permission of John Wiley & Sons, Inc.]

point of initial vaporization when the pressure of the liquid is reduced) curve, ADC, and the dew-point (the point of initial condensation when the pressure of the gas is increased) curve, BEC. These two curves meet at the critical point C which, belonging to both curves, indicates the identity of the liquid and vapor phases. At this point, viewing from the isothermal perspective,

$$\left(\frac{\partial p}{\partial v}\right)_T = \left(\frac{\partial^2 p}{\partial v^2}\right)_T = 0. \tag{3.1}$$

In pure fluid systems the phenomenon of condensation is associated with lowering the temperature and raising the pressure and vice versa for the phenomenon of vaporization.

In a fluid mixture system we have besides the external parameters: temperature and pressure, the internal parameters which identify the composition. The phase behavior of the system can be more complicated than that of a pure fluid system due to many factors such as the possibility of various kinds of retrograde phenomena, the occurrence of azeotropic mixtures of positive or negative types etc. In a binary system, for example, on the basis of an analysis of the phase diagrams by means of the van der Waals equation of state, nine major types of phase diagram may be obtained(42-44). The complete phase behavior of a binary system is represented by the four dimensional surface, $p = p(v,t,x)$ where $x$ is the mole fraction of one of the two components. Consequently, the critical point of a mixture has to be redefined as the point where liquid and vapor become identical, subject to the constraint of equality of composition.

Since this work deals with a binary mixture of carbon dioxide and ethane, attention throughout will be mainly focused on the relevant information for this mixture. Carbon dioxide and ethane form an azeotropic mixture at the appropriate composition. This binary system deviates positively from the ideal solution, which obeys Raoult's law. In this case a critical point locus follows a curve between

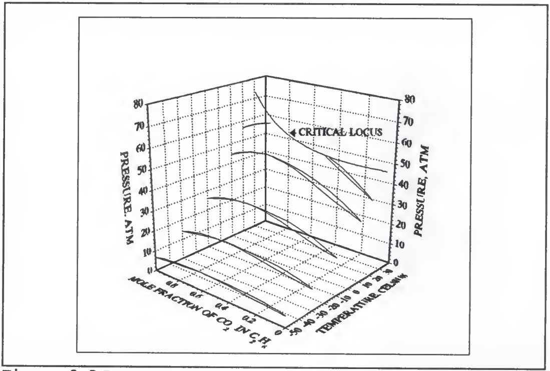

Figure 3.2 Pressure-Temperature-Mole fraction relationship of system of carbon dioxide and ethane.

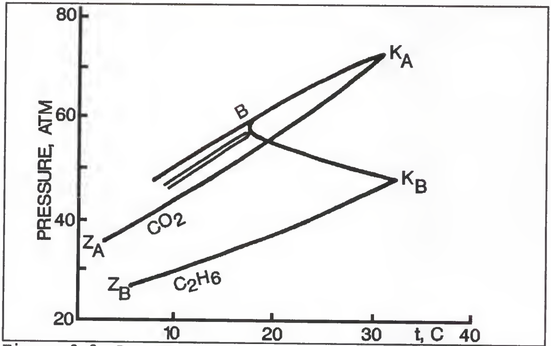

Figure 3.3. Pressure-temperature projection of the system carbon dioxide-ethane in the critical region. Lines $Z_AK_A$ and $Z_BK_B$ are vapor pressure curves of pure carbon dioxide and of pure ethane respectively.

the critical point of pure carbon dioxide and that of pure ethane. Figures 3.2 and 3.3 illustrate the pressure-temperature-mole fraction diagram and critical locus of this mixture, respectively. In figure 3.3 at point B the maximum azeotrope is tangent to the critical curve ($K_ABK_B$), which has a minimum in temperature.

## Determinations of Critical Point

Conventionally, there are three principal methods of locating the critical point. These are described briefly below.(45)

### Isotherm Approach

Critical temperature may be estimated to within a few hundredths of a kelvin by an analysis of the geometry of the isotherms(46). The isotherms in the immediate neighborhood of the critical temperature are measured with sufficient accuracy to allow the critical temperature to be determined from the inflection points of the isotherms. The minimum values of the derivative of pressure with respect to volume at constant temperature, $\left(\frac{\partial p}{\partial v}\right)_T$ found graphically are plotted as a function of temperature (or pressure or molar volume.) The intersection of this line with the horizontal axis gives the critical parameters ($T_c$, $P_c$, $v_c$.) Figures 3.4-3.6 illustrate this approach.

Isobar Approach

This method is sometimes called the rectilinear diameter method of Cailletet and Mathias.(48) If $\rho_l$ and $\rho_g$ are the densities of liquid and of saturated vapor in equilibrium with it (so called orthobaric densities), their mean is a linear function of temperature.

$$\frac{1}{2}(\rho_l + \rho_g) = \rho_0 + at \tag{3.2}$$

where $\rho_0$ = mean density of liquid and its saturated vapor at 0 °C

t = temperature in celsius

a = constant.

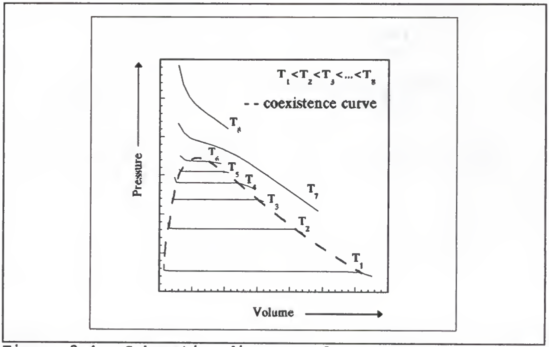

Figure 3.4. Schematic diagram of pressure and volume relationship of carbon dioxide with several isotherms in a broad region.

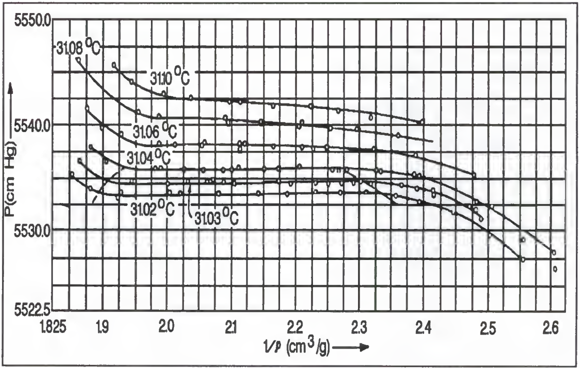

Figure 3.5. Pressure and density relationship of carbon dioxide with several isotherms around critical point[47].

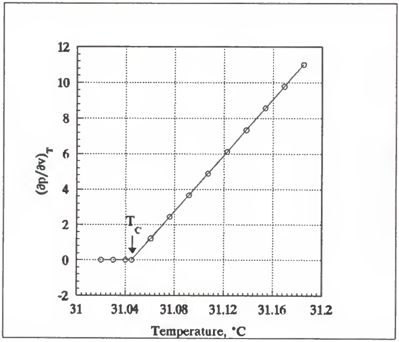

Figure 3.6. Schematic diagram of graphical determination of critical temperature of carbon dioxide.

Thus, if $\rho_g$ and $\rho_l$ are separately plotted against the temperature t, the locus of the points bisecting the joins of corresponding values of $\rho_l$ and $\rho_g$ is a straight line (see figure 3.7.) The point where this straight line cuts the coexistence curve is the critical point. In many cases this empirical law of rectilinear diameters holds very well, but sometimes over a large range of temperature the actual behavior shows a slight curvature. Furthermore, very near the

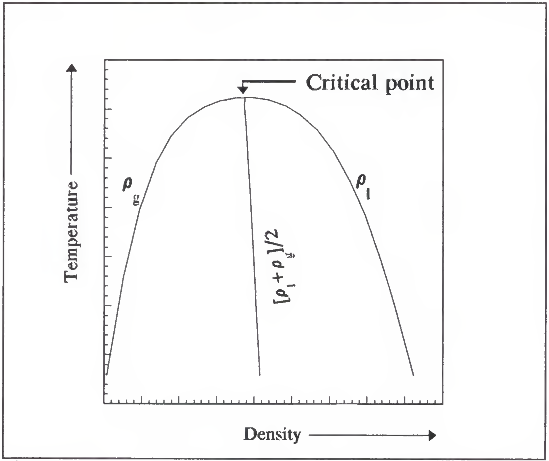

Figure 3.7. Schematic diagram of critical point determination from measurements of the liquid density $\rho_l$ and the vapor density $\rho_g$ according to the method of Cailletet and Mathias.

critical point (within several mK of $T_c$) real systems show a deviation from linearity.

Isochore Approach

There are two slightly different ways for taking this approach. The first one is to study the discontinuity of the isochore curve.⁽⁴⁹⁾ This method begins with loading a bomb of constant volume with a series of known weights of the substance and then studying the behavior of the pressure as

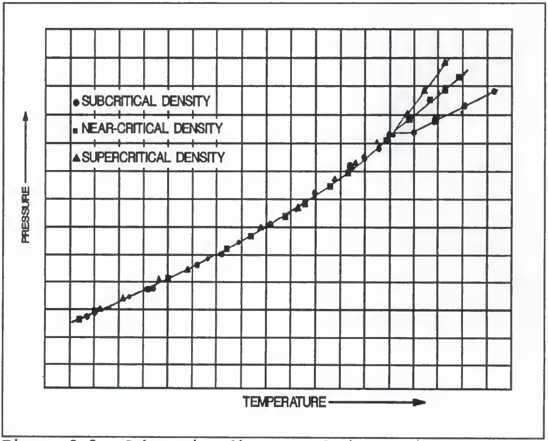

Figure 3.8. Schematic diagram of isochoric method of critical point determination.

the temperature changes. The following possible kinds of isochoric curves could result if the charging density $\rho$,is greater than the critical density $\rho_c$, the isochore curve shows an upward bend as in C, or if $\rho$ is less than $\rho_c$ the curve shows downward bend as in A. However, if $\rho$ is equal to $\rho_c$ the isochore exhibits no break as in B. This method is less demanding in terms of skillful technique and special apparatus, but the accuracy is poor. Figure 3.8 shows data illustrating all three possibilities described above.

The second established isochoric method is to study the appearance and disappearance of the meniscus between the phases near the critical temperature.(19) The procedure is the same as above except that, instead of measuring pressure as temperature changes, the behavior of the meniscus separating the liquid and gaseous phases is observed. There are also three possible phenomenon:

If $\rho < \rho_c$ the meniscus falls until the entire container is filled with gas.

If $\rho > \rho_c$ the meniscus rises until the entire container is filled with liquid.

If $\rho = \rho_c$ the meniscus approximately located at a point halfway up the container will flatten, then become very faint and finally disappear.

The temperature and density at which the meniscus disappears are taken to be the critical parameters.

## Speed of Sound as a Probe for the Critical Point

By conventional methods the critical point can be located indirectly as the zero point of the first derivative of pressure with respect to volume or of volume with respect to temperature on an isotherm or isobar, respectively, or by analyzing the slope of lines plotted as the first derivative of pressure with respect to temperature versus temperature for isochores. The technique involving use of the principle of appearance and disappearance of a meniscus is to some degree subjective due to the heuristic effect. A better alternative would be to use some thermodynamic property which shows a significant change at the critical point. In 1962 Bagatski and his coworkers (50,51) experimentally observed the asymptotic behavior of heat capacity at constant volume of argon in the immediate vicinity of the critical point. As expected $C_p$ falls off rapidly and it appeared that this could be used to detect the critical point. Measuring heat capacity, however, is not an easy task. On the other hand, the speed of sound similarly shows an abrupt change toward zero at the critical point since it is inversely proportional to $C_v$ which diverges weakly and is directly proportional to $C_p$ which diverges strongly and to the first derivative of pressure with respect to molar volume at constant temperature, which also vanishes at the critical state. The appropriate equation is:

$$C_0^2 = \tilde{V}\left[-\frac{\gamma}{M}\left(\frac{dP}{d\tilde{V}}\right)_T\right]^{1/2} \qquad (3.3)$$

where $C_0$ is the sonic speed in the limit of zero frequency. Because the sonic speed is directly proportional to the frequencies of normal mode resonance vibrations in a filled cavity resonator, one can expect to detect the approach to the critical state by observing changes in resonance frequency. Spherical cavities yield especially sharp resonances and are therefore well suited for this purpose. In the first phase of this work the isochoric approach was employed. However, unlike the conventional method of using the straightness of the pressure-temperature plot or using the appearance and disappearance of the meniscus, the speed of sound or a resonance frequency was utilized as a probe of a critical point.

# CHAPTER 4
# EXPERIMENT

## Instruments

The development of a spherical acoustic resonator as a tool to the study speed of sound in gases such as argon, butane, isobutane etc. which, in turn, leads to values of some thermodynamic and equation of state properties has been successful in the past by workers in this research group.(20-26) There are, however, some limitations on the previous work due mainly to the construction of the spherical resonator. It was made from aluminum alloy and designed to operate near atmospheric pressure. These constraints limit its applications substantially. For example, if one wishes to study natural gas mixtures, one would likely encounter the presence of some corrosive, acidic or basic gases such as hydrogen disulfide, carbon dioxide etc., and these, especially in the presence of water, attack aluminum to some extent. In addition, experiments may call for the measurements at much higher pressures than atmospheric.

The present research was undertaken to extend the applicability of the acoustic resonance technique to the study of natural gas mixtures at high pressures. To fulfil this goal a new high performance stainless steel resonator assembly was designed and built, and new data acquisition software was developed.[52] The new apparatus was used to measure the sonic speed in some carefully blended gas mixtures. Because the mixtures contained small concentrations of condensibles such as hexane for example, it was possible to cool them below their dew points and it was observed that the sonic speed faithfully revealed the precise location of the phase

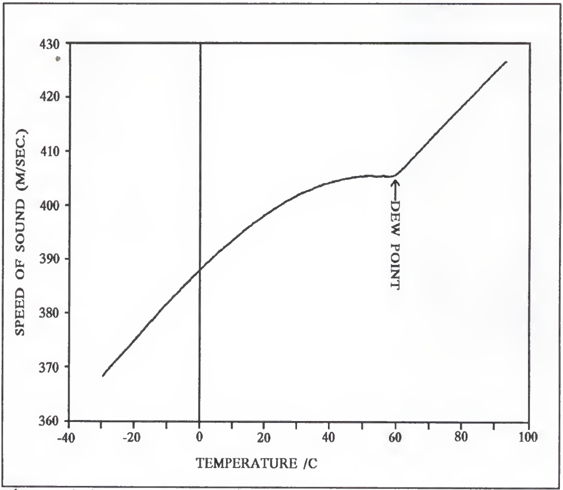

Figure 4.1. Observed sonic speed versus temperature for a North Sea natural gas mixture.(Reference 53)

change(53). This behavior was soon recognized as a valuable tool for phase equilibrium studies. Figure 4.1 shows the typical behavior in the variation of sonic speed with temperature for such a mixture. The dew point is clearly evident. Following this discovery it was decided to evaluate the use of the acoustic resonator to locate the most interesting feature of the phase diagram, namely the critical point. The work reported in this dissertation deals primarily with this difficult and challenging task.

### Spherical resonator

The resonator cavity is the heart of the apparatus. To permit its use at high pressure and in the environment of corrosive gases, the spherical resonator was built from stainless steel. Its side view is shown in figure 4.2.

The resonator cavity was fashioned from a welded spherical, type 304 stainless steel tank approximately 0.203 m.(8 in.) in diameter with a 0.24 cm.(3/32 inch.) thick wall. The tank is not perfectly spherical. This imperfection, however, does not significantly degrade the data integrity as long as appropriate measurement techniques are used as discussed in the pervious section and proven to be valid by the previous investigators.[20,21] The tank was obtained from the manufacturer (Pollution Measurement Corp.,Chicago, IL) with only a single 0.6 cm.(¼ in.) hole located at one pole ($\theta = 0$ in spherical polar coordinates). A matching hole was drilled through the opposite pole ($\theta = \pi$) and two 0.953 cm (⅜ in.)

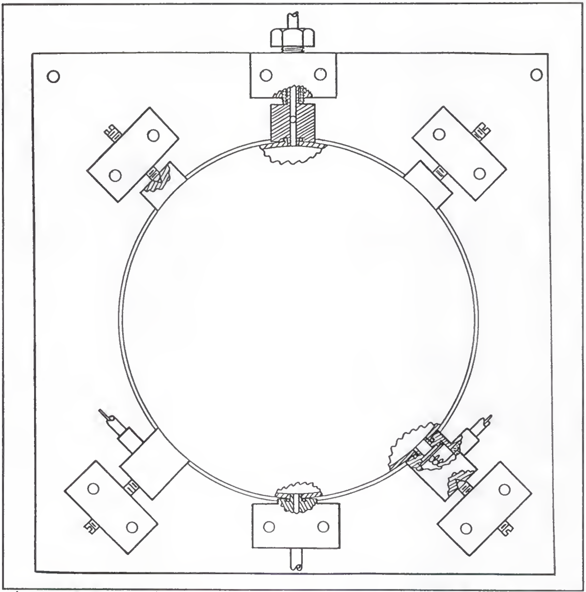

Figure 4.2. A side view of the spherical resonator equipped with the transducers.

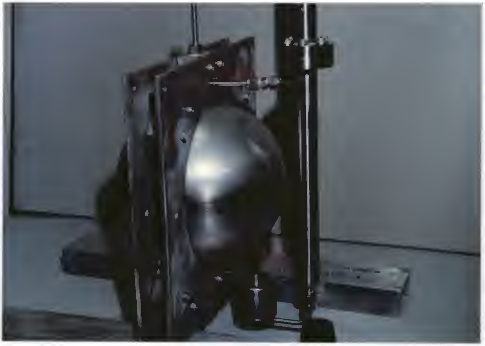

Figure 4.3. The spherical resonator.

holes drilled through the wall at $\theta = \pi/4$ with $\phi = 0$ and $\pi$, respectively. No holes were located on the equatorial weld bead ($\theta = \pi/2$). Figure 4.3 shows the overall view of the spherical resonator.

Transducers

The active element of the acoustic transducer is a 0.750 in. diameter piezoelectric ceramic bimorph (Vernitron, Bedford, Ohio) made of PZT-5A material (lead zirconate-lead titanate.) This ceramic was found to produce a signal of high volume when driven with a sinusoidal waveform of 10 volts peak-to-peak. It also has a high maximum operating temperature of 250 °C.(54) A transducer assembly was designed and fabricated. It is shown in figure 4.4. The electrical feedthrough made from brass was held in a Delrin insert to prevent a short circuit. A cross-sectional view of the transducer mounted on the resonator is also shown in figure 4.2. The transducer assemblies were mated to the resonator through short ⅛ in. diameter tubes.

Two identical transducers located at right angles to each other were used. This orientation has proved to yield a better resolution of the radial modes of vibration due to diminishing in intensity of some non-radial modes, p modes for example. One transducer functions as a speaker. It is an input transducer which mechanically deforms when a voltage is applied. The other transducer functions as a microphone. It is an output transducer which operates on a reverse mechanism of

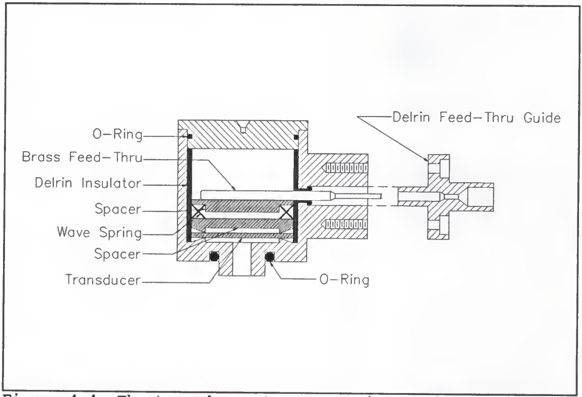

Figure 4.4. The transducer (cross-sectional view).

the input transducer: producing an electric signal when mechanically deformed by pressure waves.

### Mixing control system

A circulating pump is needed to promote mixing of system components and (or) phases and to assist with thermal equilibration by eliminating stratification. It was made from stainless steel and consists of two parts: the liquid collector and the pump. Figure 4.5 shows the design of the unit. It consists of a vertically mounted stainless steel cylinder 3.18 cm (1.25 in.) in diameter with a freely sliding internal piston 2.10 cm (0.851 in.) in diameter. The piston has a built in reed valve which is normally open under gravity but is forced closed by viscous drag as the piston descends causing the fluid to flow from top to bottom through the pump on descending motion of the piston. Piston motion is driven by interaction between an iron slug attached to the piston and an external magnet driven in turn by linkage to a motorized bell crank.

### Apparatus assembly

Tubular fittings to the spherical resonator to other parts of the system were provided with 0.6 cm (¼ in.) diameter pilot tubulations which slip into the polar holes and when pressed against the tank were sealed by elastomeric O-rings confined to glands comprised of circular grooves in the fittings around the pilot tubes and the ring like areas of the adjacent tank wall surrounding the holes. These fittings were

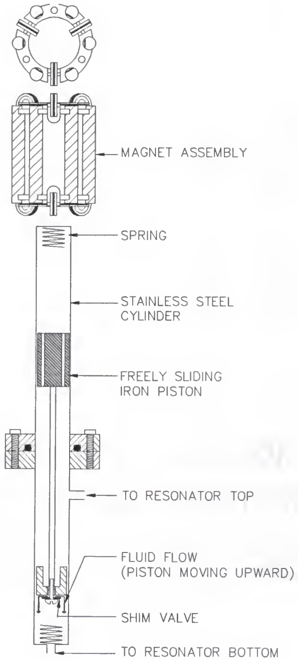

Figure 4.5. The mixing control unit.

brazed to stainless steel tubes used for charging the resonator and circulating its contents through an external loop containing the magnetically driven pump. The two identical PZT bimorph piezoelectric transducer assemblies were similarly mounted to the tank at the 0.953 cm (⅜ in.) hole positions.

The assembly support frame consists of two parallel 0.6 cm (¼ in.) thick stainless-steel plates between which an array of 2.54 cm (1 in.) thick stainless-steel blocks were attached with bolts to support the tube fittings and transducer assemblies and provide a means of applying clamping forces to the O-ring seals. The clamping force acting along the polar axis is applied by a hallow jam screw which slips over the charging tube and pushes against the brazed O-ring gland. The block which supports the lower tube fitting is rigidly fixed and provides a definite reproducible location for the tank body. The transducer assemblies were clamped against the resonator by set screws threaded through two of the blocks bolted to the mounting frame. Set screws in two additional blocks located opposite the transducer mounting holes apply counter forces against the tank to stabilize the assembly further.

The circulating pump is connected to the upper and lower tube fittings by demountable compression fittings (Swagelok.) The normal pumping rate of 4 liters per minute proved adequate for these purposes. A 0.6 cm (¼ in.) tube connected to the fluid circulation loop by a tee leads to a diaphragm-type pressure gauge and a system shut-off valve.

The resonator assembly and circulating pump were suspended from a horizontal plate which forms the cover of a stirred liquid bath in which the system is mounted. The bath was housed in a well-insulated container and connected by insulated tubing to a computer-controlled heat exchanger capable of operating from 233 to 373 K. Bath temperature was measured with a four-wire platinum resistance thermometer (RTD.) Figure 4.6 shows the instrumental setup.

### Electronic hardware

The automated systems employed in this work are shown in figures 4.7, 4.8, and 4.9. Figure 4.7 shows the setup used in the experiments on pure carbon dioxide and on a mixture of carbon dioxide and ethane. Figure 4.8 shows the setup for the experiments on pure ethane. In this latter setup we have explored the capability of using a fast-fourier transform (FFT) technique. Unfortunately, the data collected by this technique was unreliable due to leaks in the system found after the experiment was finished. While the leaks were being fixed, the instruments were transferred to another project. Consequently, the FFT exploration was discontinued for ethane and the setup shown in figure 4.9 was built to finish this project.

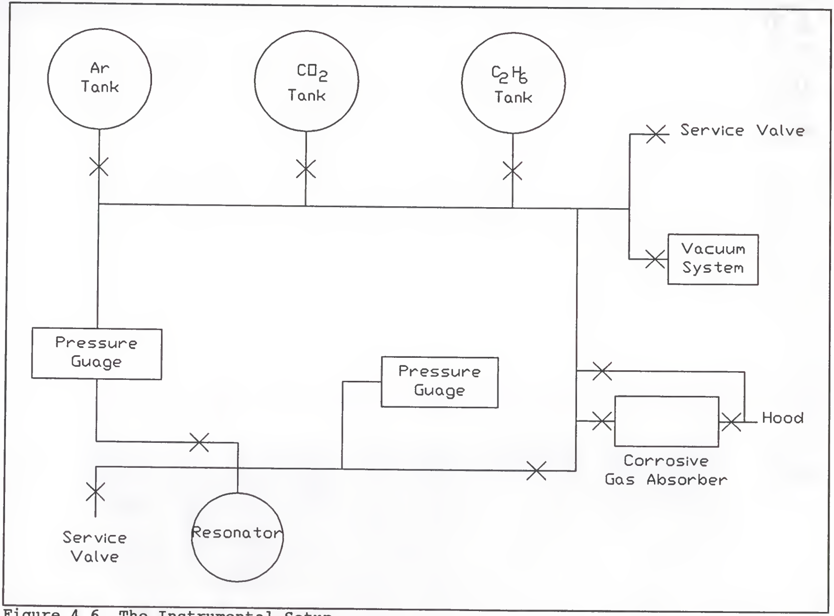

Figure 4.6. The Instrumental Setup.

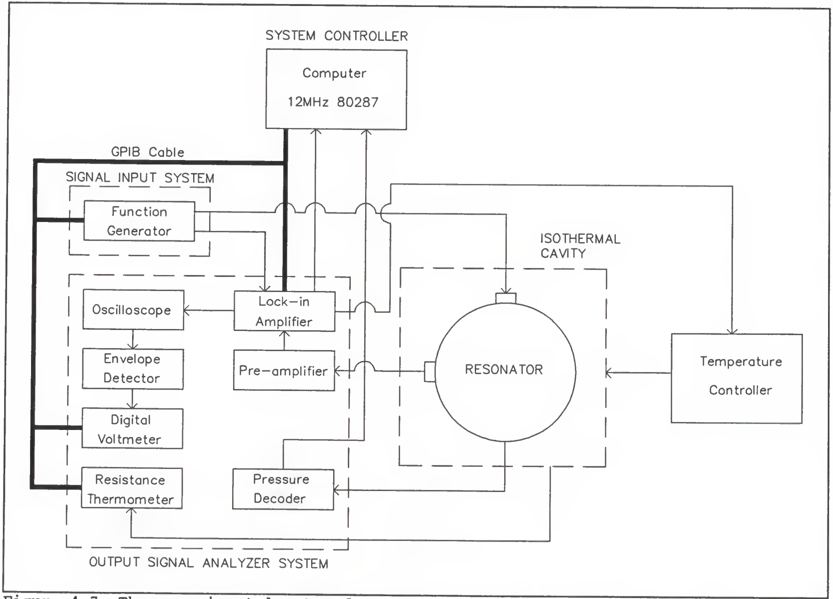

Figure 4.7. The experimental setup for $CO_2$ and $CO_2$-$C_2H_6$ mixture.

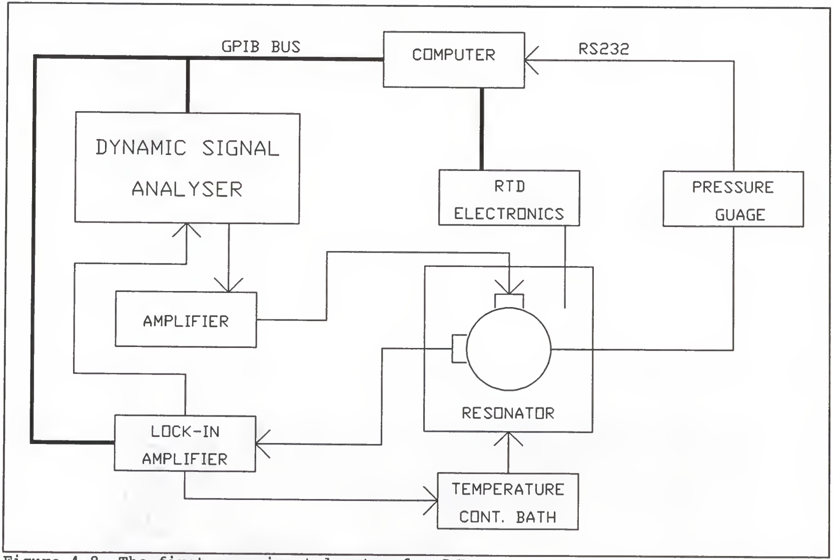

Figure 4.8. The first experimental setup for $C_2H_6$.

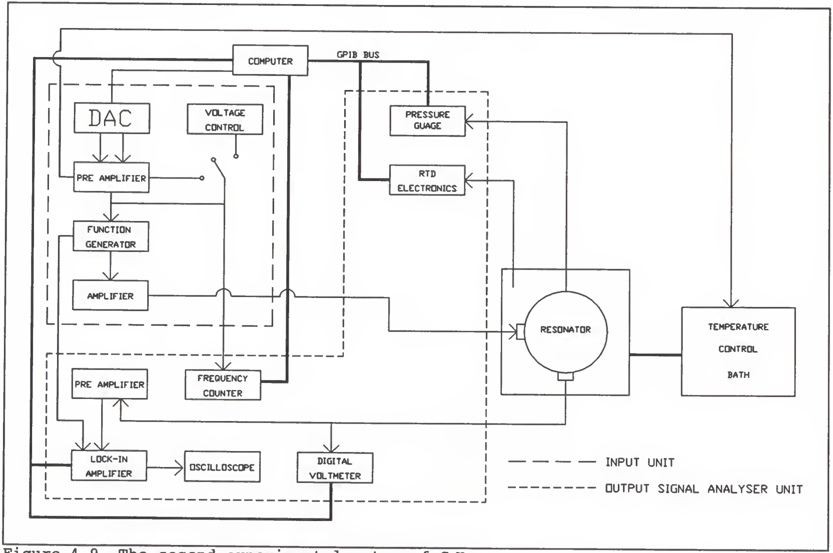

Figure 4.9. The second experimental setup of $C_2H_6$.

Even though there were different setups, the basic principles are the same and can be divided into two parts: the input signal generation part and the output signal analysis part. These are shown by dashed-line boxes in figures 4.7 and 4.9. Commands and data were transferred among the instruments and computer over the General Purpose Interface Bus (GPIB) cables. Each component on the GPIB was equipped with an IEEE-488 standard interface. The computer was always a controller-in-charge sending commands and acquiring data according to the written computer program. Each instrument was a listener and/or a talker depending on a currently executed line of the program. Table 4.1 summarizes electronic hardware components used in this work and their specifications.

### Gases

Carbon dioxide and ethane gases used were high purity grade. No further analysis was performed on carbon dioxide. Table 4.2 summarizes the pure gas qualities.

For the experiments on a mixture of $CO_2$-$C_2H_6$ quantitative analyses were performed since the results of speed of sound measurements depend on the precise composition. Both gravimetric and gas chromatography analyses were used to fulfil this task. Details of these analyses are presented in appendix B.

Table 4.1. Summary of electronic hardware.

| Item | Manufacturer | Model number | Range of operation | Accuracy (Manufacture quote) | Function |
|---|---|---|---|---|---|
| Temperature controller | Brinkmann | RKS-20D | -40 to 150 °C | 0.03 °C | Control temperature. |
| Pressure Transducer | Sensotec | TJE/743-03 | 0-3000 psia with excitation voltage = 10 volts | ±0.1% of full scale | Measure pressure. |
| Digital Strain gage transducer indicator | Beckman industrial corp. | 600 Series | -150 mv to 1 volt | 0.01 % of full scale,± 1 digit. Full scale = 3000 psia. | Accepts a strain gage type transducer input to measure pressure. |
| Lock-in amplifier | Stanford research system, Inc. | SR510 Single phase | 0.5 Hz to 100 KHz | ± 10 volt output corresponds to full scale input | AC Signal recoveries : measure signals down to 10 nv full scale while rejecting interfering signals up to $10^5$ times larger by the performance of two lines notch filters and autotracking bandpass filter. |
| Frequency counter | Sencore | FC71 | 10 Hz to 1 GHz | ± 2 digits on frequency less than 100 KHz | Measure frequency of periodic signal. |

Table 4.1. (Continued)

| Item | Manufacturer | Model number | Range of operation | Accuracy (Manufacture quote) | Function |
|---|---|---|---|---|---|
| Pre-Amplifier | Stanford research systems, Inc. | SR550 | Up to 250 mv rms input | 1 % Gain | Reduces input noise and extends the full scale sensitivity to 10 nv. |
| Voltmeter | Keithley instruments, Inc. | 177 | 200 mv to 1200 volts | 0.04 % Reading + 2 digits for minimum range or 0.035 % rdg. + 1 digit for max. range | Measure Ac or Dc Voltage. |
| Digital multimeter | Keithley instruments, Inc. | 195A | 2-Terminal & 4-terminal resistance measurements in the range of 100 $\mu\Omega$ to 20 M$\Omega$ | Depends on range. See manufacture's manual for details. | Measure resistance from Pt temperature probe. |
| Function generator | Wavetex San Diego, Inc. | 182A | 0.004 Hz to 4 MHz | Dial accuracy = ± 5 % of full scale. | Generates a precise sine /triangle/square waveform. |

Table 4.1. (Continued)

| Item | Manufacturer | Model number | Range of operation | Accuracy (Manufacture quote) | Function |
|---|---|---|---|---|---|
| Waveform synthesizer and function generator | Hewlett-Packard | 3325B | 1 $\mu$Hz to 21 MHz for sine wave with amplitude of 1 mv to 10 v p-p | ± 5X10$^{-6}$ of selected value in temperature range 20 to 30 C | Generates sine, triangular, or square wave. |
| Oscilloscope | Leader | 1020 | Input signals higher than 400 volts (Acp-p + Dc) may damage circuit. COMPONENTS | Vertical section : ± 3 % (±5% mag X 10.)<br>Horizontal section : ± 3 % | Display waveform |
| Dynamic signal analyzer | Hewlett-Packard | HP35660A | 488 $\mu$Hz to 102.4 KHz for single-channel spectrum or half of the this range for two-channel spectrum. | No information available. | Wave signal source. Also contains FFT algorithm to convert an analog input signal(time domain) to a signal displayed in the frequency domain. |

Table 4.2. Gas Specifications.

| Gas | Manufacturer | Grade | Purity |
|---|---|---|---|
| Carbon dioxide | Scott specialty gases | Research Grade | 99.99 Mole % |
| Ethane | Scott Specialty Gases | Research Grade | 99.9 % |
| Argon | Matheson gas Products | Research Grade | 99.9995 Volume % |

Table 4.3. Charging Pressure of gas systems.

| Gas system | Starting temperature (°C) | Charging pressure (psia) |
|---|---|---|
| Carbon dioxide | 36.0 | 1200 |
| $CO_2$ + $C_2H_6$ | 30.0 | 630 for $C_2H_6$ and make up to 1300 with $CO_2$ |
| $C_2H_6$ | 37.0 | 808 |

Resonance Frequency Measurements

Measurements were made on isochore samples introduced into the spherical resonator which was initially rinsed with argon gas and subsequently evacuated overnight at high temperature (40-50 °C) with a mechanical pump connected to a liquid nitrogen trap. The apparatus was then brought to a temperature above the known literature critical temperature. After that gas was introduced slowly into the resonator to bring the pressure to the calculated value (see table 4.3). The apparatus was then sealed off. The charging pressure value was calculated using the AGA8 program. Details of the calculation are given in appendix A. In the case of the mixture of $CO_2$ and $C_2H_6$, ethane was first introduced. Pressure was monitored roughly by a Bourdon pressure gauge and more precisely by a digital pressure gauge previously calibrated to yield an absolute pressure reading. The magnetic circulating pump was turned on to assure adequate mixing. Once the system was at stable conditions in temperature and pressure (which took approximately a few hours), searching for resonance frequencies began.

Fluids in the resonator were stimulated acoustically by driving one of the bimorph transducers with a 40 volt peak-to-peak sine-wave signal generated under microprocessor control (PC-AT) of a programmable signal synthesizer, HP3325B in the case of pure carbon dioxide and of the of $CO_2$ and $C_2H_6$ mixture or of a wave function generator (WAVETEX) controlled through a programmable digital-to-analog converter (DAC) in the case of pure ethane. The fluid response was determined at the other transducer which feeds its signal to a lock-in amplifier. The response of the speaker transducer in terms of voltage output signal was monitored closely to changes in frequency of the microphone transducer. At resonance, the output amplitude increased dramatically to maximum enabling a precise frequency measurement. Using an oscilloscope as a visual aid to locate the vicinity of this maximum signal and a digital voltmeter to find the precise position of the signal peak, resonance frequency could be found with high accuracy. Usually, the first radial mode of vibration was selected as the tracked peak throughout this work.

The approximate location of the desired peak, first radial mode for example, was initially calculated from the AGA8 equation using pressure, temperature, and composition as input. Then the actual location of the peak was experimentally searched using a program called SCAN. Scanning was performed in a reasonable frequency range around the center frequency identified as the output value of the AGA8 calculation. Once the peak(s) was found, location of another mode was calculated as described in the theoretical background section. The purpose of this routine was to increase the degree of confidence that each experimentally found peak was indeed correctly identified. Similarly, if more than one peak appeared together in the range while scanning, each was checked against the other radial modes to sort out the best candidate for labeling as a resonance mode based on the hypothesis that if it is a genuine system peak, its frequency should reveal the correct position of the other peaks. Figure 4.11 shows an example of a series of scans performed chronologically. The figure in the first row is an acoustic spectrum scanned in a wide frequency range. The figure in the second row is the acoustic spectrum scanned in a narrower frequency than the one in the previous figure. In this incident there were three peaks near the predicted frequency of the first radial mode peak (peak 1 in figure 4.11). Each of these was investigated closely as shown in the subsequent four rows. Each figure in the third row is a spectrum of a single peak of row two scanned in a much narrower frequency range. Frequencies found for each peak in this row were used to calculate the second, third, and forth radial frequencies. Peaks corresponding to these calculated frequencies were searched as shown the figures in the forth, fifth, and sixth row. Apparently, the third peak (peak 3 in figure 4.10) is not the correct peak as it failed to predict the location of higher radial modes. Peaks 1 and 2 give similar predictions since they lie very close together; about 5 Hz apart. Predictions of overtones based on peak 1 were in better agreement with experiment than from peak 2 therefore peak 1 is correctly interpreted as the first radial mode peak. Note that the SCAN program was used for pure carbon dioxide and for the CO2-$C_2H_6$ mixture experiments. For pure $C_2H_6$ experiment this process was performed manually via a voltage-control-generator (VCG) box since the instrumental setup was altered.

Having established the location of the peak to be tracked, data collection was begun. For pure $CO_2$ and for the mixture of $CO_2$-$C_2H_6$ experiments programs called VIKING and VIKAN were used. In this version only data corresponding to the maximum amplitude were recorded for each sweep frequency range. For the pure $C_2H_6$ experiment, however, data of the entire sweep frequency range were recorded (via the program

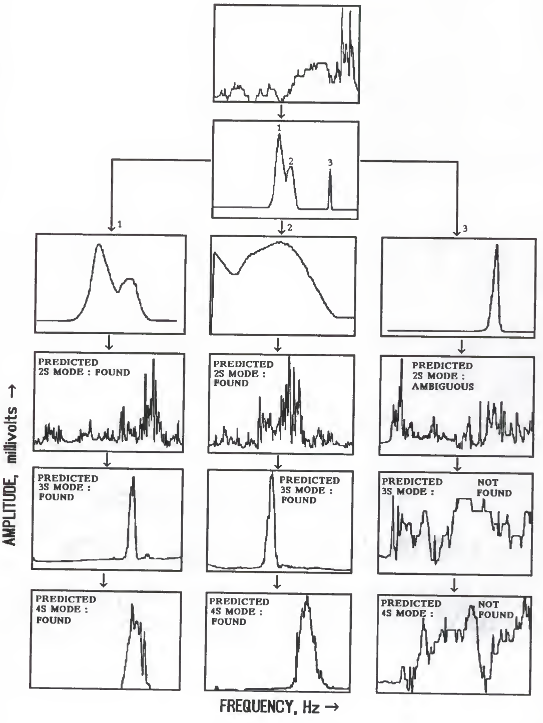

Figure 4.10. Series of scanning routine.

called MAX) since it was believed the more detailed information would be instructive. This change was possible because of advances in the available data acquisition hardware. In both cases the programs locked onto the tracked peak for the entire process as bath temperature was lowered (or raised) at a rate of a few millikelvin per minute over a period of several hours. Pressure and temperature measurements were simultaneously collected along with frequency and amplitude. Upon completion of the experiment the temperature of the system was brought back to the starting value. A small amount of gas was removed to change the density of the system, and then another data collection was begun. Typically, the density of the system was initially at a supercritical value ($\rho_g > \rho_c$) and was finally at a subcritical value ($\rho_g < \rho_c$). The usual number of runs for a system was about fifty.

Note also that the resonance frequency may also be determined accurately by observation of the phase change of the output voltage relative to the excitation. This approach is necessary for the most accurate determination of absolute sonic speeds, but great care must be taken since the phase meter is extremely sensitive and responds to peaks at even the noise level. All programs were written in FORTRAN 77. They are shown in appendix E. Figure 4.11 shows typical output response of these two approaches.

Once data collection was complete the corresponding speed of sound were calculated with a computer program called

GETSPG. This program utilizes the principle of relative measurement mentioned earlier in the theory section. Also the theoretical speeds of sound were calculated from the AGA8 equation through a computer program call TOTDAT for comparison purposes. Finally the results were manipulated and graphically displayed using popular software including: LOTUS-123, QUATTRO, GRAFTOOL, and GRAPHER. Figure 4.12 shows a schematic diagram of the entire process of data collection.

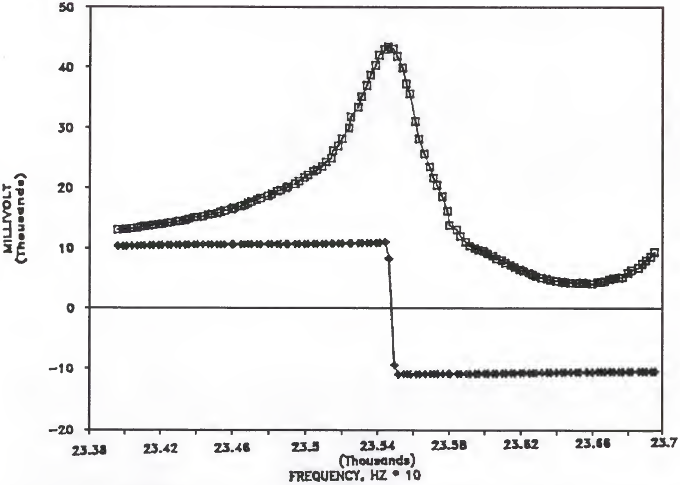

Figure 4.11. Two experimental approaches of resonance frequency determination: the maximum amplitude approach and the voltage phase change approach.

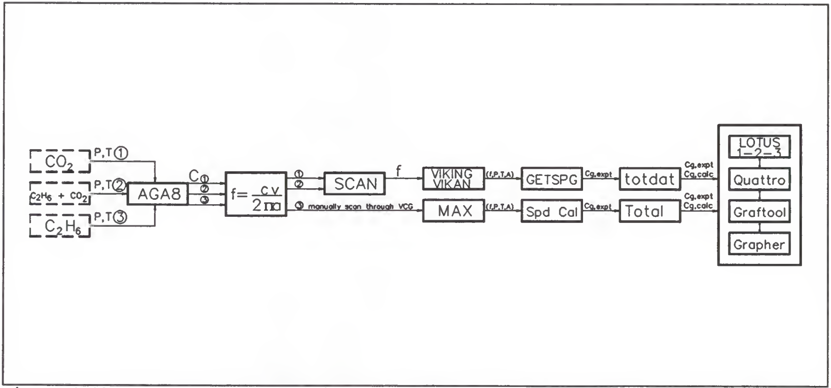

Figure 4.12. Flow chart of experimental scheme and data processing. The broken-line boxes represent the experimental systems of interest. The thick-line boxes represent the computer programs.

# CHAPTER 5
# RESULTS AND DISCUSSIONS

## Carbon Dioxide

As mentioned in the introduction, due to its well-established values, carbon dioxide was chosen to be the first candidate used to test this new acoustic resonance technique for locating critical point parameters. Learning how best to do this required considerable effort, often involving trial and error procedures. Many adjustments had to be made to both instruments and programs to identify the optimum conditions for performing this experiment.

Figure 5.1 shows the typical relationship between the first radial mode resonance frequency (hereafter abbreviated resonance frequency) and the temperature of carbon dioxide in the resonator charged near its critical density. It shows the results of four runs of this same isochore. For each run the curve may be roughly divided into two parts for the sake of discussion. The first one is a curve where the system temperature is greater than or equal to the critical temperature, $T_c$. In this region the speed of sound is directly proportional to the system temperature, i.e. as temperature

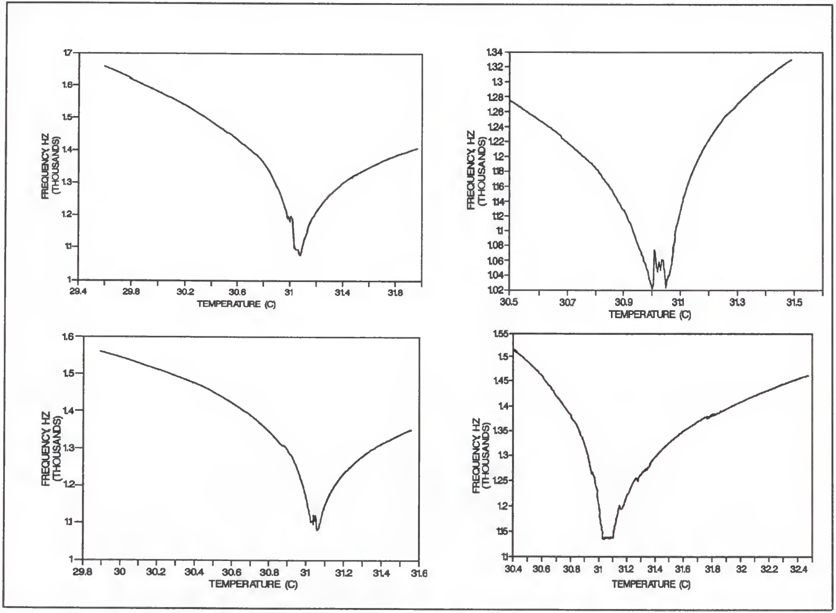

**Figure 5.1.** Relationship between resonance frequency and temperature of carbon dioxide for an isochore near its critical density.

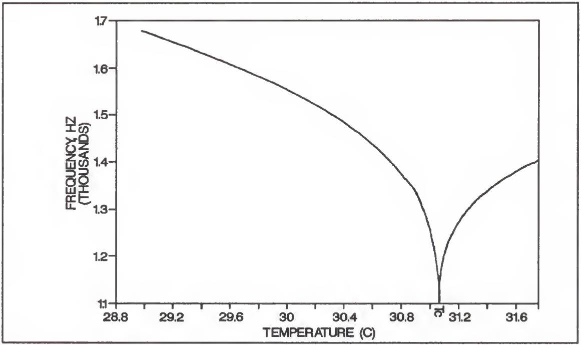

Figure 5.2. Relationship between first radial mode resonance frequency and temperature of carbon dioxide for an isochore near the critical density.

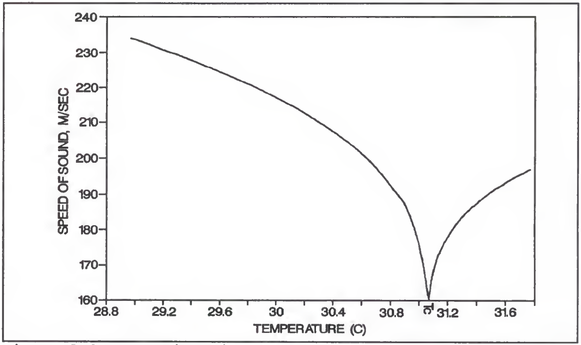

Figure 5.3. Relationship between the speed of sound and temperature of carbon dioxide for an isochore near the critical density.

decreases, resonance frequency and, hence speed of sound, decreases. This represents a single phase region of the fluid. The second part is a curve where the system temperature is less than the critical temperature. Unlike the first region, the speed of sound is inversely proportional to the system temperature, i.e. as temperature decreases, resonance frequency increases. This represents a two-phase region where both gas and liquid are present in equilibrium. Each of the experimental plots has a broken tip which occurs in the critical region indicating loss of signal and hence loss of precise track of the resonance peak in this vicinity. This is understandable in view of the extremely fast dynamic behavior of the resonance frequency in the critical vicinity and the simultaneous dramatic reduction in signal amplitude. The best experimental result was obtained during a run in which the temperature of the well insulated system was initially set at a value above the estimated critical temperature, and the system was then allowed to cool down naturally to room temperature (around 296 K.) The cooling time was approximately 17 hours during which approximately 1000 data points were collected. Figures 5.2 and 5.3 represent results of this particular run showing the relationships between system temperature and resonance frequency and sonic speed respectively. Results of this run clearly show the extremely sensitive dependence of sonic speed on temperature in the critical region. Figure 5.4 shows a plot of the first

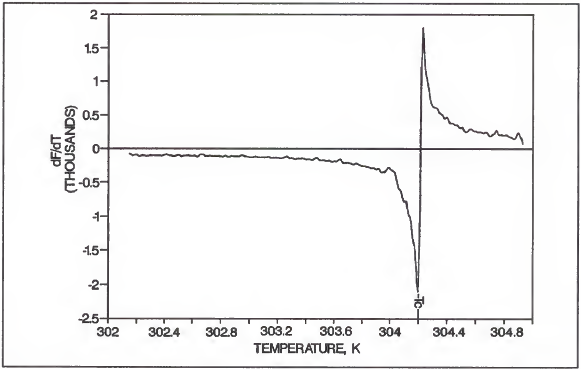

Figure 5.4. First derivative of resonance frequency versus temperature.

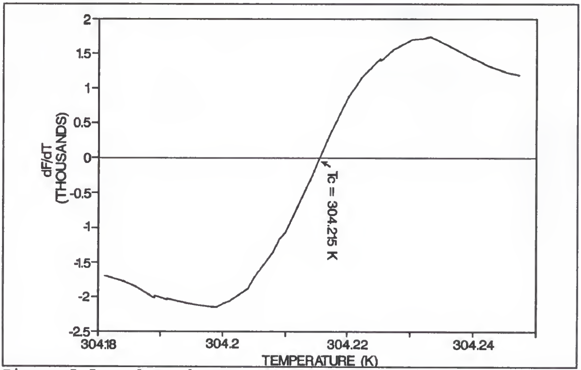

Figure 5.5. Enlarged temperature scale of figure 5.4 showing the critical temperature to be at 304.215 K.

derivative of resonance frequency with respect to temperature versus system temperature for the data of figure 5.3. It gives a precise value of the critical temperature as seen in figure 5.5 which is a portion of figure 5.4 with an expanded temperature scale. The critical temperature obtained from this plot is 304.215±0.007 kelvin. Figure 5.6 displays the relationship between the system pressure and temperature for this same run. It shows a nearly straight line with no evidence of phase separation.

Experiments were also run with subcritical density charges. These show the phase boundary location (dew points) as changes in slope of resonance frequency versus system temperature. Table 5.1 gives a comparison of results found by the present method with available literature values. The present results are in good agreement with the other experimental values and with predictions based on an equation of state(55) and a correlation model developed at the National Institute of Standards and Technology (NIST, formerly NBS)(56). The acoustic data and NIST predictions are shown graphically in figure 5.7. Table 5.2 gives a chronological collection of experimental values of critical point parameters ($T_c$ and $P_c$) reported by several authors. The value obtained by this sonic method is only 0.0016 percent different from the best value obtained in the NIST laboratories (Morrison and Kincaid, 1984. Reference 96).

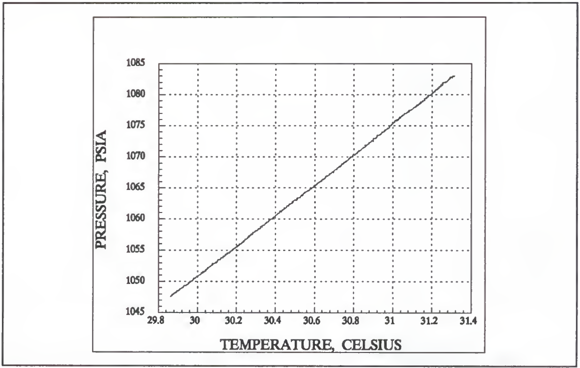

Figure 5.6. Pressure and temperature behavior of carbon dioxide for isochore near the critical density.

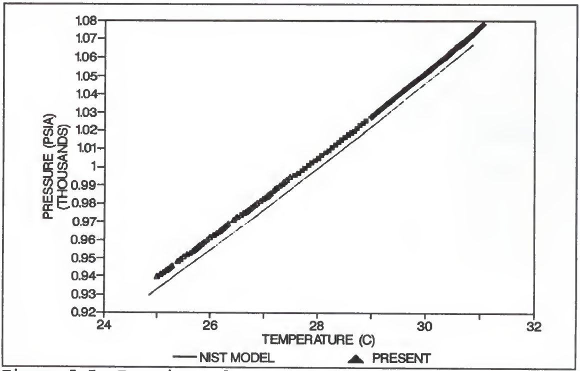

Figure 5.7. Experimental vapor pressure curve compared with the NIST model.

Table 5.1. Comparison of Dewpoint Pressures of Carbon Dioxide.

| No. | T (K) | Dewpoint pressure, psia | | | | Percent difference | | |
|---|---|---|---|---|---|---|---|---|
| | | Present sonic method | Equation of state[a] (I) | Burnett method[b] (II) | NIST Model[c] (III) | I | II | III |
| 1 | 299.905 | 971.46 | 971.045 | 971.10 | 971.53 | +0.0427 | +0.037 | -0.0072 |
| 2 | 301.012 | 995.60 | 995.418 | 996.56 | 996.41 | +0.0183 | -0.096 | -0.081 |
| 3 | 301.915 | 1015.30 | 1015.632 | 1017.10 | 1017.16 | -0.0327 | -0.177 | -0.183 |
| 4 | 303.046 | 1041.74 | 1041.379 | 1044.23 | 1043.75 | +0.0347 | -0.239 | -0.192 |

[a] Reference 55.
[b] Reference 57.
[c] Reference 56.

Table 5.2. Values of critical point parameters from the literature.

| Temperature K | Pressure | | Density | Author(s)* |
|---|---|---|---|---|
| | atm. | psia. | Kg/m$^3$ | |
| 304.07 | 73.0 | 1072.77 | - | Andrews (58) |
| 304.15 | - | - | - | Hautefeuille Cailletet (59) |
| 305.05 | 77.0 | 1131.55 | - | Dewar (60) |
| 304.50 | 72.9 | 1071.30 | - | Amagat (61) |
| 304.55 | - | - | - | Chappuis (62) |
| 304.85 | - | - | - | Villard (63) |
| 304.15 | - | - | - | Verschaffelt (64) |
| 304.25 | 73.26 | 1076.59 | - | Kuenen (65) |
| 304.55 | - | - | - | De Heen (66) |
| 304.10 | - | - | - | Von Wesendonck (67) |
| 304.13 | 72.93 | 1071.74 | - | Keesom (68) |
| 304.27 | - | - | - | Brinkmann (69) |
| 304.135 | - | - | - | Onnes & Fabius (70) |
| 304.41 | - | - | - | Bradley, Brown, & Hale (71) |
| 304.25 | 73.00 | 1072.77 | - | Dorsman (72) |
| 304.15 | 72.85 | 1070.56 | - | Cardoso & Bell (73) |
| 304.12 | - | - | - | Hein (74) |
| 304.35 | - | - | - | Dieterici C. (75) |
| 304.10 | - | - | - | Pickering S.F. (76) |
| 304.25 | 72.95 | 1072.03 | - | Meyers & Van Dusen (77) |
| 304.11±0.01 | - | - | - | Kennedy H.T., Cyril H., and Meyer (78) |

Table 5.2. (Continued)

| Temperature K | Pressure | | Density | Author(s)* |
|---|---|---|---|---|
| | atm. | psia. | Kg/m³ | |
| 304.11 | - | - | - | Kennedy (79) |
| 304.19 | - | - | - | Michael A.<br>Blaisse S.<br>Michael C. (80) |
| 304.19 | - | - | - | Lorentzen and Han Ludvig (81) |
| 304.19 | 72.80 | 1069.83 | - | Tielsch H. (82) |
| 304.16 | 75.20 | 1105.10 | - | Ernst S. and Thomas W. (83) |
| 304.21 | 72.87 | 1070.86 | - | Wentorf R.H. (84) |
| 304.16 ±0.03 | - | - | - | Ambrose D. (85) |
| 304.15 ±0.01 | 75.282 | 1106.30 | - | Ernst S. and Traube K. (86) |
| 304.2 | 72.83 | 1070.34 | 468 | Matthews J.F. (87) |
| 304.150 ±0.004 | 72.79 | 1069.68 | 467.8 | Moldover (88) |
| 304.19 | 72.86 | 1070.78 | 468 | Altunin V. (89) |
| 304.13 | - | - | - | Krynicki (90) |
| 304.16 | - | - | - | Lesnevskaya (91) |
| 304.13 | 72.79 | 1069.62 | 467 | Sengers J.V. (92) |
| 304.20 | - | - | - | Morrison G. (93) |
| 304.13 | - | - | 467.4 | Adamov (94) |
| 304.13 | 72.79 | 1069.66 | 467.8 | Shelomentsev (95) |
| 304.206 ±0.001 | 72.87 ±0.01 | 1070.96 ±0.01 | 468.248 ±0.008 | Morrison Kincaid (96) |
| 304.215 ±0.007 | 73.28 ±3.00 | 1076.88 ±3.00 | - | This work |

* Numbers in parenthesis refer to references in bibliography.

Encouraged by the apparent success of this approach to the location of phase boundaries, including critical points, for a pure substance, we opted to proceed to the next stage of the study and perform similar tests an a simple fluid mixture. The properties of mixtures are not so well documented as those of carbon dioxide, and there are few previously well characterized binary systems to choose from. Carbon dioxide-ethane is one of these, and a mixture of these two was selected for this study. The results obtained are presented in the next section.

## A Mixture of Carbon Dioxide and Ethane

Since an acoustic resonance technique has been successfully used to detect phase changes along the coexistence curve of a single component system, it is a naturally logical forward step to investigate its suitability for use with more complex systems. What is needed are specific mixtures with well characterized phase behavior. A binary mixture of 74.25 mole percent carbon dioxide and ethane was selected for this purpose. The carbon dioxide-ethane system has been studied by several researchers beginning in 1897. The first critical measurements were carried out by Kuenen in 1897(97) and 1902(98) followed by Khazanova and Lesnevsicaya in 1967(99), Fredenslund and Mollerup in 1974(100) and Morrison and Kincaid in 1984(96). Phase boundary studies have been performed by Clark and Din in 1953(101), Jensen and Kurata in 1971(102), Gugnoni and Eldridge in 1974(103), Nagahama et al. in 1974(104), Dabalos in 1974(105), and Stead and Williams in 1980(106). In 1978 Moldover and Gallagher(107) presented a correlation for this mixture in an analogy with pure fluids. The specific mixture selected for this study is one which was studied by Khazanova and Lesnevsicaya(99). Figures 5.8, 5.9, and 5.10 show the behavior of the resonance frequency versus temperature of this mixture at three different gas densities: supercritical density ($\rho_{gas} > \rho_c$), subcritical density ($\rho_{gas} < \rho_c$), and near critical density ($\rho_{gas} \approx \rho_c$). Note the sharper turning point in the curve around the critical region in figure 5.10 compared to the turning points of the curves of figure 5.8 and 5.9. The former is a distinctive characteristic of a system at its critical conditions ($T_c$, $P_c$, and $\rho_c$.) The latter are characteristic of a system reaching a coexistence boundary at other conditions (bubble points or dew points) than the critical. Figure 5.11 displays typical experimental results for a near-critical-density gas mixture. Curve 1 represents a run for which the bath temperature was ramped downward from ~30 to ~12 °C. Curve 2 shows data for an upward ramp from ~10 to ~22 °C. In both cases the tracked peak (first radial mode resonance frequency) was lost over a small temperature interval in the critical vicinity due to the extremely fast change of sonic speed and drop in amplitude. Curve 3 is like curve 2 except that the temperature of the well-insulated

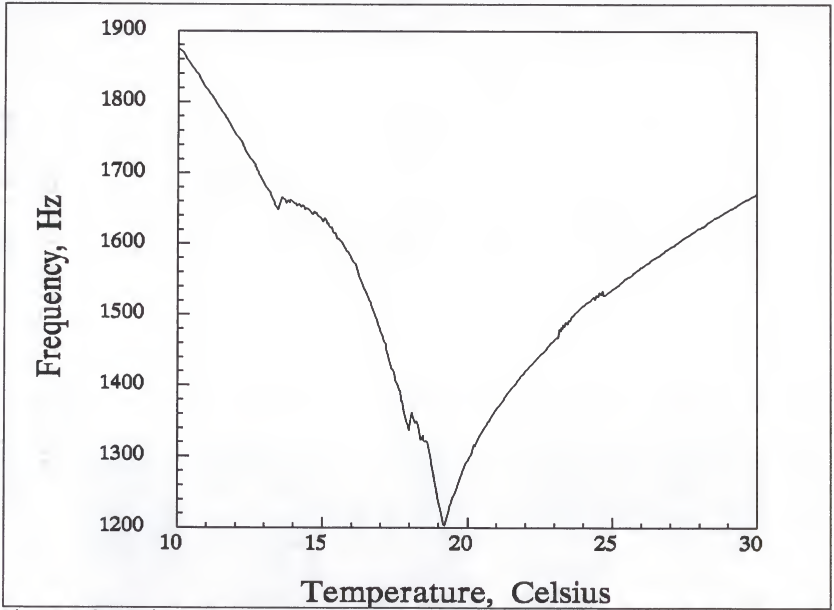

Figure 5.8. Typical behavior of resonance frequency versus temperature of the carbon dioxide-ethane mixture at a supercritical density.

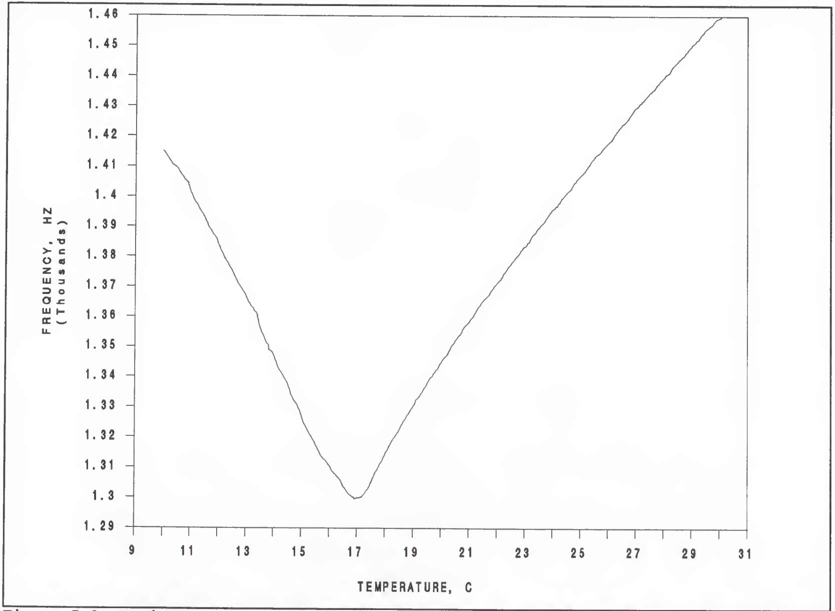

Figure 5.9. Typical behavior of resonance frequency versus temperature of the carbon dioxide-ethane mixture at a subcritical density.

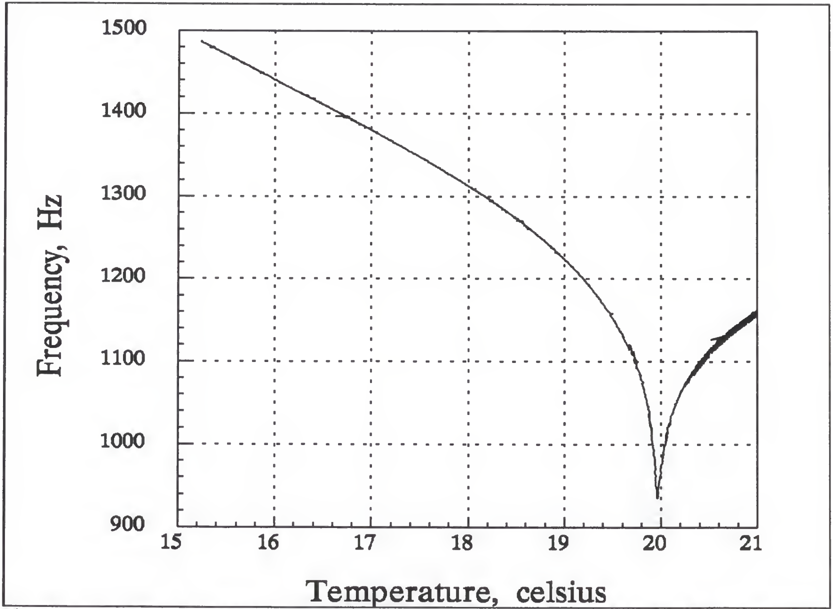

Figure 5.10. Typical behavior of resonance frequency versus temperature of the carbon dioxide-ethane mixture near critical density.

system was allowed to raise naturally from 15 °C to room temperature. This procedure was similar to the one utilized in the experiments with carbon dioxide (and also with ethane as will be seen later) except that the run went from low to high temperature as the critical temperature of this particular mixture is lower than room temperature. Again, the peak is easier to track if the system temperature changes very slowly. The speed of sound is very sensitive to temperature change in the critical region. Note that a sharp turning point gives a quite accurate value of the transition temperature but not necessarily of speed of sound. Figure 5.12 is similar to figure 5.11 but illustrates how other modes of vibration reveal the same critical point temperature. In principle every normal mode resonance exhibits a discontinuity at the critical point, so there are very many possible indicators which are equally capable of locating the critical point.

Figure 5.13 shows the behavior of pressure versus temperature for several isochoric runs representing different fluid densities. The upward direction of the breaks in these curves shows them each to result from approaching the phase boundary on cooling from a supercritical density. The breaks mark individual bubble points on the phase envelope. Approaches from subcritical densities would break downward at the corresponding dewpoints, and the critical isochore would exhibit no break at all. These facts are helpful in searching

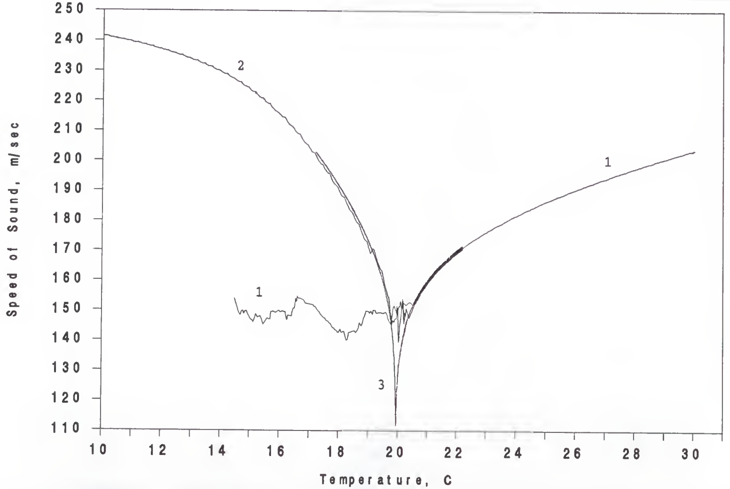

Figure 5.11. Typical experimental results of near-critical density gas of the carbon dioxide-ethane mixture. Curve 1 shows a forced cooling run. Curve 2 shows a forced warming run. Curve 3 is a slow naturally warming run.

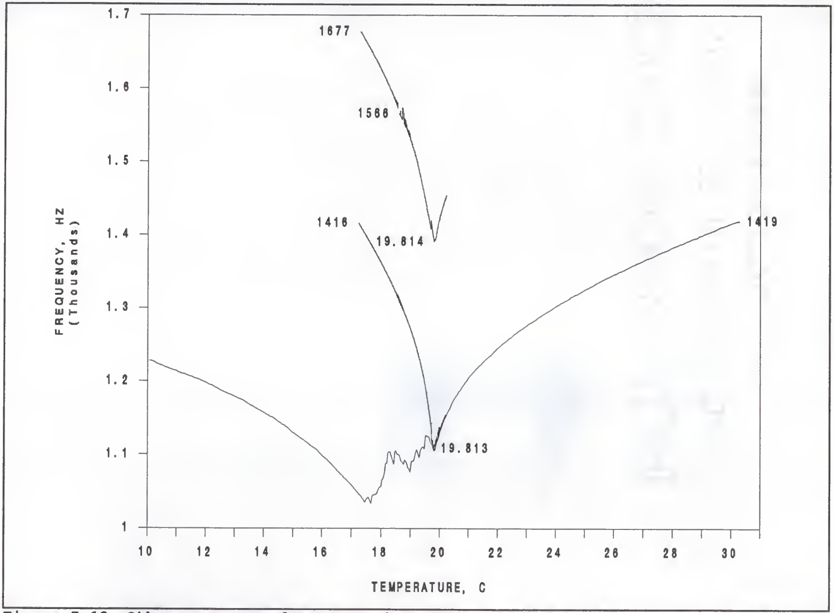

Figure 5.12. Other resonance frequency (top curve) results in same critical temperature as first radial resonance frequency (bottom curve.)

for the critical point of a system when it is not previously known. For example the starting pressure at 30 °C for the critical isochore could be approximately calculated from the information in figure 5.13 in the following fashion. For each isochore the two branches, supercritical vapor above the bubble point and two phase equilibrium below it, were fit to straight lines by linear regression. The angle θ between the two branches is directly related to the slopes of these lines. A plot of initial charging pressure versus θ indicates by extrapolation the approximate critical density charging pressure for which θ = 0. The results for the data of figure 5.13 are tabulated in table 5.3, and the plot of charging

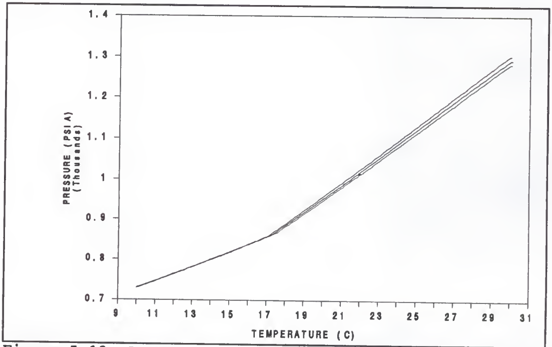

Figure 5.13. A sequence of supercritical pressure versus temperature isochores of the carbon dioxide-ethane mixture.

pressure versus θ is shown in figure 5.14. This technique revealed the magnitude of the charging pressure to be used when data were to be collected in search of the critical point.

Table 5.3. Angles between pressure-temperature lines before and after phase boundary of supercritical density fluid of carbon dioxide and ethane.

| File # | Slope of line before phase boundary | Slope of line after phase boundary | Angle between two lines (degree) |
|---|---|---|---|
| 729 | 34.637 | 18.444 | 14.733 |
| 731 | 34.074 | 18.293 | 14.479 |
| 801 | 33.562 | 18.371 | 14.091 |
| 802 | 32.842 | 18.444 | 13.594 |
| 807 | 27.882 | 18.690 | 10.356 |
| 811 | 25.149 | 18.607 | 7.992 |
| 815 | 24.701 | 18.846 | 7.191 |

This prediction was important here since the system volume is fixed. The only way to change the system density was to

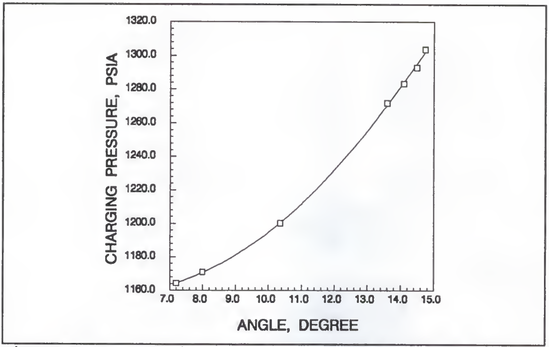

Figure 5.14. Relationship between the angles θ and the charging pressures of the carbon dioxide-ethane mixture.

release some of the material, and this process was potentially troublesome because of the possibility of inducing unwanted composition changes. Care was taken to release gas only from the system in the single phase condition and then only after it had been blended thoroughly by continued mixing. Typically, when the system was close to the critical density, only small amounts of gas were released for each successive run. The drop in charging pressure at 30 °C was typically one or two psia. For this work the total number of runs was fifty.

Table 5.4 lists the experimental results needed to construct phase diagrams of this system. Figures 5.15 to 5.19 show various types of phase diagram created from different combinations of the parameters in table 5.4. Figure 5.15 shows the relationship between starting pressure at 30 °C and the

Table 5.4. Experimental results for construction of phase diagrams of a mixture of carbon dioxide and ethane.

| FILE NAME | Starting point | | | Point of minimum frequency | | | |
|---|---|---|---|---|---|---|---|
| | T (°C) | Pressure psia | Frequency Hz | T (°C) | Frequency Hz | Sonic speed m/sec | Pressure psia |
| TDA729 | 30.004 | 1303.6 | 1976.38 | 17.006 | 1554.82 | 216.72 | 857.0 |
| TDA731 | 29.993 | 1292.9 | 1951.08 | 17.200 | 1533.44 | 213.70 | 860.7 |
| TDA801 | 30.002 | 1283.3 | 1925.92 | 17.485 | 1507.68 | 210.11 | 865.8 |
| TDA802 | 30.002 | 1271.9 | 1895.52 | 17.632 | 1470.04 | 204.87 | 869.4 |
| TDA807 | 30.003 | 1200.2 | 1669.91 | 19.228 | 1203.10 | 167.71 | 901.2 |
| TDA820 | 30.013 | 1156.6 | 1535.02 | 19.860 | 935.06 | 130.33 | 914.5 |
| TDA907 | 30.007 | 1135.3 | 1460.87 | 19.950 | 802.36 | 111.83 | 915.9 |
| TDA914 | 30.011 | 1114.8 | 1425.97 | 19.964 | 934.84 | 130.30 | 916.3 |
| TDA917,925 | 30.060 | 1107.1 | 1420.32 | 19.920 | 1030.75 | 143.66 | 915.6 |
| TDA926 | 30.039 | 1101.2 | 1426.42 | 19.885 | 1073.42 | 149.61 | 914.9 |
| TDA928 | 30.020 | 1098.6 | 1416.55 | 19.851 | 1086.70 | 151.46 | 914.1 |

Table 5.4. (Continued)

| FILE NAME | Starting point | | | Point of minimum frequency | | | |
|---|---|---|---|---|---|---|---|
| | T (°C) | Pressure psia | Frequency Hz | T (°C) | Frequency Hz | Sonic speed m/sec | Pressure psia |
| TDA929 | 30.020 | 1098.6 | 1416.55 | 19.835 | 1087.73 | 151.61 | 913.5 |
| TDA1003 | 30.018 | 1095.7 | 1416.57 | 19.800 | 1105.21 | 154.04 | 913.2 |
| TDA1004 | 30.006 | 1090.1 | 1415.82 | 19.737 | 1132.31 | 157.86 | 911.3 |
| TDA1006 | 30.015 | 1083.6 | 1417.73 | 19.596 | 1158.91 | 161.58 | 909.2 |
| TDA1007 | 30.005 | 1077.6 | 1419.66 | 19.476 | 1182.36 | 164.80 | 906.3 |
| TDA1009 | 30.007 | 1066.1 | 1425.68 | 19.181 | 1217.97 | 169.81 | 899.8 |
| TDA1010 | 30.001 | 1057.3 | 1431.13 | 18.899 | 1239.56 | 172.76 | 893.8 |
| TDA1011 | 29.997 | 1047.7 | 1437.77 | 18.532 | 1258.82 | 175.44 | 886.3 |
| TDA1012 | 30.000 | 1037.9 | 1444.67 | 18.043 | 1274.82 | 177.67 | 876.8 |
| TDA1013,14 | 29.992 | 1027.6 | 1452.33 | 17.800 | 1289.80 | 179.75 | 870.7 |
| TDA1015(1) | 30.029 | 1017.0 | 1459.64 | 17.200 | 1300.55 | 181.24 | 859.2 |

Table 5.4. (Continued)

| FILE NAME | Starting point | | | Point of minimum frequency | | | |
|---|---|---|---|---|---|---|---|
| | T (°C) | Pressure psia | Frequency Hz | T (°C) | Frequency Hz | Sonic speed m/sec | Pressure psia |
| TDA1015(2) | 30.029 | 1017.0 | 1459.64 | 17.174 | 1300.34 | 181.22 | 858.8 |
| TDA1016,17 | 30.047 | 1006.7 | 1468.85 | 16.750 | 1313.48 | 183.04 | 850.1 |

temperature of phase change. Experimental results are represented by points. The smooth curve is a result of a third order polynomial curve fitting procedure. The corresponding equation is as follows:

$$T = a + b*p + c*p^2 + d*p^3$$

where T = temperature, celsius

p = pressure, psia

$a = -8.137773 \times 10^2$

$b = 2.020012$

$c = -1.616095 \times 10^{-3}$

$d = 4.260451 \times 10^{-7}$

r = correlation coefficient

= 0.99749.

Figure 5.16 shows the relationship between starting pressure and the speed of sound at the phase change. A sharp change in the speed of sound at the critical point is evident compared to the slow change of temperature shown figure 5.15. Figure 5.17 shows a coexistence curve. Note that the curve is so slim that the bubble-point line almost overlaps the dew-point line. Recall that a similar plot for a pure fluid yields a nearly straight line (see figure 5.23 of ethane.) This clearly reveals a property of this mixture as being nearly azeotropic. It behaves much as if it were a pure fluid. The literature value of the azeotrope composition of this binary mixture is reported to be 0.255 mole fraction of ethane(108). This is very close to the composition of the mixture studied in this work

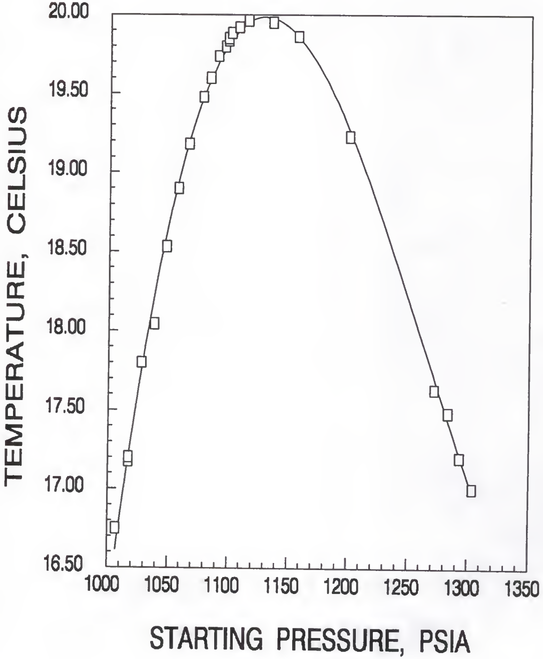

Figure 5.15. Relationship between the starting pressures and the temperatures of phase change of the carbon dioxide-ethane mixture.

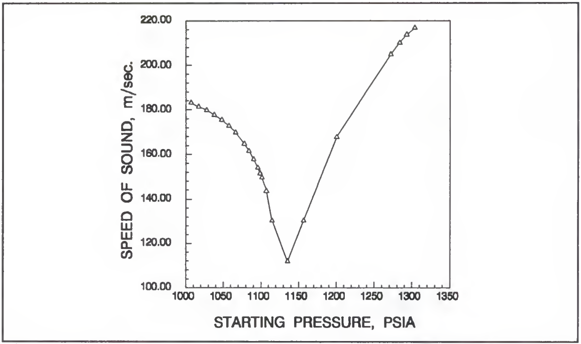

Figure 5.16. Relationship between the starting pressures and the speed of sound at a phase change of the carbon dioxide-ethane mixture.

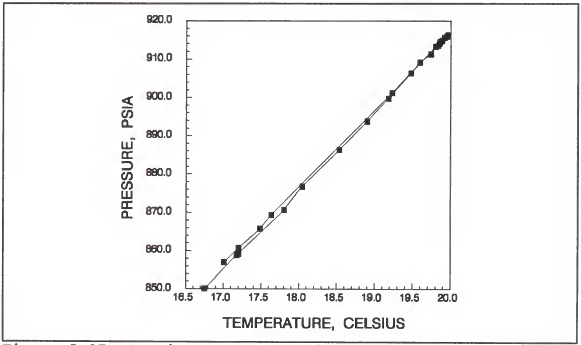

Figure 5.17. Coexistence curve of the carbon dioxide-ethane mixture near azeotrope composition.

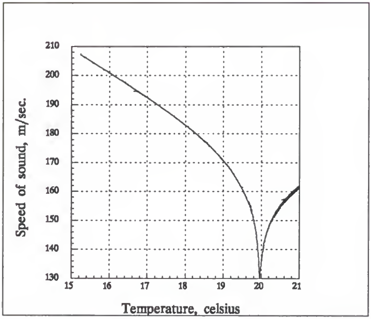

Figure 5.18. The sonic speed versus temperature of the carbon dioxide-ethane mixture for an isochore near critical density.

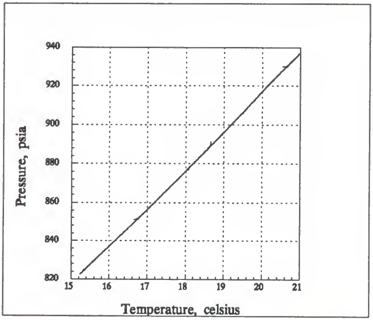

Figure 5.19. Pressure and temperature behavior of the carbon dioxide-ethane mixture charged near its critical density.

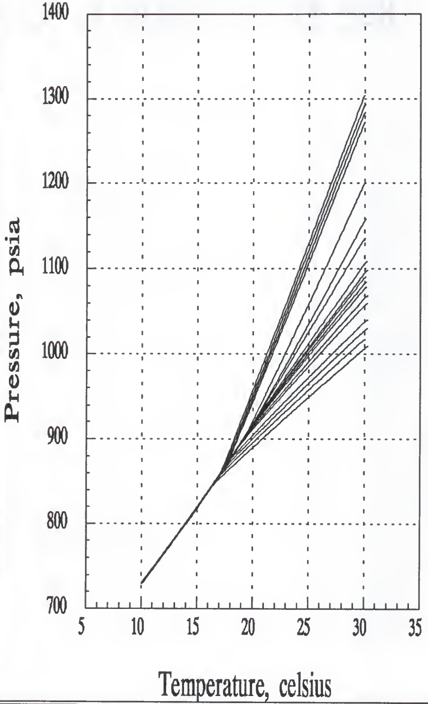

Figure 5.20. Pressure and temperature relationship of a set of several isochores of the carbon dioxide-ethane mixture.

Table 5.5. Comparison of Dewpoint Pressures of $CO_2$ + $C_2H_6$ Mixture ($X_{CO2}$ = 0.7425).

| No. | Temperature (K) | Dewpoint pressures, psia | | | Percent Difference | |
|---|---|---|---|---|---|---|
| | | Present sonic method | Equilibrium cell of the vapor recirculation type (interpolated)[1] (I) | NIST DDMIX Model[2] (II) | I | II |
| 1 | 290.156 | 850.88 | 849.950 | 862.296 | -0.109 | -1.34 |
| 2 | 290.350 | 854.55 | 853.500 | 866.068 | +0.123 | -1.35 |
| 3 | 290.635 | 859.62 | 858.620 | 871.580 | +0.116 | -1.39 |

[1] A. Fredenslund and J. Mollerup, J. Chem. Soc. Faraday Trans. I, 70, 1653 (1974).

[2] DDMIX model developed by NBS (1988) uses Peng-Robinson equation of state for coexisting-phase composition calculations and NBS corresponding states model with shape factors and van der Waals one-fluid mixing rules for phase properties. The uncertainties in DDMIX model are principally due to the uncertainties associated with the mixing rules.

(0.256) confirming the explanation. Figures 5.18 and 5.19 show the relationships near the critical density between temperature of phase change and speed of sound and the pressure respectively. As expected the sonic speed (figure 5.18) shows a pronounced change in the critical region while the pressure (figure 5.19) shows a smooth passage from the one-phase to the two-phase region. Figure 5.20 shows a composite plot of pressure and temperature data representing 23 separate isochoric runs. Those loadings with supercritical densities show phase change by upward breaks at the corresponding bubble points. Those loadings at subcritical densities show downward breaks at the corresponding dew points. Loading at the critical density leads to no break at all. Table 5.5 compares dew point pressures observed in this work with those available in the literature. Clearly, the agreement is quite good. The critical temperature for this mixture obtained in this work was 293.134±0.007 K. The only available literature experimental value for this composition was found to be 293.072 K (96). These values differ by only 0.021 percent.

## Ethane

The graphs shown in figures 5.21 to 5.24 represent the isochoric behavior of the system charged with pure ethane at near critical density. Figure 5.21 shows a typical relationship between a resonance frequency and the system

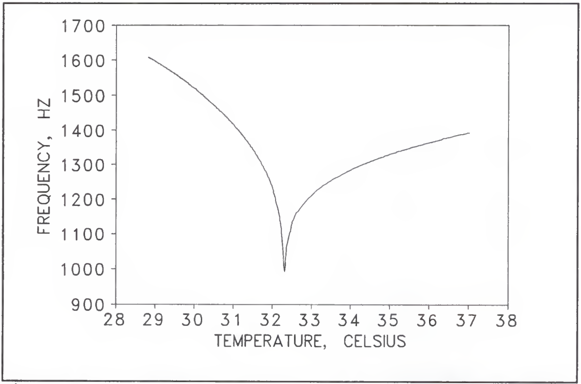

Figure 5.21. Resonance frequency (1s mode) and temperature relationship of ethane near the critical density.

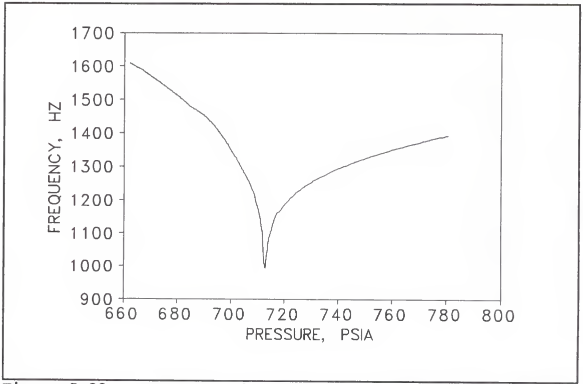

Figure 5.22. Resonance frequency (1s mode) and pressure relationship of ethane near the critical density.

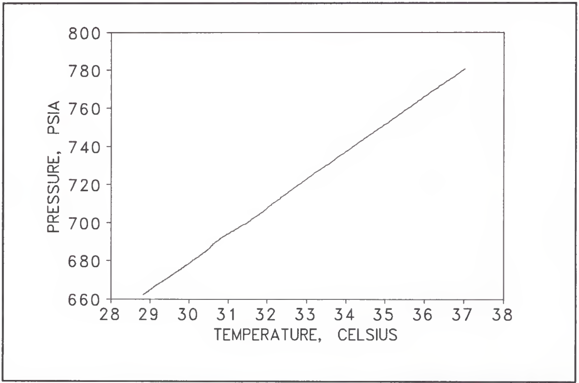

Figure 5.23. Pressure and temperature relationship of 1s mode resonance frequency of ethane near the critical density.

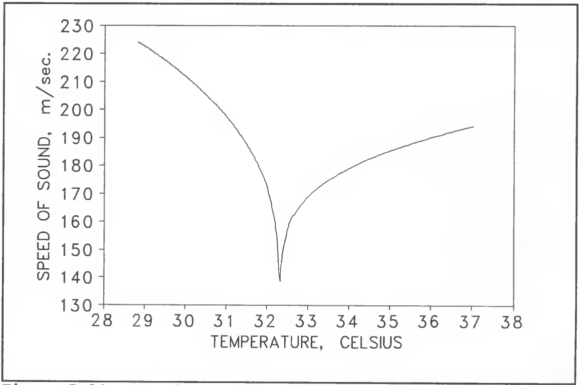

Figure 5.24. Speed of sound and temperature of 1s mode resonance frequency of ethane near the critical density.

temperature. Figure 5.22 is similar to figure 5.21 but with pressure plotted instead of temperature. These two figures have the same characteristics implying a linear relationship between temperature and pressure as expected for this condition. This is even more evident in figure 5.23. Figure 5.24 shows plot of the speed of sound as a function of temperature. It is similar to figure 5.21 since the speed of sound is directly proportional to the resonance frequency. Figure 5.25 shows the relationship between the initial charging pressure and the coexistence (liquid-vapor equilibrium) temperature. Experimental data points were fitted to a polynomial of the sixth order. Its coefficients, along with some statistical values generated from the data by GRAPHER

Table 5.6. Sixth order polynomial fit statistics of GRAPHER program applied to experimental data points in figure 5.25.

| Degree | Polynomial Coefficients | Sums of Squares of Residuals |
|---|---|---|
| 4 | 2.15029E+007 | 0.952964 |
| 4 | -166034 | 0.909732 |
| 2 | 533.701 | 0.0191329 |
| 3 | -0.914178 | 0.00389193 |
| 4 | 0.000880105 | 0.0019246 |
| 5 | -4.51543E-007 | 0.00192265 |
| 6 | 9.64558E-011 | 0.00192195 |
| Total points = 23 | | |
| Points in fit interval = 23 | | |

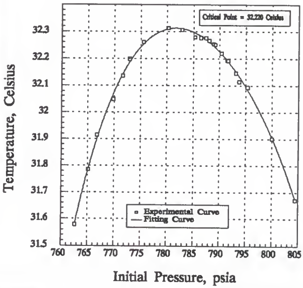

Figure 5.25. Phase diagram of pure ethane showing temperature of phase changes as a function of starting pressure.

software, are listed in table 5.6. Figure 5.26 shows a collection of pressure and temperature data of 23 isochores which cover a broad range of densities from supercritical to subcritical values. These curves coincide within experimental uncertainty in the liquid-vapor equilibrium region. Figure 5.27 shows a trajectory plot of a collection of 23 pressure-temperature-speed of sound data sets of different densities. It clearly shows the pronounced trend of decreasing sonic speed as the system approaches critical conditions. Table 5.7 is a compilation of all necessary experimental data to construct the phase diagram in different views as shown in the above listed figures. Tables 5.8 gives the comparison between

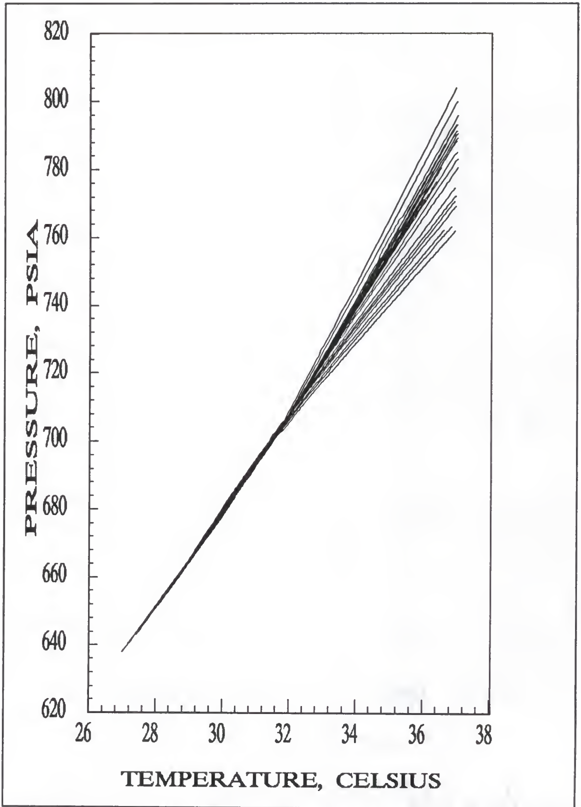

Figure 5.26. Phase diagram of ethane showing pressure and temperature behavior of 23 different isochores.

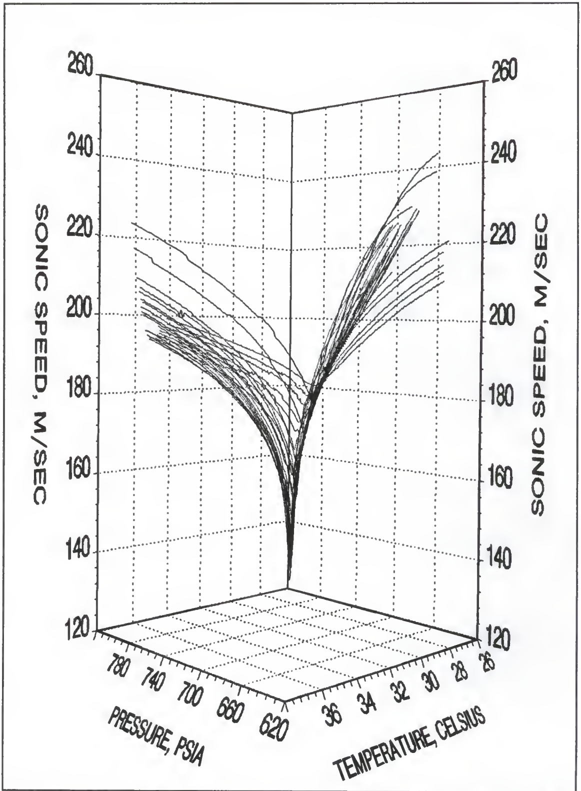

Figure 5.27. Trajectory plot of temperature, pressure, and sonic speed of ethane at different densities. The one nearest the critical density reaches the lowest sonic speed.

the present experimental bubble point pressures and available literature values. These include the experimental values measured in the compressibility apparatus of Douslin and Harrison(109) and the values predicted by DDMIX(56), a correlation model developed at the National Institute of Standards and Technology (NIST, formerly NBS). Table 5.9 compares the present vapor pressures with those of the predictive equation proposed by Sychev et. al.(110) This equation derived from a compilation of vapor pressures of ethane by Goodwin et. al.(111) The Sychev equation is:

$$\ln p_s = a + bx + cu + du^2 + eu^3 + fu(1-u)^\epsilon$$

where $x(T) = [1-(T_{tr}/T)]/[1-(T_{tr}/T_{cr})]$

$u(T) = [T-T_{tr}]/[T_{cr}-T_{tr}]$

$T_{tr}$ = Temperature at the triple point

= 90.348 ± 0.010 K

$T_{cr}$ = Critical Temperature

= 305.33 ± 0.02 K

$a = -11.38996$

$b = 18.84523$

$c = -7.635425$

$d = 5.428443$

$e = -1.362327$

$f = 0.7692493$

$\epsilon = 1.30.$

Table 5.7. Summary of results for ethane measurements.

| File Number | Conditions at start of run (T = 37 °C) | | Sonic speed at phase boundary * (m/sec.) | Conditions at minimum resonance frequency | | | | |
|---|---|---|---|---|---|---|---|---|
| | Frequency (Hz) | Pressure (psia) | | T (°C) | P (psia) | Frequency (Hz) | Sonic speed (m/sec) | Amp. (mv) |
| 919 | 1616.2 | 800.5 | 179.89 | 31.568 | 697.65 | 1287.0 | 179.37 | 254 |
| 920 | 1563.8 | 796.0 | 172.19 | 31.799 | 700.83 | 1227.3 | 171.05 | 4958 |
| 924 | 1500.9 | 791.4 | 162.40 | 31.991 | 703.71 | 1154.6 | 160.92 | 1799 |
| 9284 | 1485.0 | 789.8 | 156.15 | 32.011 | 704.30 | 1119.6 | 155.69 | 1891 |
| 1002 | 1477.5 | 789.1 | 154.15 | 32.043 | 704.70 | 1103.1 | 153.74 | 718 |
| 1007 | 1458.9 | 787.5 | 147.93 | 32.090 | 705.40 | 1067.2 | 148.73 | 862 |
| 1008 | 1449.6 | 786.4 | 143.99 | 32.116 | 706.09 | 1036.2 | 144.41 | 741 |
| 1010 | 1440.5 | 785.2 | 141.75 | 32.149 | 706.39 | 1020.7 | 142.25 | 506 |
| 1012 | 1436.1 | 784.9 | 139.19 | 32.151 | 706.59 | 1004.6 | 140.01 | 274 |
| 10141 | 1436.6 | 784.0 | 139.01 | 32.163 | 706.79 | 998.1 | 139.10 | 279 |

Table 5.7. (Continued)

| File Number | Conditions at start of run (T = 37 °C) | | Sonic speed at phase boundary* (m/sec.) | Conditions at minimum resonance frequency | | | | |
|---|---|---|---|---|---|---|---|---|
| | Frequency (Hz) | Pressure (psia) | | T (°C) | P (psia) | Frequency (Hz) | Sonic speed (m/sec) | Amp. (mv) |
| 10170 | 1430.7 | 783.4 | 138.76 | 32.173 | 705.89 | 935.0 | 139.39 | 64 |
| 1021 | 1428.5 | 782.4 | 136.72 | 32.175 | 707.08 | 979.2 | 136.47 | 92 |
| 10262 | 1408.4 | 781.4 | 136.51 | 32.176 | 707.08 | 987.8 | 137.66 | 144 |
| 10291 | 1399.4 | 778.9 | 138.00 | 32.203 | 707.78 | 947.4 | 141.47 | 163 |
| 1031 | 1393.0 | 776.3 | 137.19 | 32.210 | 707.78 | 993.6 | 138.47 | 108 |
| 1102 | 1393.8 | 771.6 | N/A | 32.158 | 706.49 | 1155.0 | 160.97 | 2929 |
| 1105 | 1399.5 | 769.0 | N/A | 32.095 | 705.40 | 1199.4 | 167.16 | 1707 |
| 1107 | 1403.0 | 767.7 | N/A | 32.033 | 704.50 | 1233.5 | 171.92 | 1686 |
| 1108 | 1408.5 | 765.9 | N/A | 31.946 | 703.11 | 1248.3 | 173.98 | 1949 |
| 1109 | 1417.6 | 762.8 | N/A | 31.812 | 700.53 | 1280.2 | 178.42 | 1305 |

Table 5.7. (Continued)

| File Number | Conditions at start of run (T = 37 °C) | | Sonic speed at phase boundary* (m/sec.) | Conditions at minimum resonance frequency | | | | |
|---|---|---|---|---|---|---|---|---|
| | Frequency (Hz) | Pressure (psia) | | T (°C) | P (psia) | Frequency (Hz) | Sonic speed (m/sec) | Amp. (mv) |
| 1110 | 1434.2 | 761.2 | N/A | 31.682 | 698.54 | 1296.2 | 180.63 | 1079 |
| 1111 | 1430.0 | 758.7 | N/A | 31.475 | 696.16 | 1314.3 | 183.16 | 1124 |

* The sonic speed at the phase boundary was determined by a Simplex routine from the experimental data. See curve fitting section.

Table 5.8. Comparison of Bubble-Point Pressures of Ethane.

| No. | T (K) | Bubble-point Pressures, psia | | | Percent Difference | |
|---|---|---|---|---|---|---|
| | | Present sonic method | Compressibility apparatus[1] (I) | NIST DDMIX Model (II)[2] | I | II |
| 1 | 304.718 | 697.67 | 697.645 | 697.497 | +0.003 | +0.024 |
| 2 | 304.949 | 700.83 | 701.020 | 700.978 | -0.027 | -0.021 |
| 3 | 305.141 | 703.71 | 703.830 | 703.735 | -0.017 | +0.009 |
| 4 | 305.161 | 704.30 | 701.020 | 704.025 | +0.026 | +0.039 |
| 5 | 305.193 | 703.71 | 701.020 | 704.605 | +0.014 | +0.013 |
| 6 | 305.240 | 705.40 | 705.450 | 705.330 | -0.008 | +0.009 |

[1] D. R. Douslin and R. H. Harrison, J. Chem. Thermodynamics, 5, 491, 1973.
[2] See footnote of table 5.5 for explanation.

Table 5.9. Comparison of experimental vapor pressures and those calculated with an equation of state of ethane proposed by Sychev.(110)

| Experimental | | Predicted pressure psia | Percent difference |
|---|---|---|---|
| T (K) | P (psia) | | |
| 304.72 | 697.65 | 697.36 | 0.0410 |
| 304.95 | 705.89 | 700.79 | 0.0053 |
| 305.18 | 703.71 | 703.96 | 0.0062 |
| 305.16 | 704.30 | 703.96 | 0.0421 |
| 305.19 | 700.79 | 704.45 | 0.0360 |
| 305.27 | 705.40 | 705.16 | 0.0896 |
| 305.27 | 704.45 | 705.55 | 0.0764 |
| 305.30 | 704.30 | 704.45 | 0.0475 |
| 305.30 | 706.59 | 706.49 | 0.0713 |
| 305.30 | 705.23 | 706.27 | 0.0735 |
| 305.30 | 705.89 | 706.42 | -0.0747 |
| 305.30 | 707.08 | 706.49 | 0.0896 |
| 305.30 | 704.38 | 706.47 | 0.0874 |
| 305.30 | 707.08 | N/A* | N/A |
| 305.36 | 707.78 | N/A* | N/A |
| 305.31 | 706.49 | 706.19 | 0.0421 |
| 305.27 | 705.40 | 705.23 | 0.0231 |
| 305.18 | 706.59 | 704.30 | 0.0292 |
| 305.10 | 703.11 | 702.99 | 0.0176 |
| 304.96 | 700.53 | 700.98 | -0.0648 |
| 304.83 | 698.54 | 699.05 | -0.0726 |
| 304.62 | 696.16 | 695.99 | 0.0242 |

* Equation diverges at this temperature.

Table 5.10. Chronological collection of critical point parameters of ethane.

| Temperature K | Pressure | | Density | Author(s) * | Year |
|---|---|---|---|---|---|
| | atm | psia | kg/m$^3$ | | |
| 305.2 | - | - | 212 | Wiebe et. al. (112) | 1930 |
| 306.7 | - | - | - | Sage et. al. (113) | 1937 |
| 305.4 | 48.5 | 712.1 | - | Kay (114) | 1938 |
| 305.41<br>(0.01) | 48.2<br>(0.02) | 707.8 | 203 (2) | Beattie et. al. (115) | 1939 |
| 305.25 | 48.6 | 713.6 | 213 | Lu et. al. (116) | 1941 |
| 305.11 | 48.12 | 707.2 | - | Kay and Brice (117) | 1953 |
| 305.31 | - | - | - | Whiteway and Mason (118) | 1953 |
| 305.47 | - | - | - | Palmer (119) | 1954 |
| 305.33 | 48.180 | 708.05 | - | Schmidt and Thomas (120) | 1954 |
| 305.42 | - | - | - | Khazanova et. al. (99) | 1967 |
| 305.43 | - | - | - | Kudchadker et. al. (121) | 1968 |
| 305.33 | - | - | - | Sliwinski (122) | 1969 |
| 305.35 | - | - | 206.2 | Bulavin et. al. (123) | 1971 |
| 305.35 | 48.112 | 707.04 | 205.8 | Miniovich and Sorina (124) | 1971 |
| 305.340 | 48.2<br>(0.1) | 707.8 | 203.9 | Khazanova and Sominskaya (125) | 1971 |
| 305.360 | - | - | - | Voronel et. al. (126) | 1972 |
| 305.3633 | - | - | - | Berestov et. al. (127) | 1973 |

Table 5.10. (Continued)

| Temperature K | Pressure | | Density | Author(s) [*] | Year |
|---|---|---|---|---|---|
| | atm | psia | kg/m$^3$ | | |
| 305.35 | 48.112 | 707.04 | 204.3 | Miniovich and Sorina (128) | 1973 |
| 305.3627 | - | - | 205 | Shmakov (129) | 1973 |
| 305.330 | 48.0805 | 706.589 | 206.581 | Douslin and Harrison (109) | 1973 |
| 305.368 (0.005) | - | - | 205.5 | Strumpf et. al. (130) | 1974 |
| 305.37 | 48.117 | 707.30 | 202.7 | Goodwin (131) | 1975 |
| 305.340 | 48.076 | 706.50 | 206.9 | Moldover and Gallagher (107) | 1978 |
| 305.360 | - | - | - | Berestov et. al. (132) | 1979 |
| 305.379 | - | - | - | Morrison (93) | 1981 |
| 305.393 ±0.001 | 47.16 ±0.01 | 692.99 ±0.01 | 205.860 ±0.005 | Morrison and Kincaid (96) | 1984 |
| 305.370 ±0.007 | 48.16 ±3.00 | 707.78 ±3.00 | - | This work | 1990 |

[*] Numbers in parenthesis refer to references in bibliography.

The predictive and experimental pressures are in good agreement. Notice that this equation is indeterminate when temperature is greater than 305.33 K since the u(T) term is more than unity. Table 5.10 chronologically collects the literature values of the critical parameters of ethane and the value obtained in this work.

## Analysis of Ethane Data

As mentioned earlier in the section on experimental procedure, the ethane experiment was performed differently from those on carbon dioxide and the carbon dioxide-ethane mixture. This resulted from advances in the experimental technique as the research progressed. In the case of ethane all data points along the entire frequency sweep range were saved on memory discs. These data can, in turn, be examined and analyzed later to obtain more understanding of the behavior of the gas under acoustic excitation. The analysis, however, is still very difficult and time consuming due in part to the large number of data points. Graphic methods are appropriate for this purpose. For example, in the ethane experiment for each isochoric density there are approximately 400 data files each containing 120 sets of four parameters: temperature, pressure, resonance frequency, and amplitude. For two dimensional observations one would have to pick two out of four parameters to plot each data set for the total of 120X400 plots. The practicability of doing this is limited by many factors such as the available graphics capability, computer

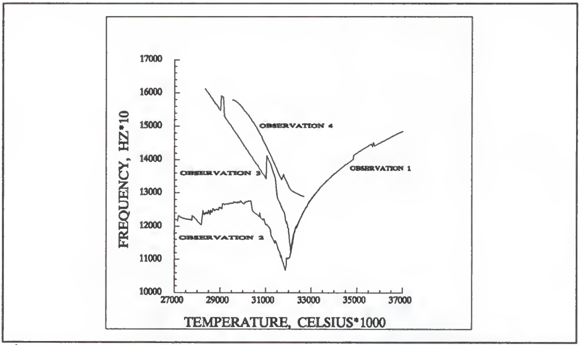

Figure 5.28. Resonance frequency and temperature relationship revealing some phenomena observed in the experiment on pure ethane.

memory size and resolution of the display monitor etc. At present only limited observations were practical.

Figure 5.28 is used in conjunction with the following observations. Note that each curve in this figure does not necessarily represent a system having the same density as the others. They are considered together for the purpose of the following comparison.

Observation 1

At temperatures above the critical temperature the first radial mode of vibration (the 1s peak) and the first nonradial mode of vibration (the 1f peak) were in close proximity (about 15-20 hz apart). Consequently, the 1f peak tended to interfere with tracking of the 1s peak. The data acquisition program selected the signal of highest amplitude in the observation window, and this was prone to shift between these two on occasion. This situation caused an unsmooth experimental curve as shown in the curve labeled observation 1 of figure 5.28.

Observation 2

On cooling below the critical temperature in some runs the tracking program locked onto some peak other than the desired 1s peak and showed aberrant behavior on continued cooling. The curve labeled observation 2 of figure 5.28 shows a behavior of this sort. No further investigation was done to identify the spurious signal.

Observation 3

If the situation in observation 2 did not occur, the peak emerging after the critical condition is the 1s peak[3]. At still lower temperatures, however this is lost intermitentally to a companion peak which grows in amplitude beyond that of the 1s peak. The partial history of the scanned signal is depicted in the plots of figures 5.29 and 5.30 which show the splitting of the tracked peak. The scans are shown in proper time order but those for which the peak is single are mainly omitted. Curves 4 and 5 of figure 5.29 show the onset of splitting. As the system moved away from the critical point

---

[3] Based on the technique used in this work one cannot say confidently what the emerged peaks are. The only sure way to solve this is to collect all peaks in the entire frequency range (from 0 to 10,000 khz) and observe the relationships among them. This, however, was beyond the scope of this work. Other work in this laboratory, however, is directed to this problem.

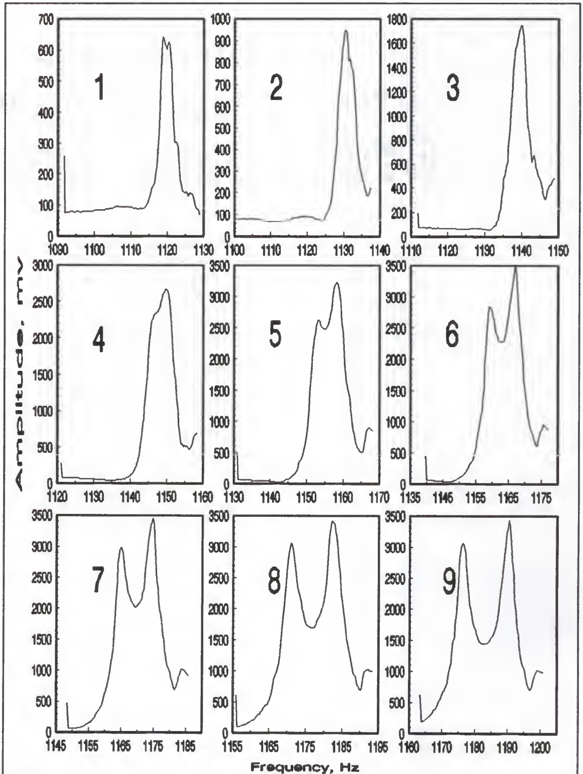

Figure 5.29. Movement of tracked peak and its neighbor below the critical temperature. These curves are numbered in the proper time sequence but many curves showing only one strong peak have been omitted.

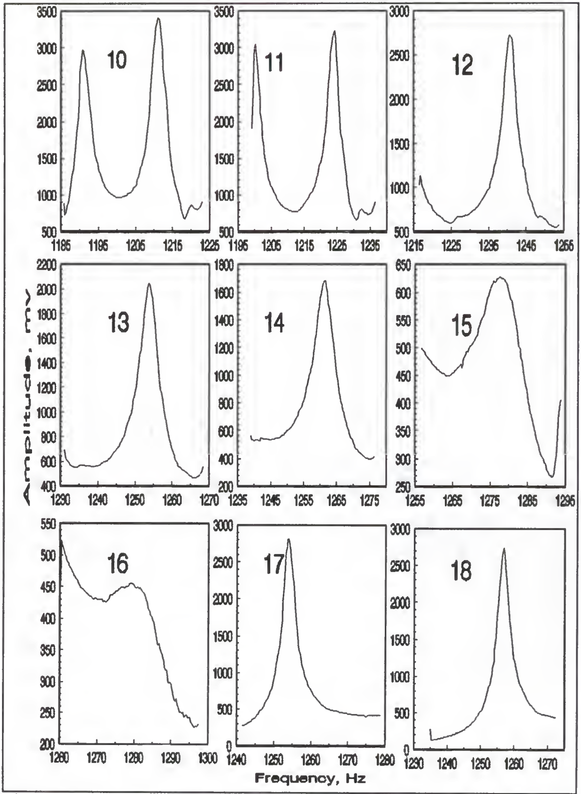

Figure 5.29. Continued movement of tracked peak and its neighbor below the critical temperature.

the separation of these two peaks increased (curves 6 through 11 of figure 5.29.) The right hand peak (peak one) was bigger and moved faster than the left peak (peak two.) It moved so fast that peak two was eventually out of the sweep range (see curve 12 of figure 5.29.) This single peak remained strong until the temperature was around 31 °C. At that temperature the other peak (possibly peak two) reappeared in the sweep range (curves 15 and 16 of figure 5.29.) It was at this time

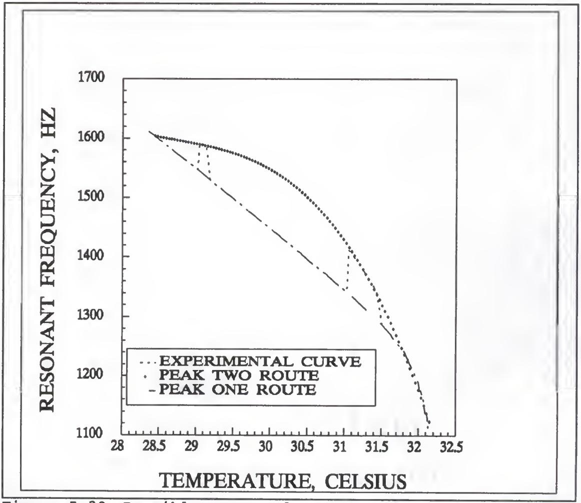

Figure 5.30. Possible routes of movement of two neighbor peaks (peak one and peak two) below the critical temperature.

stronger than peak one leading to switching of the tracked peak from peak one to peak two. The window then shifted from peak one which became lost. The peak in curve 16 is peak one but that of curve 17 is peak two. This is apparently so since the peak in curve 17 is lower in frequency than the peak in curve 16.) The reverse of this phenomenon happened around 29.5 °C where peak one re-entered the window as the dominant signal. Finally, these two peaks merged together at around 29 °C. Data were not collected below about 29 °C, so the subsequent behavior of these peaks was not observed. This type of behavior is interesting and unexpected, but it is not central to the objective of the present research. It is probably associated with the fact that below the critical temperature there are two phases present and their relative proportions in the resonator cavity change according to the effects of the magnetically driven circulating pump.

The plausible routes of these two peaks based on the above situations are depicted in figure 5.30. A full interpretation of these phenomena would require further experimentation to characterize the contents of the cavity in the two phase region. In the early stage of phase separation the bubbles or dew drops are believed to be small and entrained in the dominant phase as foam or fog, so the location of the phase transition is not obscured by massive phase separations which occur well away from the phase boundary.

Observation 4

An attempt at running the experiment with ascending temperature was made. The same uncertainties about phase distribution obscures the identify of the peak selected for tracking. The possibility of selecting a peak which evolves irregularly or fades into the background exists. The curve labeled observation 4 in figure 5.28 shows this type of observation.

## Curve Fitting

Over a small temperature interval in the critical vicinity the task of single peak tracking is quite severe, and the peak is often lost. This is due to two main effects. First, in terms of dynamics, the rate of decrease in resonance frequency, hence speed of sound, with respect to temperature is extremely high approaching infinity, i.e. the speed of sound exhibits a mathematical singularity at the critical point. Second, the amplitude of the tracked peak decreases dramatically toward zero or at least below the noise level of the system. As a consequence, an ambiguity of the critical point arises. In order to solve this problem a mathematical model describing the relationship between the speed of sound and temperature near the critical was applied. This model was originally derived by Stell et. al.(133) to fit data of latent heat of vaporization and temperature and later modified to satisfy a corresponding states principle by Sivaraman et. al.(134,135) and applied to speed of sound data by the same

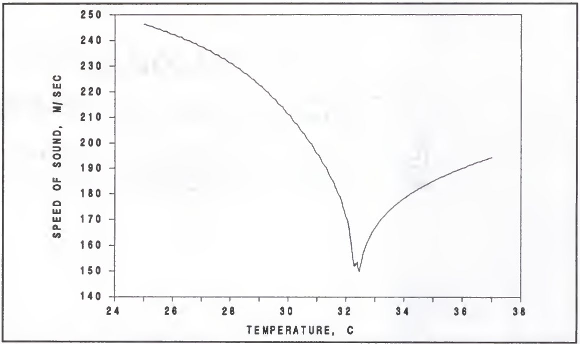

Figure 5.31. Experimental curve of ethane showing dynamic behavior of speed of sound near critical point.

author. It has a root from rigorous mathematical derivations by Wegner[(136)] and further by Green and Ley-koo[(137,138)] based on renormalization group theory.

$$\frac{C}{\sqrt{\frac{(R)(T_c)}{M}}} = A_1 T_r^{\beta} + A_2 T_r^{\beta+\Delta} + A_3 T_r^{1-\alpha+\beta} + A_4 T_r + A_5 T_r^2 + A_6 T_r^3 \qquad (5)$$

where $C$ = Speed of sound, m/sec

$R$ = Gas constant, J/sec

$T_c$ = Critical Temperature, K

$M$ = Molecular mass, Kg/mole

$A_i$ = Equation coefficients

$T_r$ = Reduced Temperature

$\alpha$, $\beta$, $\Delta$ = Critical exponents.

To fit this non linear equation to experimental data of speed of sound and temperature, eleven system-dependent coefficients must first be searched. This task was accomplished by the simplex mathematical optimization technique. (A computer program written by the author for this purpose is given in appendix C.) In general the experimental data of speed of sound and corresponding system temperature were divided into two parts according to temperature. The first one is all data at temperatures above the critical temperature (roughly estimated from the literature value.) The second one is all data at temperature below the critical temperature. Each data set was independently fitted to the above equation resulting in a set of eleven coefficients.

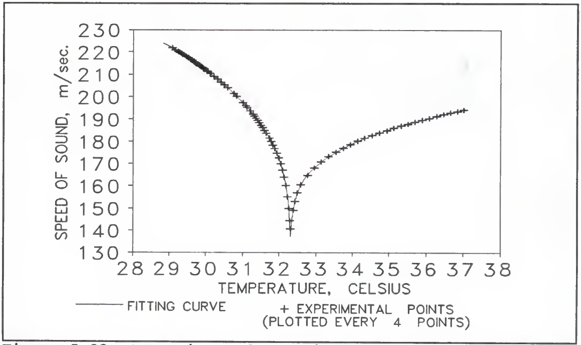

Figure 5.32. Comparison of experimental data for the ethane and curve generated by renormalization group theory equation.

Temperature and speed of sound at the intersection of these two smooth curves were treated as turning-point parameters of the corresponding experimental data set. Table 5.11 shows results of searching coefficients of experimental data shown in figure 5.31 by the simplex optimization program. Figure 5.32 compares the experimental data and fitting curve generated by this method for ethane at the critical density. Note that in this figure only one-forth of the experimental points were plotted to preserve picture clarity. Clearly, this equation represents very well the behavior of the speed of sound in the vicinity of the critical point. Furthermore, it also yields an equally satisfactory result for the mixture of carbon dioxide and ethane described in the previous section.

Table 5.11. Coefficients Obtained by Simplex Optimization Method.

| Coefficients | High Temperature Side | Low Temperature Side |
|---|---|---|
| $A_1$ | 11.95399178 | 4.4228669 |
| $A_2$ | -897.98691534 | 360.1419335 |
| $A_3$ | -3400.8303361 | 2448.9833655 |
| $A_4$ | 2976.6473117 | -1666.3105786 |
| $A_5$ | 7325.7816766 | -7444.4800181 |
| $A_6$ | -56033.5889588 | 52720.3509156 |
| $T_c$ | 305.3979294 | 305.9057717 |
| $\alpha$ | 0.1250001 | 0.1250000 |
| $\beta$ | 0.3333333 | 0.3333333 |
| $\Delta$ | 0.5000000 | 0.5000000 |

## Three Dimensional Phase Diagram

Conventionally the phase diagram in three dimensions is represented by using parameters of temperature, pressure, and molar volume leading to three well-known two dimensional projections: isotherm, isobar, and isochore curves. Figure 3.1 illustrates an example of this type of plot for a typical pure fluid. The critical point is located at the top of a coexistence curve. It can be found by a null change of slope in the critical isotherm or isobar or by a smooth curve without break in the critical isochore. These are among the traditional indicators, but their response to the critical point is not highly sensitive.

For more accurate measurements a more sensitive indicator is needed. The sonic speed or cavity resonance frequency serves nicely for this purpose due to their dramatic change at the critical point. Replacing molar volume by speed of sound in the conventional phase diagram plot leads to a pyramid shape curve as shown in figure 5.33 for a mixture of carbon dioxide and ethane. Exploring in a much narrower range of temperature around the critical point leads to an outstanding tornado shape curve as shown in figure 5.34 for ethane. These two curves were constructed from experimental data. The critical point is apparently easily located as an extrumum point on these surfaces. It corresponds to the point of minimum speed of sound, which theoretically speaking, should be zero. In that case P-T-C phase diagram curve would have much more prominent tornado-in-action shape.

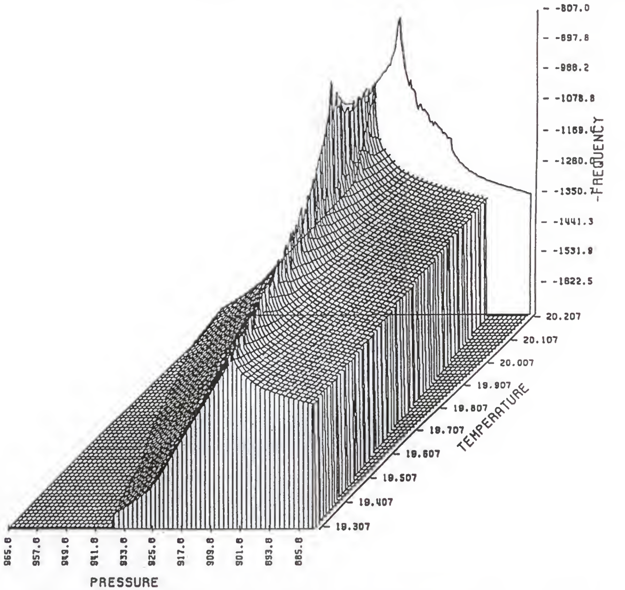

Figure 5.33. Three dimensional phase diagram of a mixture of carbon dioxide and ethane.

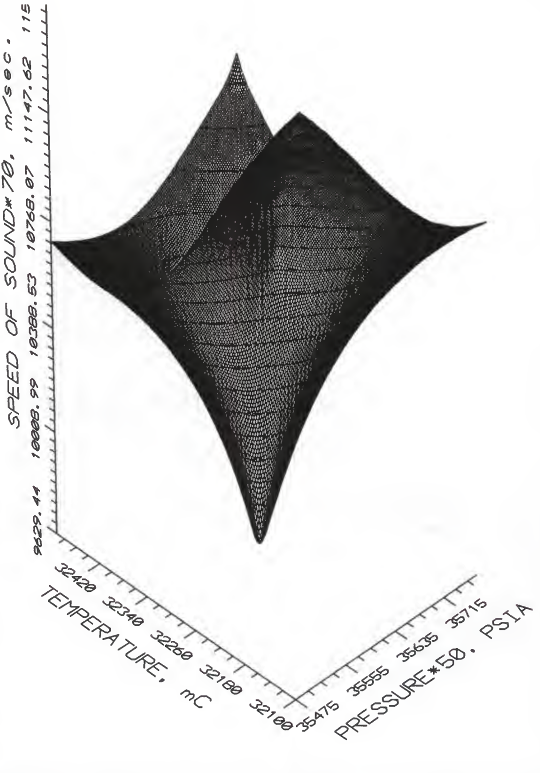

Figure 5.34. Three dimensional phase diagram of ethane.

# CHAPTER 6
# CONCLUSION

A new approach using an acoustic resonance technique for phase boundary detection may be summarized as follows:

1. Measure several resonance frequencies of standing acoustic waves excited inside a fluid filled spherical acoustic cavity.

2. Identify each resonance frequency.

3. Track an assigned resonance frequency as system parameters such as temperature, pressure, or density are varied.

4. Locate phase equilibria by abrupt changes in resonance frequency (hence speed of sound) as the system state traverses a phase boundary.

5. Locate critical points as minima on (P,T,C) or ($\rho$,T,C) diagrams.

The principal results of this work are tabulated and compared with the available literature values in table 6.1. Apparently, the present results are in good agreement with established literature values, proving the viability of this new technique. The largest discrepancy is in the system consisting of a $CO_2$-$C_2H_6$ mixture. This is not surprising inasmuch as the literature value was obtained by extrapolation of the reported experimental data and thus is subject to greater uncertainty. This comparison is intended principally to show the capability of the acoustic method to detect the critical point of the more complicated system and should be judged more on the precision than the accuracy of the outcome since the basis for judging the latter is not sufficiently strong.

Generally speaking, considering the results for pure gases, even though the values of this work are not all within the reported uncertainty of the literature values, the work should not be judged a failure. In the first place the maximum disparity between the different methods is only 1 mK, and an increase in the estimated limits of uncertainty of only ±1 mK would bring the divers results into accord. There are reasons, however, to suspect that the present results may be more reliable. Consider, for example, the conventional method of detecting the critical point. This involves the direct observation of the transition from two phases to one, with the critical state taken to be the single condition for which the meniscus disappears when the volumes of liquid and vapor are just the same. Ideally, critical points would be determined by the direct observation of this phenomena at the exact middle of the cylindrical sample cell. Realistically, such a measurement is experimentally impracticable(96) and the appearance of the meniscus elsewhere is used as a to determine the critical parameters. In practice these are determined by interpolation of data taken when the meniscus appears just above and just below the middle of the cell. This method is then subject to an heuristic effect. Besides, near the critical condition the phenomena of critical opalescence (light scattering effect) may obscure the observation to some extent. In the acoustic method, the instrument is generally capable of measuring frequencies with an accuracy of at least 1 mHz. In the course of these experiments data were taken over a 4 K range around the critical temperature over a period of twelve hours. The recorded data show that nearest the observed critical state the temperature gradient of resonance frequency exceeds 2000 Hz/K on both sides of the frequency minimum for which the corresponding temperature was taken as a critical temperature. A remarkably abrupt change in frequency is evident. The sharpness of this turning point together with the stated precision of frequency measurements illustrates how the present technique can locate the extremum to a resolution of about one part per million in the temperature. Demonstrating this fact was indeed the principal goal of this research. That the acoustic resonance method is vastly more sensitive (ca. three orders of magnitude) than the visual method is far more important than whether of not the accuracy of temperature measurement at a small poorly funded university laboratory is

Table 6.1. Comparison of Critical Temperatures and Pressures.

| No. | System | Critical Temperature (K) | | Percent Different | Sources |
|---|---|---|---|---|---|
| | | This work | Literature | | |
| 1 | Carbon Dioxide | 304.215 ±0.007 | 304.206 ±0.001 | 0.003 | Morrison & Kincaid (1984) |
| 2 | Ethane | 305.370 ±0.007 | 305.379 | -0.003 | Morrison (1981) |
| 3 | 74.25 mole % $CO_2$<br>25.75 mole % $C_2H_6$ | 293.134 ±0.007 | 293.072* | 0.021 | Morrison & Kincaid (1984) |
| | | Critical Pressure Psia | | | |
| 1 | Carbon dioxide | 1069.23 ±3.00 | 1070.96 ±0.01 | -0.01 | Morrison & Kincaid (1984) |
| 2 | Ethane | 707.78 ±3.00 | 707.8 ±0.1 | -0.002 | Khazanova & Sominskaya (1971) |
| 3 | 74.25 % mole $CO_2$<br>25.75 % mole $C_2H_6$ | 916.76 ±3.00 | N/A | N/A | N/A |

* Extrapolated value.

comparable to that at the major standards laboratory of the nation. Given equivalency of thermometric accuracy, the new method of critical point determination is clearly superior and is a good candidate to become the method of choice in future studies. Even so improvements are possible and some of these are being incorporated in the next generation version of this apparatus. The major change will be the inclusion of a volume change capability so that data can be taken isothermally or isobarically as well as isochorically.

The spherical resonator is a remarkably accurate and convenient tool for the measurement of thermophysical properties of fluids. The speed of sound in a gas of interest can be measured with high accuracy merely by measuring the frequencies of the radial normal modes of vibration. A relative measurement against a reference gas such as argon further simplified the procedure. This technique offers a proven alternative experimental approach to valuable physical properties including phase boundaries, thermodynamic properties and equation of state parameters, all of which are useful to both pure and applied science. Applications are numerous and only now beginning to be explored. One important application is indirectly determining the intermolecular potentials of fluids from acoustic virial coefficients via an inversion technique without using the parameter optimization techniques for model potentials such as Lennard-Jones. Accurate sonic speed data as a function of temperature of both pure fluids and mixtures would be useful source of this information. The properties of bulk matter derive ultimately from the interactions between its molecules, and information about these interactions supports the development of useful correlations and of statistical mechanics in general.

It is apparent from this work and others that the natural vibrations of fluid masses convey a vast storehouse of encoded information. Learning to acquire and interpret that information is the long range goal of this laboratory.[4]

---

[4] Some work has already begun. See reference 139.

# APPENDIX A
# CHARGING PRESSURE CALCULATIONS

Since in this work data were collected in the isochoric mode, the density of the system was constant throughout each run as well. To locate the critical without further addition of gas required that the initial runs be made on samples at supercritical densities. Density was not directly measured but was infered from the AGA8 equation of state$^{(5)}$; therefore the starting conditions were specified by composition, temperature, and pressure. The procedures followed:

Pure Fluid (Carbon dioxide or Ethane)

1. Obtain literature values of the critical point parameters ($T_c$, $P_c$, $\rho_c$.)

2. Use the AGA8 equation to calculate a series of densities corresponding to varying pressures in the vicinity of the critical pressure at a charging temperature which must be higher than the critical temperature by about five to seven degrees celsius. This set of densities should span the critical density.

3. Plot the calculated densities as a function of the corresponding charging pressures, then apply a suitable curve fit regression, generally polynomial of the nth order, to these data.

4. Charging pressure corresponding to literature critical density is now calculated from the best curve fitting equation found in step 3. This value plus about 10 psia is taken as a charging pressure of fluid at the starting temperature. The extra 10 psia is added as a safety factor due to the possibility of error in the literature critical density.

Fluid Mixture

1. Decide on the composition of carbon dioxide-ethane mixture to be studied.

2. Approximate charging pressure at starting temperature from closest literature critical point parameters available.

3. Calculate the density of the gas mixture corresponding to the charging pressure estimated in step 2 at the starting temperature and mole fractions of carbon dioxide and ethane using the AGA8 equation.

4. Calculate the density of ethane from the density of the gas mixture obtained from step 3.

5. Follow procedures in step 2 to 4 for a pure fluid. The calculated density obtained in step 3 for this procedure is taken as the literature critical density called for in step 4 of pure fluid. The resulting pressure is taken as the target charging pressure of ethane.

6. Ethane was charged first to the pressure calculated in the previous step. Carbon dioxide was subsequently introduced to the resonator while mixing until the desired total pressure was obtained (estimated value in step 2.)

# APPENDIX B
# QUANTITATIVE ANALYSIS OF GAS MIXTURE

Reported values of critical point parameters for gas mixtures are meaningless unless accompanied by their quantitative compositions. For this particular mixture of carbon dioxide and ethane two methods were used for quantitative analysis: a gravimetric method for carbon dioxide and a gas chromatography method for ethane. Carbon dioxide was not analyzed by the latter method due to an unavailability of a suitable detector during the course of analysis. The assumption used through out this analysis was that there were no significant impurities since the mixture was carefully prepared in this laboratory from highly pure gases.

## Gravimetric Method

Carbon dioxide reacts with base to form carbonate salt which readily dissolves in water as shown in the following chemical equation:

$$CO_2 + 2\ OH^- = CO_3^{2-} + H_2O$$

The difference between weights of reaction vessels before and after carefully passing carbon dioxide is the weight of the gas. The weight of ethane was calculated by subtracting the measured weight of carbon dioxide from the weight of the sample.

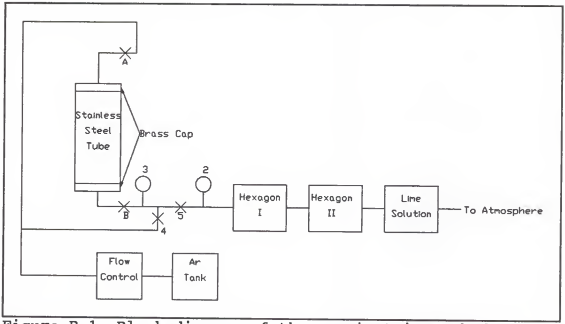

Figure B.1. Block diagram of the gravimetric method.

A block diagram of the experimental setup is shown in figure B.1. A gas sampling container was made from a stainless steel tube provided with high pressure needle valves A and B. The experiment started with pre-conditioning the system by flowing argon gas to the reaction vessels (hexagonal absorber array [5], see figure B.2) through valves 4 and 5 for one-half hour. After that valves 4 and 5 were closed followed by opening valve B. The pressure of gas in the gas sampling container was shown on gauge 3 (typical pressure was around 1200 psia.) Then valve 5 was opened carefully to bleed gas

---

[5] The hexagon absorber arrays of vertical tubes each having a wash board shape were designed to prolong contact time of gas with absorbant to assure completeness of the reaction. Each section of the first five tubes was filled with 1M NaOH. The last tube was filled with drierite (moister absorbent.)

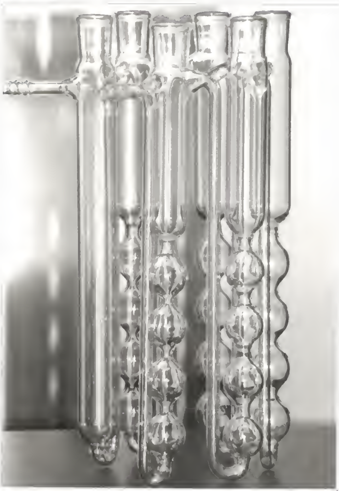

Figure B.2. The hexagon reaction vessel for a gravimetric analysis.

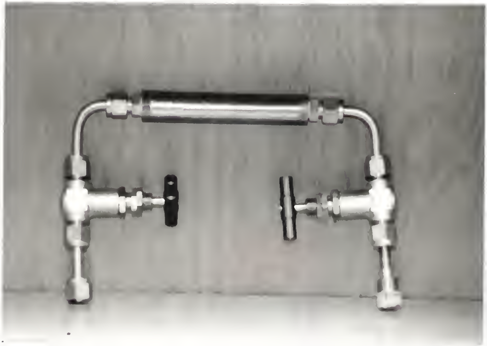

Figure B.3. The high pressure gas sampling container.

slowly to the hexagon reaction vessels. Opening of valve 5 was judged from the rate of bubbles rising up in the absorber tubes. If valve 5 was opened too wide, carbon dioxide gas would not have time to react efficiently with sodium hydroxide in the absorber. The completeness of the reaction was checked by passing exiting gas from the second absorber array through a lime water, saturated $Ca(OH)_2$ solution. Turbidity of the solution due to forming of $CaCO_3$ indicates incompleteness of the reaction. Once bubbles stopped rising up (about 2-3 hours) argon was delivered to the system through valve A to flush out all sample gas remaining in the lines for one-half hour. After that, screw clamps of the entrance and exit tygon tubes to the absorber array were tightly closed. The vessels were disconnected from the system and weighed on an analytical balance. During the entire course of these experiments the lime solution remained clear. The total absorption time was about 3-4 hours. Note that before analyzing the sample gas a blank test was performed by continuously flowing argon through the system for 3-4 hours. No significant change in weight (comparable with the uncertainty of the balance, 1 mg.) of the absorbers before and after passing argon was observed. Despite its tedious procedure this method worked reasonably well, provided that sufficient care was exercised.

### Gas Chromatography Method

Description of standard procedures for performing gas chromatography can be found elsewhere.(140,141) A calibration curve for ethane was made first using pure ethane. Both calibration and sample analysis were performed on the same day basis to minimize errors. Details of the equipment and optimized conditions, which were determined by trial and error methods, are summarized as follows:

Gas chromatograph: Varian model 3700

Syringe: Pressure-Lock gas syringe series A with side port. Dynatech Precision Sampling Corporation.

Column: Fused silica megabore column GSQ, 0.53 mm i.d., 30 m long, open tubular. J&W Scientific.

Optimized conditions:

Temperature(°C) - Injector: 100
- Flame Ionization Detector: 100
- Column : 80

Flow rate(ml/min) - Helium : 6
- Hydrogen : 30
- Air : 300

Count rate on the integrator : 12,000 cpm.

Sample results of calibrations are summarized in table B.1. Figure B.3 shows the calibration curve for ethane.

Table B.1. Data for calibration curve of ethane.

| No.of repetitions | Attenuation factor | No.of counts | No.of adjusted counts | Volume of gas injected, μl |
|---|---|---|---|---|
| 5 | 32 | 414±52 | 13±2 | 5.0 |
| 6 | 256 | 192±9 | 48±2 | 15.0 |
| 6 | 256 | 399±7 | 100±2 | 15.0 |
| 7 | 1024 | 131±5 | 131±5 | 20.0 |
| 6 | 1024 | 188±2 | 188±2 | 25.0 |
| 5 | 1024 | 252±4 | 252±4 | 30.0 |
| 6 | 1024 | 310±2 | 310±2 | 35.0 |
| 6 | 1024 | 367±2 | 367±2 | 40.0 |
| 6 | 1024 | 423±2 | 423±2 | 45.0 |
| 6 | 1024 | 483±2 | 483±2 | 50.0 |

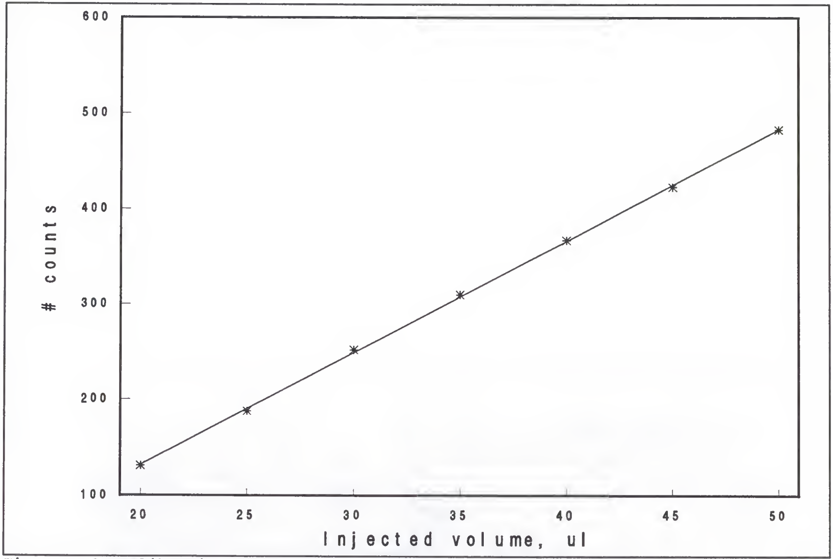

Figure B.4. Calibration curve of ethane for gas chromatography.

# APPENDIX C
# SIMPLEX

There are three programs for searching for minimum points of speed of sound (points along coexistence curve). The first is the simplex optimization program used to search for eleven coefficients in an equation (5). The second program is used to calculate speed of sound with coefficients found in program one. The last program finds the common point of two curves generated from programs one and two.

## Program I. Simplex Optimization

```
C234567
      IMPLICIT REAL*8 (A-H,O-Z)
      DIMENSION C(4000),T(4000),B(20,20)
      DIMENSION SSRSD(500)
      WRITE(*,*) 'INPUT MOLECULAR WEIGHT IN KG/MOLE'
      READ (*,*) W
      OPEN (10,FILE='DATA.RAW',STATUS='OLD')
      L=1
 20   READ(10,*,END=30) T(L),C(L)
      L=L+1
      GOTO 20
 30   CLOSE(10)
      L=L-1
      WRITE(*,*) 'L=',L
      WRITE(*,*) 'W=',W
      OPEN (40,FILE='INITIAL.DAT',STATUS='OLD')
      READ(40,*) ((B(I,J),I=1,10),J=1,11)
      CALL INITLCOOR (B,SSRSD,L,T,C,W)
      OPEN (5,FILE='START.DAT',STATUS='NEW')
       DO 80 J=1,11
        DO 90 I=1,10
         WRITE (5,*) B(I,J)
 90   CONTINUE
         WRITE (5,*) 'SSRSD',J,'=',SSRSD(J)
         WRITE (5,*) '  '
 80   CONTINUE
```

```
      CLOSE(5)
   50 IF (SSRSD(1).LT.1.0E-17) THEN
C         WRITE(*,*) 'FIN CON 1'
        GOTO 100
      END IF
      CALL SHELL(B,SSRSD,WORST)
      CHECKER=CHECKER+SSRSD(1)
      KOUNT=KOUNT+1
C      WRITE(*,*) '*************************KOUNT=',KOUNT
      KKOUNT=KKOUNT+1
      IF (KKOUNT.EQ.300) THEN
C      IF (KKOUNT.EQ.200) THEN
        KKOUNT=0
        CHECKER=(CHECKER/300.0)-SSRSD(1)
C         CHECKER=(CHECKER/200.0)-SSRSD(1)
        IF (CHECKER.LT.1.00000E-17) THEN
C         IF (CHECKER.LT.1.0E-16) THEN
          GOTO 100
        END IF
        CHECKER=0.0
      END IF
      IF (SSRSD(11).EQ.WORST) THEN
C         WRITE(*,*) 'FLAG RAISED FLAG RAISED FLAG RAISED'
       Z=SSRSD(10)
       SSRSD(10)=SSRSD(11)
       SSRSD(11)=Z
       DO 140 J=1,10
         ZZ=B(J,10)
         B(J,10)=B(J,11)
         B(J,11)=ZZ
  140  CONTINUE
      END IF
C      WRITE(*,*) 'START REFLEX'
      CALL REFLEX (SSRSD,B,L,T,C,W)
C      WRITE(*,*) 'PASS REFLEX'
      IF (SSRSD(13).LT.SSRSD(1)) THEN
       CALL EXPAND(B,SSRSD,C,T,L,W)
C        WRITE(*,*) 'PASS EXPAND'
       GOTO 50
      ELSE IF (SSRSD(13).GT.SSRSD(1).AND.
     CSSRSD(13).LT.SSRSD(10)) THEN
       SSRSD(11)=SSRSD(13)
       DO 70 I=1,10
        B(I,11)=B(I,13)
   70  CONTINUE
C        WRITE(*,*) 'PASS BETWEEN'
       GOTO 50
      ELSE IF (SSRSD(13).GT.SSRSD(10)) THEN
       IF (SSRSD(13).LT.SSRSD(11)) THEN
        CALL CNTR(B,SSRSD,C,T,L,W)
C         WRITE(*,*) 'PASS CNTR'
       ELSE IF (SSRSD(13).GT.SSRSD(11)) THEN
```

```
          CALL CNTW(B,SSRSD,C,T,L,W)
C           WRITE(*,*) 'PASS CNTW'
         END IF
         GOTO 50
        END IF
        CLOSE(40)
  100 OPEN (60,FILE='COOR.OUT',STATUS='NEW')
         DO 800 J=1,11
          DO 900 I=1,10
           WRITE (60,*) B(I,J)
  900 CONTINUE
           WRITE (60,*) 'SSRSD',J,'=',SSRSD(J)
           WRITE (60,*) '  '
  800 CONTINUE
      WRITE(60,*) 'NUMBER OF ITERATIONS = ',KOUNT
      CLOSE(60)
      STOP
      END
C
C
C
      SUBROUTINE INITLCOOR (B,SSRSD,L,T,C,W)
      IMPLICIT REAL*8 (A-H,O-Z)
      DIMENSION B(20,20),T(4000),C(4000),SSRSD(500),A(10)
      DO 10 I=1,11
       DO 20 J=1,10
        A(J)=B(J,I)
   20  CONTINUE
       A1=A(1)
       A2=A(2)
       A3=A(3)
       A4=A(4)
       A5=A(5)
       A6=A(6)
       TC=A(7)
       ALPHA=A(8)
       BETA=A(9)
       DELTA=A(10)
       CALL RESIDUAL(A1,A2,A3,A4,A5,A6,TC,ALPHA,BETA
     C,DELTA,C,T,L,ST,W)
       SSRSD(I)=ST
C       WRITE(*,*) 'SSRSD',I,'=',SSRSD(I)
 10   CONTINUE
      RETURN
      END
C
C
C
      SUBROUTINE RESIDUAL(A1,A2,A3,A4,A5,A6,TC,ALPHA,BETA
     C,DELTA,C,T,L,ST,W)
       IMPLICIT REAL*8 (A-H,O-Z)
      REAL*8 DABS,DSQRT
      DIMENSION C(4000),T(4000)
      GAS=8.3144
C       W=40.539/4000.0
C       W=0.040441
      CON=GAS*TC/W
      ST=0.0
      DO 10 I=1,L
        TR=DABS((T(I)-TC)/TC)
        RS=(C(I)/DABS(DSQRT(CON)))-(A1*TR**BETA+A2*TR**(BETA
     C+DELTA)+A3*TR**(1.0-ALPHA+BETA)+(A4*TR)+(A5*TR**2.0)
     C+(A6*TR**3.0))
C          WRITE(*,*) 'RS=',RS
        RS=RS**2
        ST=ST+RS
 10   CONTINUE
      RETURN
      END
C
C
C
      SUBROUTINE REFLEX (SSRSD,B,L,T,C,W)
      IMPLICIT REAL*8 (A-H,O-Z)
      REAL*8 DSQRT
      DIMENSION B(20,20),C(4000),T(4000),SSRSD(500),A(10)
      DO 10 J=1,10
       CUM=0.0
       DO 50 I=1,10
         CUM=CUM+B(J,I)
  50   CONTINUE
       B(J,12)=CUM/10.0
       B(J,13)=B(J,12)+(B(J,12)-B(J,11))
  10  CONTINUE
      DO 200 I=12,13
 350   DO 300 J=1,10
        A(J)=B(J,I)
 300   CONTINUE
       A1=A(1)
       A2=A(2)
       A3=A(3)
       A4=A(4)
       A5=A(5)
       A6=A(6)
       TC=A(7)
       ALPHA=A(8)
       BETA=A(9)
       DELTA=A(10)
C      IF (I.EQ.13.AND.TC.LT.292.15) THEN
C       WRITE(*,*) 'LOWER BOUNDARY LOWER BOUNDARY'
C        TC=292.15
C        FACTOR=(TC-B(7,11))/(B(7,13)-B(7,11))
C        DO 600 J=1,10
C         B(J,13)=FACTOR*(B(J,13)-B(J,11))+B(J,11)
```

```
C 600    CONTINUE
C        GOTO 350
C        ELSE IF (I.EQ.13.AND.TC.GT.294.15) THEN
C       WRITE(*,*) 'UPPER BOUNDARY UPPER BOUNDARY'
C        TC=294.15
C         FACTOR=(TC-B(7,11))/(B(7,13)-B(7,11))
C        DO 700 J=1,10
C         B(J,13)=FACTOR*(B(J,13)-B(J,11))+B(J,11)
C 700    CONTINUE
C        GOTO 350
C       END IF
       CALL RESIDUAL(A1,A2,A3,A4,A5,A6,TC,ALPHA,BETA
     C ,DELTA,C,T,L,ST,W)
       SSRSD(I)=ST
C       WRITE(*,*) 'SSRSD',I,'=',SSRSD(I)
 200  CONTINUE
      RETURN
      END
C
C
C
      SUBROUTINE SHELL(B,SSRSD,WORST)
      IMPLICIT REAL*8 (B,D-H,O-Z)
      DIMENSION SSRSD(500),B(20,20)
      INTEGER A,C
      WORST=SSRSD(11)
C      WRITE(*,*) 'SHELL'
      J=1
      N=11
      M=N
 90   IF (M.GE.1) THEN
       J=1
       M=M/2
       K=N-M
 50    IF (J.EQ.1) THEN
        J=0
        DO 60 I=1,K
         L=I+M
         IF (SSRSD(I).GT.SSRSD(L)) THEN
          V=SSRSD(I)
          SSRSD(I)=SSRSD(L)
          SSRSD(L)=V
          DO 70 C=1,10
           W=B(C,I)
           B(C,I)=B(C,L)
           B(C,L)=W
 70       CONTINUE
          J=1
         END IF
 60     CONTINUE
        GOTO 50
       END IF
       GOTO 90
      END IF
C      DO 900 I=1,11
C       WRITE(*,*) SSRSD(1)
C  900 CONTINUE
      RETURN
      END
C
C
C
      SUBROUTINE EXPAND(B,SSRSD,C,T,L,W)
      IMPLICIT REAL*8 (A-H,O-Z)
      DIMENSION B(20,20),C(4000),T(4000),SSRSD(500),A(10)
      DO 10 I=1,10
        B(I,14)=B(I,13)+(B(I,12)-B(I,11))
 10   CONTINUE
       DO 30 K=1,10
        A(K)=B(K,14)
 30    CONTINUE
       A1=A(1)
       A2=A(2)
       A3=A(3)
       A4=A(4)
       A5=A(5)
       A6=A(6)
       TC=A(7)
       ALPHA=A(8)
       BETA=A(9)
       DELTA=A(10)
C      WRITE(*,500) A1,A2,A3,A4,A5,A6,TC,ALPHA,BETA,DELTA
C 500   FORMAT (1X,7F8.2,3F4.2)
       CALL RESIDUAL(A1,A2,A3,A4,A5,A6,TC,ALPHA,BETA
     C ,DELTA,C,T,L,ST,W)
       SSRSD(14)=ST
C       WRITE(*,*) 'SSRSD',I,'=',SSRSD(I)
      IF (SSRSD(14).LT.SSRSD(13)) THEN
       SSRSD(11)=SSRSD(14)
       DO 20 J=1,10
         B(J,11)=B(J,14)
  20   CONTINUE
      ELSE IF (SSRSD(14).GT.SSRSD(13)) THEN
       SSRSD(11)=SSRSD(13)
       DO 50 J=1,10
         B(J,11)=B(J,13)
  50   CONTINUE
      END IF
      RETURN
      END
C
C
C
C
```

```
      SUBROUTINE CNTR(B,SSRSD,C,T,L,W)
      IMPLICIT REAL*8 (A-H,O-Z)
      DIMENSION B(20,20),C(4000),T(4000),SSRSD(500),A(10)
      DO 10 I=1,10
        B(I,14)=B(I,12)+0.5*(B(I,12)-B(I,11))
 10   CONTINUE
       DO 30 K=1,10
        A(K)=B(K,14)
 30    CONTINUE
       A1=A(1)
       A2=A(2)
       A3=A(3)
       A4=A(4)
       A5=A(5)
       A6=A(6)
       TC=A(7)
       ALPHA=A(8)
       BETA=A(9)
       DELTA=A(10)
C      WRITE(*,500) A1,A2,A3,A4,A5,A6,TC,ALPHA,BETA,DELTA
C 500   FORMAT (1X,7F8.2,3F4.2)
       CALL RESIDUAL(A1,A2,A3,A4,A5,A6,TC,ALPHA,BETA
     C ,DELTA,C,T,L,ST,W)
       SSRSD(14)=ST
       SSRSD(11)=SSRSD(14)
       DO 20 J=1,10
         B(J,11)=B(J,14)
  20   CONTINUE
      RETURN
      END
C
C
C
      SUBROUTINE CNTW(B,SSRSD,C,T,L,W)
      IMPLICIT REAL*8 (A-H,O-Z)
      DIMENSION B(20,20),C(4000),T(4000),SSRSD(500),A(10)
      DO 10 I=1,10
        B(I,14)=B(I,12)-0.5*(B(I,12)-B(I,11))
 10   CONTINUE
       DO 30 K=1,10
        A(K)=B(K,14)
 30    CONTINUE
       A1=A(1)
       A2=A(2)
       A3=A(3)
       A4=A(4)
       A5=A(5)
       A6=A(6)
       TC=A(7)
       ALPHA=A(8)
       BETA=A(9)
       DELTA=A(10)
```

```
C      WRITE(*,500) A1,A2,A3,A4,A5,A6,TC,ALPHA,BETA,DELTA
C 500   FORMAT (1X,7F8.2,3F4.2)
       CALL RESIDUAL(A1,A2,A3,A4,A5,A6,TC,ALPHA,BETA
     C ,DELTA,C,T,L,ST,W)
       SSRSD(14)=ST
       SSRSD(11)=SSRSD(14)
       DO 20 J=1,10
         B(J,11)=B(J,14)
  20   CONTINUE
      RETURN
      END
```

### Program II. Speed of Sound Calculations

```
C234567
      IMPLICIT REAL*8 (A-H,O-Z)
      REAL*8 DABS,DSQRT
      DIMENSION C(4000),T(4000),A(12)
      OPEN (60,FILE='COOR.OUT',STATUS='OLD')
      DO 70 I=1,10
       READ (60,*) A(I)
C       WRITE(*,*) A(I)
 70   CONTINUE
      CLOSE(60)
      A1=A(1)
      A2=A(2)
      A3=A(3)
      A4=A(4)
      A5=A(5)
      A6=A(6)
      TC=A(7)
      ALPHA=A(8)
      BETA=A(9)
      DELTA=A(10)
      OPEN (10,FILE='DATA.RAW',STATUS='OLD')
      OPEN (40,FILE='TC.DAT',STATUS='NEW')
      L=1
 30   READ(10,*,END=20) T(L)
c      WRITE(*,*) T(L)
      L=L+1
      GOTO 30
 20   CLOSE(10)
      L=L-1
      GAS=8.3144
C      W=0.040441
      W=0.03007
      CON=GAS*TC/W
      DO 50 I=1,L
        TR=DABS((T(I)-TC)/TC)
C        WRITE(*,*) 'TR=',TR
       C(I)=DSQRT(CON)*(A1*TR**BETA+A2*TR**(BETA
     C+DELTA)+A3*TR**(1.0-ALPHA+BETA)+A4*TR+A5*TR**2.0
     C+A6*TR**3.0)
       WRITE(40,*)  T(I), C(I)
C       WRITE(*,*)  T(I), C(I)
 50   CONTINUE
      CLOSE(40)
      STOP
      END
```

## Program III. Crossing-Point Searching

```
c234567
      program min
      CHARACTER*20 U,V
      DOUBLE PRECISION Q,T,S,R,E,F
      DOUBLE PRECISION DEL,DSQRT,DABS,ZERO,TWO,DELE
      DOUBLE PRECISION P2L,P3L,TCL,TL,TRL
      DOUBLE PRECISION P2R,P3R,TCR,TR,TRR,DELF
      DOUBLE PRECISION A1L,A2L,A3L,A4L,A5L,A6L
      DOUBLE PRECISION ALPHAL,BETAL,DELTAL
      DOUBLE PRECISION A1R,A2R,A3R,A4R,A5R,A6R
      DOUBLE PRECISION ALPHAR,BETAR,DELTAR
      DIMENSION A(20), B(20)
      ZERO=0.0D00
      TWO=20.0D-1
      WRITE(*,*) 'RIGHT SIDE FILE NAME'
      READ(*,50) U
 50   FORMAT (A20)
      OPEN (20,FILE=U,STATUS='OLD')
      DO 40 I=1,10
       READ (20,*) A(I)
       WRITE(*,*) A(I)
 40   CONTINUE
      CLOSE(20)
      WRITE(*,*) 'LEFT SIDE FILE NAME'
      READ(*,50) V
      OPEN (30,FILE=V,STATUS='OLD')
      DO 60 I=1,10
       READ (30,*) B(I)
       WRITE(*,*) B(I)
 60   CONTINUE
      CLOSE(30)
      A1R=A(1)
      A2R=A(2)
      A3R=A(3)
      A4R=A(4)
      A5R=A(5)
      A6R=A(6)
      TCR=A(7)
      ALPHAR=A(8)
      BETAR=A(9)
      DELTAR=A(10)
      A1L=B(1)
      A2L=B(2)
      A3L=B(3)
      A4L=B(4)
      A5L=B(5)
      A6L=B(6)
      TCL=B(7)
      ALPHAL=B(8)
      BETAL=B(9)
      DELTAL=B(10)
      WRITE(*,*) 'INPUT TR & TL IN KELVIN'
      READ(*,*) TR, TL
      T=(TR+TL)/TWO
      P2L = BETAL + DELTAL
      P3L = 1.0-ALPHAL+BETAL
      P2R = BETAR + DELTAR
      P3R = 1.0-ALPHAR+BETAR
 10   TRL = DABS((T-TCL)/TCL)
      TRR = DABS((T-TCR)/TCR)
C      write (*,*) trl,trr,p2l,p3l,p2r,p3r
      S=(DSQRT(TCL))*(A1L*TRL**BETAL+A2L*TRL**P2L
     C+A3L*TRL**P3L+A4L*TRL+A5L*TRL**2+A6L*TRL**3)
      R=(DSQRT(TCR))*(A1R*TRR**BETAR+A2R*TRR**P2R
     C+A3R*TRR**P3R+A4R*TRR+A5R*TRR**2+A6R*TRR**3)
      DEL=R-S
      IF (DABS(DEL).LE.1.0D-16) THEN
       GOTO 100
C      ELSE IF (R.GT.S) THEN
      ELSE IF (DEL.GT.ZERO) THEN
       TR=T
       T=(TR+TL)/TWO
       DELE=T-E
       IF (DELE.EQ.ZERO) THEN
        GOTO 90
       END IF
       E=T
       WRITE (*,*) DEL,T,TR
       GOTO 10
C     ELSE IF (R.LT.S) THEN
      ELSE IF (DEL.LT.ZERO) THEN
       TL=T
       T=(TR+TL)/TWO
       DELF=T-F
       IF (DELF.EQ.ZERO) THEN
        GOTO 95
       END IF
       F=T
      WRITE (*,*) DEL,T,TL
      GOTO 10
     END IF
 90  WRITE (*,*) '****',T,E
     GOTO 97
 95  WRITE (*,*) '****',T,F
     GOTO 97
 97  WRITE (*,*) '-->UNABLE TO REFINE FURTHER'
100  WRITE (*,*) T,T-273.15,DEL
     R=R*(SQRT(8.3144/0.03007))
     S=S*(SQRT(8.3144/0.03007))
     WRITE (*,*) R,S
     STOP
     END.
```

# APPENDIX D
# LABORATORY STANDARD PRESSURE GAUGE

## Introduction

Pressure gauges are essential instruments of science and industry and are available in a variety of types. Most of the common types are favored for possessing one or more of the following desirable features: low cost, ease of use, rugged construction, suitability for remote sensing. The attainment of these features is generally facilitated by the use of gauges which measure pressure indirectly. Such gauges require calibration and are, therefore, not suitable for use as primary standards. Unless their calibrations are checked frequently, their readings are always somewhat suspect.

While for most purposes the common gauge types give sufficiently reliable readings, there are occasions which call for absolute pressure measurements made by gauges which measure directly the average normal force acting over a known area. The pressure range from about $10^{-3}$ to $10^{-5}$ pascal is served adequately at the low end by the McLeod gauge if suitably operated to avoid the errors associated with the mercury pumping effect[142] and at the upper end by the U-tube manometer. Higher pressures require the use of pressure gauges of the dead weight variety[143].

This paper reports on the construction and use of a simple dead weight gauge for absolute pressure measurements and a variation of that gauge which works well but requires calibration. Figure D.1 illustrates the basic features of a conventional dead weight pressure gauge. The pressure to be measured is transmitted to the floating piston through a null detector such as a mercury U-tube with adjustable electric contacts, for example. The null detector is used to isolate the system gases from the lubricating oil which surrounds the piston. This oil is continually lost by viscous flow and must

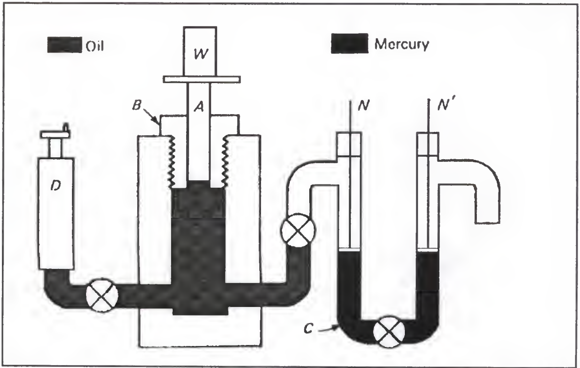

Figure D.1. Conventional dead weight pressure gauge: A = piston; B = cylinder; C = steel U tube; D = oil injector; N, N' = indicator contact needles.

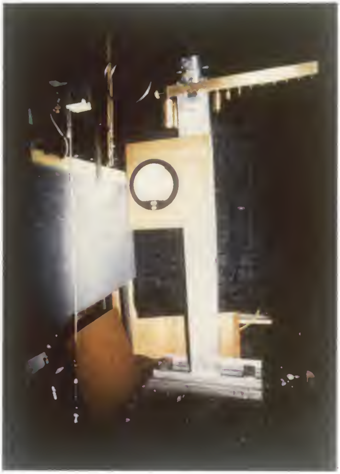

Figure D.2. The present deadweight pressure gauge.

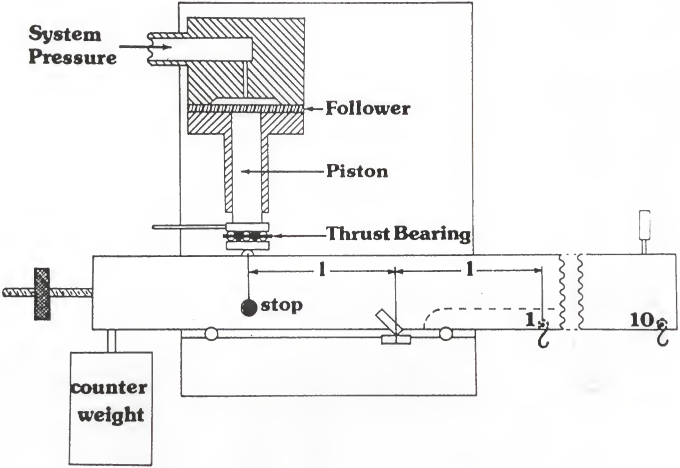

Figure D.3. The arrangement of the deadweight pressure gauge.

be replenished by means of an injection pump. The upward force on the piston is balanced by the sum of the external pressure, gravity acting on the piston and an additional masses added as required to keep the piston afloat. Although this type of pressure gauge is capable of high accuracy, its use is tedious, and commercial units are expensive, being beyond the means of many small laboratories. The present gauges were developed to avoid these problems.

## Dead Weight Pressure Gauge

The present gauge is shown in figure D.2. It differs principally from the conventional designs in the following respects:

1. The piston is inverted being forced vertically downward by the system pressure.

2. The loading weight is generated by standard masses suspended from accurately spaced hooks on a pivoted balance beam.

3. The load is transferred to the piston by point contact with a hardened precision ball accurately located on the beam with respect to the hooks.

4. A thin flexible membrane across the top of the cylinder acts as a piston follower thereby separating the piston from the system gases and eliminating the need for a null detector or oil injection pump.

Figure D.3 shows the arrangement of the gauge elements. System pressure is delivered to the top surface of the follower and transmitted through it to the top of the piston which slides freely in the mating cylinder. The resultant force is countered by the upward force of the loaded balance beam. The travel of the piston is limited by a stop pin extending into an oversize hole in the beam. Total vertical displacement of the piston and angle between the beam and true horizontal influence the net downward force. For this reason the balance point is always taken as the median position, for which the beam is horizontal and the relationship $P=F_{\uparrow}/A$ holds, where $F_{\uparrow}$ is the upward force transmitted by the piston to the follower. This gauge was built for the specific purpose of measuring pressures and standardizing secondary gauges used in an ongoing research effort on sonic speeds in gases at pressures up to about $10^3$ pascal (~ 150 psi.) The stresses generated on the gauge elements at these pressures are relatively small so ordinary materials could be used. The piston, cylinder and gauge body were machined from type 303 stainless steel. For use at high pressures these elements should be made from heat treatable alloys and hardened in the conventional manner. Many materials are available for use as follower. A choice may be made principally on the basis of compatibility with the fluids to be measured and flexibility. Low permeability is desirable, of course, but since the follower is supported by dense solid surfaces, loss of gas through it is generally negligible. Some suitable follower materials are thin elastomeric sheets, plastic films and metal foils if not stressed beyond their elastic limits. The balance beam was machined from brass bar stock. The crucial features on it are the location of the contact ball and the weight suspension hook pins with respect to the knife edge. These features were located on 2.000 inch centers with maximum uncertainty of 0.0005 inch. The contact ball sits in a 60° tapered center drill hole on top of the beam, and the hardened 0.1250 inch hook pins are pressed into mating holes located along the lower edge of the beam. The S hooks fit over the pins and pivot freely in a groove machined into the bottom of the beam. The pins are numbered consecutively one to ten beginning with the one nearest the fulcrum. The beam is pivoted on a knife edge. Conventional balances have quartz or other hard crystalline knife edges and bearing pads. Because such components are expensive and not readily available, especially for supporting heavy loads, it was decided to make use of a common low cost material which seemed well suited for the purpose. Cemented carbide inserts produced by powder metallurgical techniques for use as cutting tools in machining operations are available in many standard compositions and geometries. These are harder than quartz and are manufactured to exacting dimensions with close tolerances. We used a standard insert 0.500 X 0.500 X 0.125 inch which was set into a seat cut at a 45° angle with respect to the bottom of the beam. The insert has eight useable 90° knife edges. A second insert was used as the bearing pad. It fits in a seat machined in a support member and securely fastened to the gauge frame. When not in use the beam may be elevated to lift the knife edge off of the bearing pad to prolong the life of the knife edge by supporting it on the hardened pins.

The cylinder was machined by drilling and reaming and finished by ballizing. The piston was machined on a precision lathe and polished with rouge paper. The diameter was measured with a Pratt and Whitney supermicrometer. Ten readings taken at different positions around the piston gave the average diameter 0.37383 inch with a standard deviation of 0.00001 inch.

Because in operation the contact ball moves on a circular arc and the piston is constrained to move only vertically, there is some relative motion between them resulting in some unwanted sliding friction. To avoid this problem a small thrust bearing was used between the lower surface of the piston and a hardened chip to convert the sliding motion to the less restricted rolling motion.

The gauge is mounted on a rigid beam which is securely bolted to the laboratory floor. The mounting plate is adjustable to allow the bearing pad to be precisely leveled. The vertical component of upward force exerted by the contact ball on the gauge piston is equal to

$$F_{\uparrow} = g \cos \Theta \, \Sigma \, n_i m_i \qquad \text{(D.1)}$$

where $g$ = local acceleration of gravity,

$m_i$ = added load mass

$n_i$ = position of load mass and

$\Theta$ = the angle between the top of the beam and the horizontal.

In order to use the simpler relationship

$$F_t = g \Sigma n_i m_i \tag{D.2}$$

it is necessary to adjust the position of the gauge body relative to the plane of the bearing pad so that the balance point occurs when the beam is precisely horizontal (i.e. $\cos \Theta = 1$.) To accomplish this the gauge body is mounted in a grooved way and adjusted vertically by a fine lead screw. A precision spacer is positioned between the lower end of the cylinder and the flange on the piston during the adjustments. This spacer assures that the piston can extend into the cylinder only to the median position. The beam is loaded sufficiently to hold the piston against the spacer and the gauge body adjusted vertically by means of the lead screw so that a precision level shows the beam to be horizontal. Following the adjustments the gauge body is clamped securely in place.

While the piston is held in the median position by use of the spacer, the balance scale and indicator are set to "zero". Although a conventional scale and pointer combination can be used with this apparatus, greater sensitivity is easily achieved by using an optical indicator consisting of a He-Ne laser beam reflected off a mirror attached to the balance beam onto a suitable scale. We have used a sheet of precision graph paper taped to a wall of the laboratory. The path length between the mirror and the scale is about 3 meters.

The unloaded beam is first balanced by using the adjusting weights added as necessary to restore the balance of forces on the piston. To reduce the effects of friction, which can lead to weighing errors, the piston is coated with oil and provided with a horizontal lever arm which is used to oscillate it back and forth through a small angle while it settles into its vertical equilibrium position. Freedom from sticking is evident when the balance point is constant on repeated tries including those with both positive and negative initial offsets.

### Test Results

The absolute dead weight pressure gauge was tested for accuracy by using it to determine the pressure of gaseous $CF_2Cl_2$ (freon-12) in equilibrium with its liquid phase at constant temperature. This system has been thoroughly studied by Gilkey et. al.(144, 145) using more elaborate methods. The freon container was placed in an adjustable subambient constant temperature bath and connected to the gauge inlet. Air was purged from the gauge and lines by vacuum pumping and repeated flushing with small aliquots of freon. After equilibrium was reached the beam was balanced and the requisite masses and their positions noted. The atmospheric pressure was determined using a mercury barometer noting the usual corrections for thermal expansions of mercury and brass. The measured pressure was calibrated from the relationship

$$P = P_{atm} + (g\ \Sigma\ n_i m_i)/A \qquad (D.3)$$

where $A = \pi r^2$ = cross sectional area of the piston
The local acceleration of gravity must be known or measured. In this laboratory it is 979.284 cm/sec.$^2$ and the resulting gauge constant is 0.0200584 psig/g.

Table D.1 gives the results of these tests at two temperatures, along with the corresponding vapor pressures which may be inferred from the precise measurements of Gilkey et. al.(144, 145) The close agreement shows that the present gauge works well. These results are not intended to serve as a calibration of the gauge but rather as a check of its performance.

The freon used was manufactured for refrigeration service and was of unknown purity. The consistency of the gauge readings indicates that the absolute pressure gauge is accurate to within the limits of the smallest mass difference which may be reproducibility discerned. Using a 30 μm polyimid film follower (DuPont Kapton) the loading mass could be measured easily to within ± 0.5 g, which corresponds to the limits of uncertainty stated in the table. The gauge is a little more responsive if a 15 μm latex follower is used (ca. ± 0.1 g) but the lubricating oils used thus far permeate or react with the latex causing operational difficulties. Thin films of synthetic elastometers such as neoprene, viton, silicone rubbers etc. should work well, but have not thus far been available for testing.

The tests included comparison of the readings of a precision Bourdon gauge connected to the pressure line. Table D.1. shows that this particular gauge is in error or requires calibration.

## Deadweight Gauge with Bellows Sensor

The basic pressure gauge herein described was designed to accommodate interchangeable sensing elements. It can, for example, be fitted with piston/cylinder combinations of different diameters or with entirely other types of sensors. In particular it was intended to investigate the suitability of a thin walled metallic bellows for use as a balance detector. An electroformed nickel bellows with 0.0018 inch

Table D.1. Experimental Test of Dead Weight Pressure Gauge.

| Temperature, K | Vapor Pressure R-12, psia (in parenthesis is % deviation from literature value) | | |
|---|---|---|---|
| | Gilkey (1947) | This work | Bourdon Gauge |
| 271.92 | 43.04 | 42.97±0.01<br>(0.16%) | 42.47<br>(1.3%) |
| 287.45 | 69.87 | 69.66<br>(0.31%) | 68.90<br>(1.4%) |

walls, 0.375 inch o.d., 0.25 inch i.d. and 24 convolutions was brazed to fittings which permitted it to be utilized as a re-entrant pressure sensor (see figure D.4.) System pressure is applied externally around the bellows causing it to contract or shorten. A push rod extending through the bellows is acted upon by the contact ball as before. The beam is loaded to counteract the downward force due to the system pressure. The bellows are very flexible axially but stiff in the radial direction. The downward force is then equal to the magnitude of the system pressure times the active cross sectional area, $A_{eff}$ or

$$P = f_{\downarrow}/A_{eff} = P_{atm} + g\Sigma m_i n_i/A_{eff}. \tag{D.4}$$

$A_{eff}$ is given approximately by the bellows manufacturer as 0.0723 inch$^2$, but lack of accuracy in this value and uncertainty in the effects of the brazing operations on it require that it be determined by calibration. Freon-12 was used for calibrating the bellows. The weight required to balance the system pressure was measured versus temperature of the vapor-liquid equilibrium. If the bellows does behave as a piston of fixed active cross section, a plot of system pressure versus the mass required to balance the beam should be a straight line with slope of $g/A_{eff}$. Figure D.5 shows a plot of the calibration data. The slope was determined by a linear regression and is equal to 0.03000273 psig/g. The correlation coefficient of the linear fit is 0.99995 which shows the gauge to perform in accordance with equation D.4

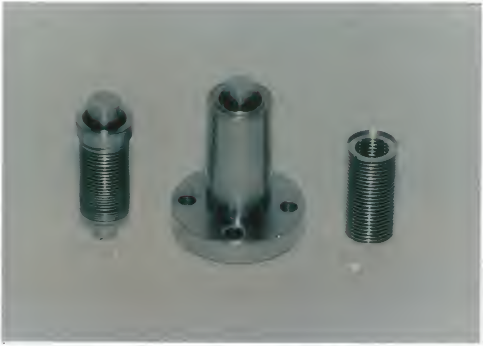

Figure D.4. An electroformed nickel bellow pressure sensor.

over the range of pressures tested. The effective area inferred by the calibration is 0.0734 inch$^2$.

The disadvantage of this gauge relative to the piston type is the need for calibration. The advantage is the intrinsic greater sensitivity available with the bellows. The present sensor responds to mass differences of 0.05 gram which corresponds to pressure differences of 0.0015 psi.

## Conclusion

This work shows that even small laboratories can have reliable pressure standards at relatively low cost. The gauges described here were constructed from readily available materials at a total cost of less than $300 (excluding the laser.) Commercial dead weight pressure gauges cost several thousand dollars and are generally beyond the means of many of the laboratories which could benefit from their use. Perhaps gauges based on the technology presented here will bridge the present gap between conventional secondary gauges and high cost absolute ones. They are at least working well in this laboratory by increasing the confidence in the determination of pressure sensitive acoustic and thermodynamic properties.

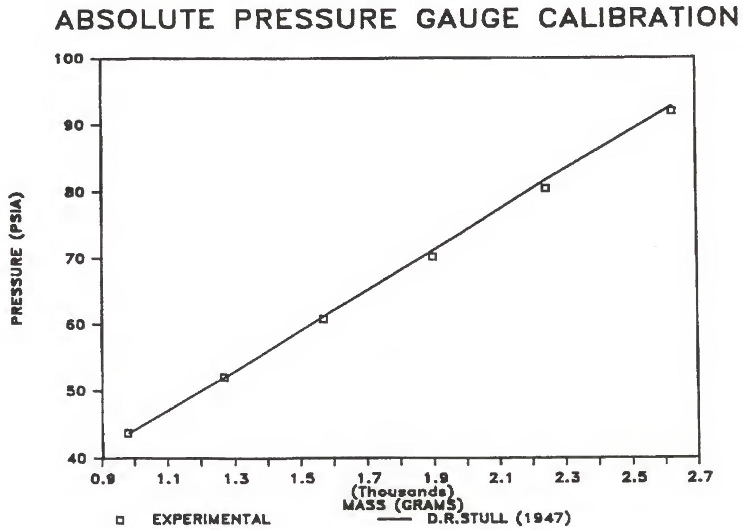

Figure D.5. The calibration curve for dead weight pressure gauge.

# APPENDIX E
## COMPUTER PROGRAMS

Since most of the programs are lengthy only programs VIKING and MAX3 are showed in full. The others are listed only main programs. Most of these programs were written in fortran 77 by Dr. McGill. The remaining by the author.

PROGRAM VIKING

```
$large
    INTERFACE TO SUBROUTINE TIME (N,STR)
    CHARACTER*10 STR [NEAR,REFERENCE]
    INTEGER*2 N [VALUE]
    END
    REAL*4 DX(2000),DY(2000),XMAX,XMIN,YMAX,YMIN
    CHARACTER*1 KOL
    CHARACTER*2 SWEEP
    CHARACTER*10 DNAME
    CHARACTER*7 DTEMP
    CHARACTER*10 TSTR
    INTEGER*2 HR,MIN,SEC
    INTEGER READS,T,TC,T0,T00,POINTS
    SWEEP='30'
    WIDTH = 8.0
    READS = 124
    KOUNT = 0
    STP = 0.0025
    CALL KEITHA(TZERO)
    OPEN(60,File='c:DATA.BUF',STATUS='OLD')
    READ(60,*) VOLT,IG
    CALL GAINSET(IG)
    CLOSE(60)
C***********************************************************
C      VOLTE = (25.0-TZERO)*0.01 + VOLT
C TO BE USED IN NORMAL SCAN
C***********************************************************
      VOLTE = 0.0175
    CLOSE(10)
    DTEMP='c:DATA.'
    OPEN(70,File='c:NAME.NUM',STATUS='OLD')
    READ(70,301) DNAME
 301    FORMAT(1X,A10)
    CLOSE (70)
    READ(DNAME,'(7X,I3)') NUM
    NUM=NUM+1
```

```
        OPEN(70,File='c:NAME.NUM',STATUS='NEW')
        WRITE(70,302) DTEMP,NUM
        WRITE(*,302) DTEMP,NUM
 302    FORMAT(1X,A7,I3)
        CLOSE (70)
        OPEN(20,FILE=DNAME,STATUS='NEW')
        OPEN(30,File='c:Peak.buf',STATUS='OLD')
        READ(30,*) F,TI
        TI=TI+273.15
        CALL KEITHA(TF)
        TF=TF+273.15
        F=SQRT(TF/TI)*F
        CLOSE(30)
        IXT=3
c        IXT=1
        NA = 21/IXT
        IDELY=2*NA
C***********************************************************
C        M=1000/NA/IXT-IDELY/NA
C USED ONLY FOR CENTERING
C***********************************************************
        M=61
C USED AFTER CENTERING
C***********************************************************
        XMIN=1.0
        XMAX=FLOAT(M)
 1001   CALL TIME(10,TSTR)
        READ(TSTR,'(I2)',ERR=1001) HR
        READ(TSTR,'(3X,I2)',ERR=1001) MIN
        READ(TSTR,'(6X,I2)',ERR=1001) SEC
        T00 = HR*3600+MIN*60+SEC
  100   CALL TEMPSET(VOLT)
  101   DO 30 I=1,READS
  500      SF=F-WIDTH/2.0
           SPF=F+WIDTH/2.0
           INDEX=1
           POINTS=M
           ISTART=1
  200      CALL HP(SF,SPF,SWEEP)
           AMAX=0.0
           XMIN=200000.0
           DO 42 ID=1,IDELY
              CALL KEITH(MV)
  42       CONTINUE
           DO 40 J=ISTART,POINTS,INDEX
           AVG=0.0
           DO 41 JA=1,NA
  300         CALL KEITH(MV)
              KOUNT=KOUNT+1
              IF(KOUNT.EQ.2*NA) THEN
                IG=IG+1
                CALL GAINSET(IG)
```

```
               ENDIF
               IF(KOUNT.GT.3*NA) THEN
                  KOUNT=0
                  GOTO 500
               ENDIF
               IF(MV.GT.20000.OR.MV.LT.100) GOTO 300
               KOUNT=0
               AVG=AVG+FLOAT(MV)
  41        CONTINUE
               AMP=AVG/FLOAT(NA)
               DX(J)=FLOAT(J)
               DY(J)=AMP
            IF(AMP.GT.AMAX) THEN
              AMAX=AMP
              JMAX=J
            ENDIF
            IF(AMP.LT.XMIN) XMIN=AMP
  40        CONTINUE
            IF(INDEX.EQ.1) THEN
               NPLOT=1
            ELSE
               NPLOT=0
            ENDIF
            YMAX=AMAX
C*******************************************************
C            CALL PLOT(M,DX,DY,XMAX,XMIN,YMAX,YMIN,NPLOT)
C ONLY USED FOR CENTERING
C*******************************************************
            IF(INDEX.EQ.1) THEN
               INDEX=-INDEX
               TEMP=SF
               SF=SPF
               SPF=TEMP
               ISTART=POINTS
               POINTS=1
               JFMAX=JMAX
               AVGA=AMAX
               CALL KEITHA(TI)
               IF(TI.LT.25.0) GOTO 169
               CALL PRES(VI)
               GOTO 200
            ELSE
               CALL KEITHA(TF)
               CALL PRES(VF)
               JRMAX=JMAX
               FO=FLOAT(JFMAX+JRMAX)/2.0
               CALL MAX(F,WIDTH,FO,M)
               F=FO
               AMP=(AMAX+AVGA)/2.0
               IF(JFMAX.EQ.1.OR.JFMAX.EQ.M.OR.JRMAX.EQ.1.OR.
     CJRMAX.EQ.M) THEN
                 OPEN(30,File='c:Peak.buf',STATUS='OLD')
                 READ(30,*) F,TI
                 CLOSE(30)
                 TI=TI+273.15
                 TF=TF+273.15
                 F=SQRT(TF/TI)*F
                 GOTO 500
               ENDIF
 1003          CALL TIME(10,TSTR)
               READ(TSTR,'(I2)',ERR=1003) HR
               READ(TSTR,'(3X,I2)',ERR=1003) MIN
               READ(TSTR,'(6X,I2)',ERR=1003) SEC
               T = HR*3600+60*MIN+SEC
               T=T-T00
               IF(T.LT.0.0) THEN
                  T00=T00-24*3600
                  T = HR*3600+60*MIN+SEC
                  T=T-T00
               ENDIF
             IF(AMP.LT.7000) THEN
               IG=IG-1
               IF(IG.GE.7) CALL GAINSET(IG)
             ENDIF
             IF(AMP.GT.19000) THEN
               IG=IG+1
               IF(IG.LE.24) CALL GAINSET(IG)
             ENDIF
             RATIO=F/SQRT((TI+TF+273.15*2.0)/2.0)
             WRITE(20,*) TI,TF,VI,VF,AMP,F,T,IG
C***********************************************************
C          DO 18 IF=1,19
C                WRITE(*,*)
C  18         CONTINUE
C             WRITE(*,390) SPF,SF
C  390        FORMAT(1X,'FREQUENCY= ',F10.3,48X,F10.3)
C                WRITE(*,*)
C             IF (JRMAX .GT. JFMAX ) M=M-1
C             IF (JRMAX .LT. JFMAX ) M=M+1
C             DF=0.0
C USED ONLY FOR CENTERING
C***********************************************************
         WRITE(*,400)TI,TF,VI,VF,M,F,T,JRMAX,JFMAX,RATIO
  400      FORMAT(1X,2F8.3,2F8.1,I6,F10.3,I8,2I4,F9.3)
C***********************************************************
           DT=TF-TI
           DF=FLOAT(JRMAX-JFMAX)/FLOAT(M)*WIDTH
C USED ONLY AFTER CENTERING
C***********************************************************
           F=F+DF*1.5
           ENDIF
  30   CONTINUE
C       IF(ABS(DT).GT.0.02) READS=READS+1
C       IF(ABS(DT).GT.0.03) READS=READS+1
```

```
C        IF(ABS(DT).GT.0.04) READS=READS+1
C        IF(ABS(DT).GT.0.05) READS=READS+1
C        IF(ABS(DT).GT.0.06) READS=READS+1
C        IF(ABS(DT).GT.0.07) READS=READS+1
C        IF(ABS(DT).GT.0.08) READS=READS+1
C        IF(ABS(DT).LT.0.05.AND.READS.GT.2) READS=READS-1
C        IF(ABS(DT).LT.0.04.AND.READS.GT.2) READS=READS-1
C        IF(ABS(DT).LT.0.03.AND.READS.GT.2) READS=READS-1
C        IF(ABS(DT).LT.0.02.AND.READS.GT.2) READS=READS-1
C        IF(ABS(DT).LT.0.015.AND.READS.GT.2) READS=READS-1
C        IF(ABS(DT).LT.0.01.AND.READS.GT.2) READS=READS-1
C        IF(ABS(DT).LT.0.005.AND.READS.GT.2) READS=READS-1
       WRITE(*,380) VOLT
 380   FORMAT (1X,'SET POINT VOLTAGE = ',F9.4)
       OPEN(30,File='c:Peak.buf',STATUS='NEW')
       WRITE(30,*) F,TF
       CLOSE(30)
       IF(TF.GT.100.0) GOTO 169
       IF(VOLT.LE.VOLTE) THEN
         VOLT=VOLT+STP
         OPEN(60,File='c:VOLT.BUF',STATUS='NEW')
         WRITE(60,*) VOLT
         CLOSE(60)
         GOTO 100
C***********************************************************
C        ELSE
C          IF(VOLT.GT.VOLTE-0.4) THEN
C            VOLT=VOLTE-0.5
C            OPEN(60,File='c:VOLT.BUF',STATUS='NEW')
C            WRITE(60,*) VOLT
C            CLOSE(60)
C           GOTO 100
C          ENDIF
C          GOTO 101
C USED IN NORMAL SCAN
C***********************************************************
       ENDIF
 169   OPEN(70,File='c:STOP.RUN',STATUS='NEW')
       CLOSE(70)
       CALL TEMPSET(0.0)
       STOP
       END
C
C
C
       SUBROUTINE KEITHA(T)
       common /ibglob/ ibsta,iberr,ibcnt
       'COMMON GROUP 1.'
       integer*4      cmd(10),rd(512),wrt(512)
       character*8  bname,bdname,TEMP
       'COMMON GROUP 2.'
       character*50 flname
```

```
        KLA = IBFIND ('K195A ')
        I24 = 2**24
        I16 = 2**16
        I8 = 2**8
 1004   CALL IBRD (KLA,RD,12)
        I5 = RD(2)/I24
        I6 = (RD(2)-I5*I24)/I16
        I7 = (RD(2)-I5*I24-I6*I16)/I8
        I88 = RD(2)-I5*I24-I6*I16-I7*I8
        I9 = RD(3)/I24
        I10 = (RD(3)-I9*I24)/I16
        I11 = (RD(3)-I9*I24-I10*I16)/I8
        I12 = RD(3)-I9*I24-I10*I16-I11*I8
     WRITE(TEMP,'(8A1)')char(I88),char(I7),char(I6),char(I5),
    CCHAR(I12),CHAR(I11),CHAR(I10),CHAR(I9)
        READ(TEMP,'(F8.3)',ERR=1004) R
        R0=99.99
        ALPHA=0.0039042
        DELTA=1.5205
c        R0=100.06
c        ALPHA=.0039046
c        DELTA=1.5205
        ALDEL=ALPHA*DELTA
        RC=R/R0-1.0
        PART1=ALPHA+ALDEL/100.0
        PART2=(ALDEL/100.0+ALPHA)**2
        PART3=4.0*RC*ALDEL/10000.0
        PART4=2.0*ALDEL/10000.0
        TEMP2=PART1-SQRT(PART2-PART3)
        T=TEMP2/PART4
        RETURN
        end
C
C
C
      SUBROUTINE HP(SF,SPF,SWEEP)
      common /ibglob/ ibsta,iberr,ibcnt
      'COMMON GROUP 1.'
      integer*4      cmd(10),rd(512),wrt(512),IP(4)
      character*1 ch(40)
      CHARACTER*9 STARTF,STOPF
      CHARACTER*2 SWEEP
      character*8  bname,bdname
      'COMMON GROUP 2.'
        call ibinit(ibsta)
        IP(1) = 1
        IP(2) = 2**8
        IP(3) = 2**16
        IP(4) = 2**24
        IHP = IBFIND ('hp3325 ')
        CH(1) = 'F'
        CH(2) = 'U'
CH(3) = '1'
CH(4) = 'A'
CH(5) = 'M'
CH(6) = '0'
CH(7) = '1'
CH(8) = 'V'
CH(9) = 'O'
CH(10) = 'S'
CH(11) = 'T'
WRITE(STARTF,'(F9.3)') SF
READ(STARTF,'(A1)') CH(12)
READ(STARTF,'(1X,A1)') CH(13)
READ(STARTF,'(2X,A1)') CH(14)
READ(STARTF,'(3X,A1)') CH(15)
READ(STARTF,'(4X,A1)') CH(16)
READ(STARTF,'(5X,A1)') CH(17)
READ(STARTF,'(6X,A1)') CH(18)
READ(STARTF,'(7X,A1)') CH(19)
READ(STARTF,'(8X,A1)') CH(20)
READ(STARTF,'(9X,A1)') CH(21)
CH(22) = 'H'
CH(23) = 'Z'
CH(24) = 'S'
CH(25) = 'P'
WRITE(STOPF,'(F9.3)') SPF
READ(STOPF,'(A1)') CH(26)
READ(STOPF,'(1X,A1)') CH(27)
READ(STOPF,'(2X,A1)') CH(28)
READ(STOPF,'(3X,A1)') CH(29)
READ(STOPF,'(4X,A1)') CH(30)
READ(STOPF,'(5X,A1)') CH(31)
READ(STOPF,'(6X,A1)') CH(32)
READ(STOPF,'(7X,A1)') CH(33)
READ(STOPF,'(8X,A1)') CH(34)
READ(STOPF,'(9X,A1)') CH(35)
CH(36) = 'H'
CH(37) = 'Z'
CH(38) = 'T'
CH(39) = 'I'
READ(SWEEP,'(A1)') CH(40)
READ(SWEEP,'(1X,A1)') CH(41)
CH(42) = 'S'
CH(43) = 'E'
CH(44) = 'S'
CH(45) = 'S'
CH(46) = 'S'
CH(47) = 'S'
N=12
M=47
DO 30 I=1,N
   WRT(I) = 0
   DO 40 J=1,4
```

```
              IF((I-1)*4+J.LE.M) THEN
                 WRT(I) = WRT(I) + ICHAR(CH((I-1)*4+J))*IP(J)
              ENDIF
 40         CONTINUE
 30       CONTINUE
          CALL IBWRT(IHP,WRT,M)
          RETURN
          end
c
c
c
         subroutine error
         common /ibglob/ ibsta, iberr, ibcnt
         write (*,100) ibsta,iberr,ibcnt
100      format (' Error',i6,i6,i6)
         return
         end
C
C
C
        SUBROUTINE TEMPSET(VS)
        common /ibglob/ ibsta,iberr,ibcnt
        'COMMON GROUP 1.'
        integer*4      cmd(10),rd(512),wrt(512),IP(4)
        CHARACTER*1 CH(20)
        CHARACTER*6  VOLTS
        character*8  bname,bdname
        'COMMON GROUP 2.'
          LK = IBFIND ('LOCKIN ')
          IP(4) = 2**24
          IP(3) = 2**16
          IP(2) = 2**8
          IP(1) = 1
          WRITE(VOLTS,'(F6.3)') VS
          CH(1) = 'X'
          CH(2) = '6'
          CH(3) = ','
          READ(VOLTS,'(A1)') CH(4)
          READ(VOLTS,'(1X,A1)') CH(5)
          READ(VOLTS,'(2X,A1)') CH(6)
          READ(VOLTS,'(3X,A1)') CH(7)
          READ(VOLTS,'(4X,A1)') CH(8)
          READ(VOLTS,'(5X,A1)') CH(9)
          DO 10 I=1,3
             WRT(I) = 0
             DO 20 J=1,4
                K=(I-1)*4+J
                IF(K.LE.9) THEN
                   WRT(I) = WRT(I) + ICHAR(CH(K))*IP(J)
                ENDIF
 20          CONTINUE
 10       CONTINUE
```

```
        CALL IBWRT(LK,WRT,9)
        RETURN
        end
C
C
C
      SUBROUTINE GAINSET(IG)
      common /ibglob/ ibsta,iberr,ibcnt
      'COMMON GROUP 1.'
      integer*4      cmd(10),rd(512),wrt(512),IP(4)
      CHARACTER*1 CH(20)
      CHARACTER*2  GAIN
      character*8  bname,bdname
      'COMMON GROUP 2.'
        LK = IBFIND ('LOCKIN ')
        IP(4) = 2**24
        IP(3) = 2**16
        IP(2) = 2**8
        IP(1) = 1
        WRITE(GAIN,'(I2)') IG
        CH(1) = 'G'
        READ(GAIN,'(A1)') CH(2)
        READ(GAIN,'(1X,A1)') CH(3)
        WRT(1)=ICHAR(CH(1))+ICHAR(CH(2))*
       CIP(2)+ICHAR(CH(3))*IP(3)
        CALL IBWRT(LK,WRT,3)
        RETURN
        end
C
C
C
      SUBROUTINE PRES(P)
        character*14 a
 300    open(10,file='com1',status='old')
        read(10,100) a
        READ(a,'(3X,F8.3)',ERR=200) P
 100    format(a14)
        RETURN
 200    CLOSE(10)
        GOTO 300
        end
C
C
C
        SUBROUTINE MAX(F,W,FO,M)
        FO=W/FLOAT(M)*FO+F-W/2.0
        RETURN
        END
C
C
C
      SUBROUTINE KEITH(MV)
      common /ibglob/ ibsta,iberr,ibcnt
      'COMMON GROUP 1.'
      integer*4      cmd(10),rd(512),wrt(512)
      character*8  bname,bdname,TEMP
      'COMMON GROUP 2.'
        kl = IBFIND ('k177 ')
        i24 = 2**24
        i16 = 2**16
        i8 = 2**8
 1006   call ibrd (KL,RD,6)
        i1 = rd(1)/i24
        i2 = (rd(1)-i1*i24)/i16
        i3 = (rd(1)-i1*i24-i2*i16)/i8
        i4 = rd(1)-i1*i24-i2*i16-i3*i8
        i5 = rd(2)/i24
        i6 = (rd(2)-i5*24)/i16
        i7 = (rd(2)-i5*i24-i6*i16)/i8
        i88 = rd(2)-i5*i24-i6*i16-i7*i8
        WRITE(TEMP,'(8A1)') CHAR(I4),CHAR(I3),CHAR(I2),
       CCHAR(I1),CHAR(I88),CHAR(I7),CHAR(I6),CHAR(I5)
       READ(TEMP,'(I6)',ERR=1006) MV
       RETURN
       end
c
c
c
      SUBROUTINE PLOT(N,DX,DY,XMAX,XMIN,YMAX,YMIN,NPLOT)
      REAL*4 DX(1),DY(1)
      REAL*4 XMAX,XMIN,YMAX,YMIN
      INTEGER*2 SYMBOL,PEN,M,DEVTYPE,ADDR
      INTEGER*2 XAXIS,YAXIS
      LOGICAL*2 LIN
      CHARACTER*40 XLBL,YLBL,TITLE
C*******************************************************
C GRAPHING PERAMETERS
C eeeeeeeeeeeeeeeeeeeeeeeeeeeeeeeeeeeeeeeeeeeeeeeeeeeee
       M=16
C eeeeeeeeeeeeeeeeeeeeeeeeeeeeeeeeeeeeeeeeeeeeeeeeeeeee
C 1 IS FOR SCREEN 2 IS FOR PLOTTER
      DEVTYPE=1
      INTERFACE=#C400
      ADDR=5
C****************************************************
      XAXIS=1
      YAXIS=0
      YLBL=' AMP¦'
      XLBL=' INDEX VARIABLE¦'
      TITLE=' AMP VS INDEX¦'
      LIN='0'
      SYMBOL=0
      PEN=10
      LEFT=0.0
      BOTTOM=0.0
      RIGHT=1.0
      TOP=0.8
      IF(NPLOT.EQ.1) THEN
        CALL SCREENMODE (M)
        CALL PLOTTER (DEVTYPE,INTERFACE,ADDR)
        CALL SCALE (XMIN,YMIN,XMAX,YMAX)
        CALL WINDOW (LEFT,BOTTOM,RIGHT,TOP)
      CALL GRAPHXY(DX,DY,N,XAXIS,XLBL,YAXIS,
     CYLBL,TITLE,LIN,SYMBOL,PEN)
      ELSE
      CALL GRAPHXY(DX,DY,N,XAXIS,XLBL,YAXIS,
     CYLBL,TITLE,LIN,SYMBOL,PEN)
      ENDIF
      RETURN
      END
```

### PROGRAM MAX3

```
      INTERFACE TO SUBROUTINE TLOOK[C](T)
      INTEGER*4 T [NEAR,REFERENCE]
      END
C
C
C
       COMMON I1,I8,I16,I24
       INTEGER*4 I1,I8,I16,I24
       INTEGER*4 NDELY,T,T0,TB,TL
       INTEGER AMP,COUNT,FREQ,FSHIFT
       REAL*8 ASUM,PHSUM
C      REAL*8 AGSUM
       INTEGER*2 AM(120),PH(120),PR(120)
       INTEGER*2 FM(120),TM(120),LARGE
C      INTEGER*2 AG(120)
       CHARACTER*20 FILERAW,FILEFORM
       N=120
       NDELY=1000
       I1=1
       I8=2**8
       I16=2**16
       I24=2**24
       Write(*,*) ' WHAT IS THE DATA OUTPUT FILE NAME?'
       READ(*,100) FILERAW
       Write(*,*) ' WHAT IS THE FORMAT OUTPUT FILE NAME?'
       READ(*,100) FILEFORM
 100   FORMAT(A)
       open(3,file='block',status='new')
       OPEN(5,FILE=FILEFORM,STATUS='NEW')
       OPEN(10,FILE=FILERAW,FORM='UNFORMATTED',STATUS='NEW')
       write(*,*) ' WHAT IS THE RESONANCE DAC SETTING?'
       READ(*,*) ICENT
```

```
        ISTART=ICENT-N/2
        CALL VOLTS0(IFLIP(ISTART))
        Write(*,*) ' WHAT IS THE INITIAL TEMPERATURE VOLTAGE?'
        READ(*,*) TBB
        ITB=INT(TBB)
        CALL VOLTS1(IFLIP(ITB))
        Write(*,*) ' WHAT IS THE FINAL TEMPERATURE VOLTAGE?'
        READ(*,*) TF
        Write(*,*)  ' HOW MANY HOURS FOR THIS TEMPERATURE
SWEEP?'
        READ(*,*) TIM
        TIM=TIM*3600000.0
        TMM=(TF-TBB)/TIM
        CALL TLOOK(T)
        T0=T
c        WRITE(*,*) ' WHAT IS THE SENSITIVITY ID NUMBER?'
c        READ(*,*) IG
c        OPEN(15,FILE='SENSE',STATUS='NEW')
        CALL TEMPGET(TEMP)
        TSHIFT=TEMP-22.0
        ITSHIFT=TSHIFT
        WRITE(5,200) TSHIFT
 200    FORMAT(1X,'TEMPERATURE SHIFT=',F8.3)
        CALL PRESGET(P)
        PSHIFT=P-3000.0
        WRITE(5,300) PSHIFT
 300    FORMAT(1X,'PRESSURE SHIFT=',F10.3)
        CALL FREQGET(FREQ)
        FSHIFT=FREQ-10000
        WRITE(5,400) FSHIFT
 400    FORMAT(1X,'FREQUENCY SHIFT=',I6)
        CALL PHASEGET(AMPL)
C        CALL LOCKIN(AMPL,ANGL)
C        ASHIFT=ANGL-80.0
C        WRITE(5,700) ASHIFT
C 700    FORMAT(1X,'ANGLE SHIFT=',F8.3)
C        WRITE(*,*) 'AMPL=',AMPL
C        WRITE(*,*) 'ANGL=',ANGL
        WRITE(5,500) N
 500    FORMAT(1X,' LOOP RANGE=',I4)
        CLOSE(5)
        KBLOCK=0
 1000   KBLOCK=KBLOCK+1
        LARGE=-20000
        COUNT=0
        ISTART=ICENT-N/2
        ISTOP=ISTART+N
        CALL VOLTS0(IFLIP(ISTART))
        CALL SECS(T,T0)
        TEMP=FLOAT(T)*TMM+TBB
        ITEMP=INT(TEMP)
        CALL VOLTS1(IFLIP(ITEMP))
```

```
C...FORWARD SWEEP
          DO 20 I=ISTART,ISTOP
             CALL VOLTS0(IFLIP(I))
             CALL SECS(T,T0)
             TB=T
             ASUM=0.0
             PHSUM=0.0
C             AGSUM=0.0
             KOUNT=0
 3000         CALL SECS(T,T0)
                CALL Ke177b(AMP)
C                CALL PHASEGET(AMPL,ANGL)
                CALL PHASEGET(AMPL)
                ASUM=ASUM+FLOAT(AMP)
                PHSUM=PHSUM+AMPL
C                AGSUM=AGSUM+ANGL
C                WRITE(*,*) 'PHSUM=',PHSUM
C                WRITE(*,*) 'ASUM=',ASUM
C                WRITE(*,*) 'AGSUM=',AGSUM
                KOUNT=KOUNT+1
                TL=T-TB
             IF(TL.LT.NDELY) GOTO 3000
             CALL TEMPGET(TEMP)
             CALL FREQGET(FREQ)
             CALL PRESGET(P)
             COUNT=COUNT+1
             AM(COUNT)=INT2(ASUM/FLOAT(KOUNT))
             PH(COUNT)=INT2((PHSUM/FLOAT(KOUNT))*1.0E6)
C             AG(COUNT)=INT2(((AGSUM/FLOAT(KOUNT))
C     C-ASHIFT)*100.0)
C             WRITE (*,*) 'AM=',AM(COUNT)
C             WRITE (*,*) 'PH=',PH(COUNT)
C             WRITE (*,*) 'AG=',AG(COUNT)
             FM(COUNT)=INT2(FREQ-FSHIFT)
             TM(COUNT)=INT2((TEMP-TSHIFT)*1000.0)
             PR(COUNT)=INT2((P-PSHIFT)*10.0)
             LARGE=MAX0(LARGE,AM(COUNT))
             IF (LARGE.EQ.AM(COUNT)) ICENT=I
C             CALL ADJUST(IG)
C             ISEN(COUNT)=INT1(IG)
  20      CONTINUE
C        WRITE(10) AM,PH,PR,FM,TM,AG
        WRITE(10) AM,PH,PR,FM,TM
C        CALL SENSET(IG)
        WRITE(*,30) AM(120),PH(120),PR(120),FM(120),
     CTM(120)+ITSHIFT*1000
C        WRITE(15,*) IG
C     C,AG(120)
 30     FORMAT(1X,5I10)
        CALL SECS(T,T0)
        IF(T.GT.INT(TIM)) GOTO 2000
        Write(*,*) 'BLOCK NUMBER',KBLOCK
        GOTO 1000
 2000   Write(3,600) KBLOCK
 600    FORMAT(1X,' NUMBER OF BLOCKS OF DATA=',I5)
        CLOSE(10)
        CLOSE(3)
c       CLOSE(15)
        END
C
C
C
      FUNCTION IFLIP(INPUT)
      IFLIP=-INPUT+4095
      RETURN
      END
C
C
C
      SUBROUTINE VOLTS0(ITEMP)
      INTEGER*2 ADAPT,DEVICE,CTRL,STAT,VDACH1
      VDACH1 = INT2(ITEMP)
      ADAPT=0
      DEVICE = 9
      CTRL = 0
      STAT = 0
      CALL AOUS (ADAPT,DEVICE,0,CTRL,VDACH1,STAT)
      RETURN
      END
C
C
C
      SUBROUTINE VOLTS1(ITEMP)
      INTEGER*2 ADAPT,DEVICE,CTRL,STAT,VDACH1
      VDACH1 = INT2(ITEMP)
      ADAPT=0
      DEVICE = 9
      CTRL = 0
      STAT = 0
      CALL AOUS (ADAPT,DEVICE,1,CTRL,VDACH1,STAT)
      RETURN
      END
C
C
C
       SUBROUTINE PHASEGET(AMPL)
       common /ibglob/ ibsta,iberr,ibcnt
       INTEGER*4 I1,I88,I166,I24
       DIMENSION I(20)
       'COMMON GROUP 1.'
       integer CR
       integer cmd(10),rd(512),wrt(512),IP(4)
       CHARACTER*1 CH(20)
       character*8  bname,bdname
       CHARACTER*20 TEMPO,TEMP
       'COMMON GROUP 2.'
       data CR/13/
         LK = IBFIND ('LOCKIN ')
         IP(4) = 2**24
         IP(3) = 2**16
         IP(2) = 2**8
         IP(1) = 1
         I24 = 2**24
         I166 = 2**16
         I88  = 2**8
         I1=1
C         CH(1) = 'P'
C         WRT(1)=ICHAR(CH(1))
C         CALL IBWRT(LK,WRT,1)
C 1004    CALL IBRD (LK,RD,12)
C         I(4) = RD(1)/I24
C         I(3) = (RD(1)-I(4)*I24)/I166
C         I(2) = (RD(1)-I(4)*I24-I(3)*I166)/I88
C         I(1) =  RD(1)-I(4)*I24-I(3)*I166-I(2)*I88
C         I(8) = RD(2)/I24
C         I(7) = (RD(2)-I(8)*I24)/I166
C         I(6) = (RD(2)-I(8)*I24-I(7)*I166)/I88
C         I(5) =  RD(2)-I(8)*I24-I(7)*I166-I(6)*I88
C         I(12) = RD(3)/I24
C         I(11) = (RD(3)-I(12)*I24)/I166
C         I(10) = (RD(3)-I(12)*I24-I(11)*I166)/I88
C         I(9) =  RD(3)-I(12)*I24-I(11)*I166-I(10)*I88
C         DO 10 J=1,12
CC          WRITE (*,*) I(J), CHAR(I(J))
C          IF (I(J).EQ.CR) THEN
C           JJ=J-1
C           GOTO 30
C          END IF
C  10     CONTINUE
C  30     IF (JJ.EQ.7) THEN
C          WRITE(TEMP,'(7A1)') CHAR(I(1)),CHAR(I(2)),
C     CCHAR(I(3)), CCHAR(I(4)),CHAR(I(5)),
C     CCHAR(I(6)),CHAR(I(7))
C         READ(TEMP,'(F7.2)',ERR=1004) ANGL
C         ELSE IF (JJ.EQ.6) THEN
C          WRITE(TEMP,'(6A1)') CHAR(I(1)),CHAR(I(2)),
c     CCHAR(I(3)),CHAR(I(4)),CHAR(I(5)),CHAR(I(6))
C         READ(TEMP,'(F6.2)',ERR=1004) ANGL
C         ELSE IF (JJ.EQ.5) THEN
C          WRITE(TEMP,'(5A1)') CHAR(I(1)),CHAR(I(2)),
C     CCHAR(I(3)),CHAR(I(4)),CHAR(I(5))
C         READ(TEMP,'(F5.2)',ERR=1004) ANGL
C         ELSE IF (JJ.EQ.4) THEN
C          WRITE(TEMP,'(4A1)') CHAR(I(1)),CHAR(I(2)),
C     CCHAR(I(3)),CHAR(I(4))
C         READ(TEMP,'(F4.2)',ERR=1004) ANGL
```

```
C         END IF
         CH(1) = 'Q'
         WRT(1)=ICHAR(CH(1))
         CALL IBWRT(LK,WRT,1)
 1005    CALL IBRD (LK,RD,12)
         I(4) = RD(1)/I24
         I(3) = (RD(1)-I(4)*I24)/I166
         I(2) = (RD(1)-I(4)*I24-I(3)*I166)/I88
         I(1) =  RD(1)-I(4)*I24-I(3)*I166-I(2)*I88
         I(8) = RD(2)/I24
         I(7) = (RD(2)-I(8)*I24)/I166
         I(6) = (RD(2)-I(8)*I24-I(7)*I166)/I88
         I(5) =  RD(2)-I(8)*I24-I(7)*I166-I(6)*I88
         I(12) = RD(3)/I24
         I(11) = (RD(3)-I(12)*I24)/I166
         I(10) = (RD(3)-I(12)*I24-I(11)*I166)/I88
         I(9) =  RD(3)-I(12)*I24-I(11)*I166-I(10)*I88
         DO 20 K=1,12
          IF (I(K).EQ.CR) THEN
           KK=K-1
           GOTO 40
          END IF
  20     CONTINUE
  40     IF (KK.EQ.10) THEN
          WRITE(TEMPO,'(10A1)') CHAR(I(1)),CHAR(I(2)),
     CCHAR(I(3)),CCHAR(I(4)),CHAR(I(5)),
     CCHAR(I(6)),CHAR(I(7)),CHAR(I(8)),
     CCHAR(I(9)),CHAR(I(10))
         READ(TEMPO,'(F10.2)',ERR=1005) AMPL
C          IF (I(10).EQ.51) AMPL=AMPL/10.0**3.0
C          IF (I(10).EQ.54) AMPL=AMPL/10.0**6.0
C          IF (I(10).EQ.57) AMPL=AMPL/10.0**9.0
         ELSE IF (KK.EQ.9) THEN
          WRITE(TEMPO,'(9A1)') CHAR(I(1)),CHAR(I(2)),
     CCHAR(I(3)), CCHAR(I(4)),CHAR(I(5)),
     CCHAR(I(6)),CHAR(I(7)),CHAR(I(8)),CHAR(I(9))
         READ(TEMPO,'(F9.2)',ERR=1005) AMPL
C          IF (I(9).EQ.51) AMPL=AMPL/10.0**3.0
C          IF (I(9).EQ.54) AMPL=AMPL/10.0**6.0
C          IF (I(9).EQ.57) AMPL=AMPL/10.0**9.0
         ELSE IF (KK.EQ.8) THEN
          WRITE(TEMPO,'(8A1)') CHAR(I(1)),CHAR(I(2)),
     CCHAR(I(3)), CCHAR(I(4)),CHAR(I(5)),
     CCHAR(I(6)),CHAR(I(7)),CHAR(I(8))
         READ(TEMPO,'(F8.2)',ERR=1005) AMPL
C          IF (I(8).EQ.51) AMPL=AMPL/10.0**3.0
C          IF (I(8).EQ.54) AMPL=AMPL/10.0**6.0
C          IF (I(8).EQ.57) AMPL=AMPL/10.0**9.0
         ELSE IF (KK.EQ.7) THEN
          WRITE(TEMPO,'(7A1)') CHAR(I(1)),CHAR(I(2)),
     CCHAR(I(3)), CCHAR(I(4)),CHAR(I(5)),CHAR(I(6)),CHAR(I(7))
         READ(TEMPO,'(F7.2)',ERR=1005) AMPL
```

```
C          IF (I(7).EQ.51) AMPL=AMPL/10.0**3.0
C          IF (I(7).EQ.54) AMPL=AMPL/10.0**6.0
C          IF (I(7).EQ.57) AMPL=AMPL/10.0**9.0
         END IF
         IF (ABS(AMPL).GT.20000.0) GOTO 1005
         RETURN
         end
C
C
C
       SUBROUTINE Ke177b(MV)
       common /ibglob/ ibsta,iberr,ibcnt
       COMMON I1,I8,I16,I24
       INTEGER*4 I1,I8,I16,I24
       'COMMON GROUP 1.'
       integer*4      cmd(10),rd(512),wrt(512)
       character*8  bname,bdname,TEMP
       'COMMON GROUP 2.'
         K177BAD=IBFIND('K177B ')
 1006    call ibrd (K177BAD,RD,6)
         i1 = rd(1)/i24
         i2 = (rd(1)-i1*i24)/i16
         i3 = (rd(1)-i1*i24-i2*i16)/i8
         i4 = rd(1)-i1*i24-i2*i16-i3*i8
         i5 = rd(2)/i24
         i6 = (rd(2)-i5*i24)/i16
         i7 = (rd(2)-i5*i24-i6*i16)/i8
         i88 = rd(2)-i5*i24-i6*i16-i7*i8
         WRITE(TEMP,'(8A1)') CHAR(I4),CHAR(I3),CHAR(I2),
     CCHAR(I1),CHAR(I88),CHAR(I7),CHAR(I6),CHAR(I5)
         READ(TEMP,'(I6)',ERR=1006) MV
         IF (ABS(MV).GT.20000) GOTO 1006
        RETURN
        end
C
C
C
       SUBROUTINE FREQGET(FREQ)
       common /ibglob/ ibsta,iberr,ibcnt
       COMMON I1,I8,I16,I24
       INTEGER*4 I1,I8,I16,I24
       INTEGER FREQ
       'COMMON GROUP 1.'
       integer SENAD
       integer*4      cmd(10),rd(512),wrt(512)
       character*8  bname,bdname
       CHARACTER*7 TEMP
       'COMMON GROUP 2.'
         i3 = ichar('3')
         i0 = ichar('0')
         SENAD=IBFIND('SENCORE ')
 1006    call ibrd (SENAD,RD,17)
```

```
         IC(1) = rd(1)/i24
         IC(2) = (rd(1)-IC(1)*i24)/i16
         IC(3) = (rd(1)-IC(1)*i24-IC(2)*i16)/i8
         IC(4) = rd(1)-IC(1)*i24-IC(2)*i16-IC(3)*i8
         IC(5) = rd(2)/i24
         IC(6) = (rd(2)-IC(5)*i24)/i16
         IC(7) = (rd(2)-IC(5)*i24-IC(6)*i16)/i8
         IC(8) = rd(2)-IC(5)*i24-IC(6)*i16-IC(7)*i8
         IC(9) = rd(3)/i24
         IC(10) = (rd(3)-IC(9)*i24)/i16
         IC(11) = (rd(3)-IC(9)*i24-IC(10)*i16)/i8
         IC(12) = rd(3)-IC(9)*i24-IC(10)*i16-IC(11)*i8
         IC(13) = rd(4)/i24
         IC(14) = (rd(4)-IC(13)*i24)/i16
         IC(15) = (rd(4)-IC(13)*i24-IC(14)*i16)/i8
         IC(16) = rd(4)-IC(13)*i24-IC(14)*i16-IC(15)*i8
         IF(IC(14).EQ.i3) THEN
         WRITE(TEMP,'(7A1)') CHAR(IC(1)),CHAR(IC(8)),
     CCHAR(IC(7)), CHAR(IC(5)),CHAR(IC(12)),
     CCHAR(IC(11)),CHAR(IC(10))
         READ(TEMP,'(I7)',ERR=1006) FREQ
         ENDIF
         IF(IC(14).EQ.i0) THEN
         WRITE(TEMP,'(7A1)') CHAR(IC(1)),CHAR(IC(8)),
     CCHAR(IC(7)),CHAR(IC(6)),CHAR(IC(5)),
     CCHAR(IC(12)),CHAR(IC(10))
         READ(TEMP,'(I7)',ERR=1006) FREQ
         ENDIF
        RETURN
        end
C
C
C
       SUBROUTINE SECS(T,T0)
       INTEGER*4 T,T0,DAY
       DAY=3600*24*1000
 100   CALL TLOOK(T)
       IF(T.GT.DAY.OR.T.LT.0) GOTO 100
       T=T-T0
       IF(T.LT.0) THEN
         T0=T0-DAY
         T=T+DAY
       ENDIF
       RETURN
       END
C
C
C
       SUBROUTINE TEMPGET(T)
       common /ibglob/ ibsta,iberr,ibcnt
       COMMON I1,I8,I16,I24
       INTEGER*4 I1,I8,I16,I24
```

```
        'COMMON GROUP 1.'
        integer*4      cmd(10),rd(512),wrt(512)
        character*8  bname,bdname,TEMP
        'COMMON GROUP 2.'
          K195AAD=IBFIND('K195A ')
  1004    CALL IBRD (K195AAD,RD,12)
          I5 = RD(2)/I24
          I6 = (RD(2)-I5*I24)/I16
          I7 = (RD(2)-I5*I24-I6*I16)/I8
          I88 = RD(2)-I5*I24-I6*I16-I7*I8
          I9 = RD(3)/I24
          I10 = (RD(3)-I9*I24)/I16
          I11 = (RD(3)-I9*I24-I10*I16)/I8
          I12 = RD(3)-I9*I24-I10*I16-I11*I8
         WRITE(TEMP,'(8A1)')char(I88),char(I7),
      Cchar(I6),char(I5), CCHAR(I12),CHAR(I11),
      CCHAR(I10),CHAR(I9)
          READ(TEMP,'(F8.3)',ERR=1004) R
          R0=99.98
          ALPHA=0.0039076
          DELTA=1.5205
          ALDEL=ALPHA*DELTA
          RC=R/R0-1.0
          PART1=ALPHA+ALDEL/100.0
          PART2=(ALDEL/100.0+ALPHA)**2
          PART3=4.0*RC*ALDEL/10000.0
          PART4=2.0*ALDEL/10000.0
          TEMP2=PART1-SQRT(PART2-PART3)
          T=TEMP2/PART4
          RETURN
          end
c
c
c
        subroutine error
        common /ibglob/ ibsta, iberr, ibcnt
        write (*,100) ibsta,iberr,ibcnt
 100    format (' Error',i6,i6,i6)
        return
        end
C
C
C
       SUBROUTINE PRESGET(P)
       common /ibglob/ ibsta,iberr,ibcnt
       COMMON I1,I8,I16,I24
       INTEGER*4 I1,I8,I16,I24
       'COMMON GROUP 1.'
       integer BMAD
       integer*4      cmd(10),rd(512),wrt(512)
       character*8  bname,bdname
       character*7  Pres
       'COMMON GROUP 2.'
         BMAD=IBFIND('BM600 ')
 1006    call ibrd (BMAD,RD,10)
         i1 = rd(1)/i24
         i2 = (rd(1)-i1*i24)/i16
         i3 = (rd(1)-i1*i24-i2*i16)/i8
         i4 = rd(1)-i1*i24-i2*i16-i3*i8
         i5 = rd(2)/i24
         i6 = (rd(2)-i5*i24)/i16
         i7 = (rd(2)-i5*i24-i6*i16)/i8
         i88 = rd(2)-i5*i24-i6*i16-i7*i8
         WRITE(Pres,'(7A1)') CHAR(I4),CHAR(I3),CHAR(I2),
     CCHAR(I1),CHAR(I88),CHAR(I7),CHAR(I6)
         READ(PRES,'(F7.1)',ERR=1006) P
        RETURN
        end
C
C
       SUBROUTINE SENSET(IG)
       common /ibglob/ ibsta,iberr,ibcnt
       INTEGER*4 I1,I88,I166,I24
       DIMENSION I(20)
       'COMMON GROUP 1.'
       integer CR
       integer cmd(10),rd(512),wrt(512),IP(4)
       CHARACTER*1 CH(20)
       CHARACTER*2 GAIN
       character*8  bname,bdname
       CHARACTER*20 TEMP
       'COMMON GROUP 2.'
       data CR/13/
         IP(4) = 2**24
         IP(3) = 2**16
         IP(2) = 2**8
         IP(1) = 1
         I24 = 2**24
         I166 = 2**16
         I88  = 2**8
         I1=1
         J=0
         K=1
         L=0
  20     LK = IBFIND ('LOCKIN ')
         CH(1) = 'Y'
         CH(2) = '4'
         WRT(1)=ICHAR(CH(1))+ICHAR(CH(2))*IP(2)
         CALL IBWRT(LK,WRT,2)
 1004    CALL IBRD (LK,RD,12)
         I(4) = RD(1)/I24
         I(3) = (RD(1)-I(4)*I24)/I166
         I(2) = (RD(1)-I(4)*I24-I(3)*I166)/I88
         I(1) =  RD(1)-I(4)*I24-I(3)*I166-I(2)*I88
        WRITE(TEMP,'(A1)') CHAR(I(1))
        READ(TEMP,'(I1)',ERR=1004) ISTATUS
        L=L+1
        IF (L.LT.3) GOTO 20
        IF (J.EQ.1.AND.ISTATUS.EQ.0) GOTO 30
        IF (J.EQ.1.AND.K.EQ.0.AND.ISTATUS.EQ.0) GOTO 30
        IF (ISTATUS.EQ.1) THEN
         IG=IG+2
         IF (IG.GT.24) IG=24
         IF (IG.LT.1) IG=1
         J=1
         GOTO 10
        ELSE IF (ISTATUS.EQ.0) THEN
         IG=IG-1
         K=0
         IF (IG.GT.24) IG=24
         IF (IG.LT.1) IG=1
         GOTO 10
        END IF
 10     WRITE(GAIN,'(I2)') IG
        CH(1) = 'G'
        READ(GAIN,'(A1)') CH(2)
        READ(GAIN,'(1X,A1)') CH(3)
         WRT(1)=ICHAR(CH(1))+ICHAR(CH(2))*IP(2)+
    CICHAR(CH(3))*IP(3)
        CALL IBWRT(LK,WRT,3)
        GOTO 20
 30     RETURN
        end
```

PROGRAM VIKAN2

```
$large
        INTERFACE TO SUBROUTINE TIME (N,STR)
        CHARACTER*10 STR [NEAR,REFERENCE]
        INTEGER*2 N [VALUE]
        END
        REAL*4 DX(3000),DY(3000),XMAX,XMIN,YMAX,YMIN
        CHARACTER*1 KOL
        CHARACTER*2 SWEEP
        CHARACTER*10 DNAME
        CHARACTER*7 DTEMP
        CHARACTER*10 TSTR
        INTEGER*2 HR,MIN,SEC
        INTEGER READS,T,TC,T0,T00,POINTS
        SWEEP='15'
        WIDTH = 30.0
        READS = 3
        KOUNT = 0
        STP = -0.00125
        CALL KEITHA(TZERO)
        OPEN(60,File='c:DATA.BUF',STATUS='OLD')
        READ(60,*) VOLT,IG
        CALL GAINSET(IG)
        CLOSE(60)
        VOLTE = (10.0-TZERO)*0.01 + VOLT
        write (*,*) volte
        CLOSE(10)
        DTEMP='c:DATA.'
        OPEN(70,File='c:NAME.NUM',STATUS='OLD')
        READ(70,301) DNAME
 301    FORMAT(1X,A10)
        CLOSE (70)
        READ(DNAME,'(7X,I3)') NUM
        NUM=NUM+1
        OPEN(70,File='c:NAME.NUM',STATUS='NEW')
        WRITE(70,302) DTEMP,NUM
        WRITE(*,302) DTEMP,NUM
302    FORMAT(1X,A7,I3)
       CLOSE (70)
        OPEN(20,FILE=DNAME,STATUS='NEW')
        OPEN(30,File='c:Peak.buf',STATUS='OLD')
        READ(30,*) F,TI
        TI=TI+273.15
        CALL KEITHA(TF)
        TF=TF+273.15
        F=SQRT(TF/TI)*F
        CLOSE(30)
        IXT=3
c        IXT=1
        NA = 21/IXT
        IDELY=2*NA
C*********************************************************
c        M=1000/NA/IXT-IDELY/NA
C USED ONLY FOR CENTERING
C*********************************************************
        M=29
C USED AFTER CENTERING
C*********************************************************
        XMAX=FLOAT(M)
 1001   CALL TIME(10,TSTR)
        READ(TSTR,'(I2)',ERR=1001) HR
        READ(TSTR,'(3X,I2)',ERR=1001) MIN
        READ(TSTR,'(6X,I2)',ERR=1001) SEC
        T00 = HR*3600+MIN*60+SEC
  100   CALL TEMPSET(VOLT)
  101   DO 30 I=1,READS
  500      SF=F-WIDTH/2.0
           SPF=F+WIDTH/2.0
           INDEX=1
           POINTS=M
           ISTART=1
  200      CALL HP(SF,SPF,SWEEP)
```

```
            AMAX=0.0
            XMIN=200000.0
            DO 42 ID=1,IDELY
               CALL KEITH(MV)
  42        CONTINUE
            DO 40 J=ISTART,POINTS,INDEX
            AVG=0.0
            DO 41 JA=1,NA
  300          CALL KEITH(MV)
               KOUNT=KOUNT+1
               IF(KOUNT.EQ.2*NA) THEN
                 IG=IG+1
                 CALL GAINSET(IG)
               ENDIF
               IF(KOUNT.GT.3*NA) THEN
                  KOUNT=0
                  GOTO 500
               ENDIF
               IF(MV.GT.20000.OR.MV.LT.100) GOTO 300
               KOUNT=0
               AVG=AVG+FLOAT(MV)
  41        CONTINUE
               AMP=AVG/FLOAT(NA)
               DX(J)=FLOAT(J)
               DY(J)=AMP
            IF(AMP.GT.AMAX) THEN
              AMAX=AMP
              JMAX=J
            ENDIF
            IF(AMP.LT.XMIN) XMIN=AMP
  40        CONTINUE
            IF(INDEX.EQ.1) THEN
               NPLOT=1
            ELSE
               NPLOT=0
            ENDIF
            YMAX=AMAX
C********************************************************
c            CALL PLOT(M,DX,DY,XMAX,XMIN,YMAX,YMIN,NPLOT)
C ONLY USED FOR CENTERING
C********************************************************
            IF(INDEX.EQ.1) THEN
               INDEX=-INDEX
               TEMP=SF
               SF=SPF
               SPF=TEMP
               ISTART=POINTS
               POINTS=1
               JFMAX=JMAX
               AVGA=AMAX
               CALL KEITHA(TI)
               IF(TI.LT.10.0) GOTO 169
              CALL PRES(VI)
              GOTO 200
           ELSE
              CALL KEITHA(TF)
              CALL PRES(VF)
              JRMAX=JMAX
              FO=FLOAT(JFMAX+JRMAX)/2.0
              CALL MAX(F,WIDTH,FO,M)
              F=FO
              AMP=(AMAX+AVGA)/2.0
              IF(JFMAX.EQ.1.OR.JFMAX.EQ.M.OR.JRMAX.EQ.1.OR.
     CJRMAX.EQ.M) THEN
                OPEN(30,File='c:Peak.buf',STATUS='OLD')
                READ(30,*) F,TI
                CLOSE(30)
                TI=TI+273.15
                TF=TF+273.15
                F=SQRT(TF/TI)*F
                GOTO 500
              ENDIF
 1003         CALL TIME(10,TSTR)
              READ(TSTR,'(I2)',ERR=1003) HR
              READ(TSTR,'(3X,I2)',ERR=1003) MIN
              READ(TSTR,'(6X,I2)',ERR=1003) SEC
              T = HR*3600+60*MIN+SEC
              T=T-T00
              IF(T.LT.0.0) THEN
                 T00=T00-24*3600
                 T = HR*3600+60*MIN+SEC
                 T=T-T00
              ENDIF
            IF(AMP.LT.7000) THEN
              IG=IG-1
              IF(IG.GE.7) CALL GAINSET(IG)
            ENDIF
            IF(AMP.GT.19000) THEN
              IG=IG+1
              IF(IG.LE.24) CALL GAINSET(IG)
            ENDIF
            RATIO=F/SQRT((TI+TF+273.15*2.0)/2.0)
            WRITE(20,*) TI,TF,VI,VF,AMP,F,T,IG
C************************************************************
c           DO 18 IF=1,19
c               WRITE(*,*)
c  18        CONTINUE
c           WRITE(*,390) SPF,SF
c  390       FORMAT(1X,'FREQUENCY= ',F10.3,48X,F10.3)
c               WRITE(*,*)
c            IF (JRMAX .GT. JFMAX ) M=M-1
c            IF (JRMAX .LT. JFMAX ) M=M+1
c            DF=0.0
C USED ONLY FOR CENTERING
```

```
C**************************************************************
           WRITE(*,400)TI,TF,VI,VF,M,F,T,JRMAX,JFMAX,RATIO
  400      FORMAT(1X,2F8.3,2F8.1,I6,F10.3,I8,2I4,F9.3)
C**************************************************************
           DT=TF-TI
          DF=FLOAT(JRMAX-JFMAX)/FLOAT(M)*WIDTH
C  USED ONLY AFTER CENTERING
C**************************************************************
           F=F+DF*1.5
           ENDIF
  30   CONTINUE
       IF(ABS(DT).GT.0.02) READS=READS+1
       IF(ABS(DT).GT.0.03) READS=READS+1
       IF(ABS(DT).GT.0.04) READS=READS+1
       IF(ABS(DT).GT.0.05) READS=READS+1
       IF(ABS(DT).GT.0.06) READS=READS+1
       IF(ABS(DT).GT.0.07) READS=READS+1
       IF(ABS(DT).GT.0.08) READS=READS+1
C       IF(ABS(DT).LT.0.05.AND.READS.GT.2) READS=READS-1
C       IF(ABS(DT).LT.0.04.AND.READS.GT.2) READS=READS-1
C       IF(ABS(DT).LT.0.03.AND.READS.GT.2) READS=READS-1
       IF(ABS(DT).LT.0.02.AND.READS.GT.2) READS=READS-1
       IF(ABS(DT).LT.0.015.AND.READS.GT.2) READS=READS-1
       IF(ABS(DT).LT.0.01.AND.READS.GT.2) READS=READS-1
       IF(ABS(DT).LT.0.005.AND.READS.GT.2) READS=READS-1
       WRITE(*,380) VOLT
 380   FORMAT (1X,'SET POINT VOLTAGE = ',F9.4)
c       Call scan(F,IG)
       OPEN(30,File='c:Peak.buf',STATUS='NEW')
       WRITE(30,*) F,TF
       CLOSE(30)
       if (tf.lt.10.0) goto 169
       IF(TF.GT.100.0) GOTO 169
       IF(VOLT.GE.VOLTE) THEN
         VOLT=VOLT+STP
         OPEN(60,File='c:VOLT.BUF',STATUS='NEW')
         WRITE(60,*) VOLT
         CLOSE(60)
         GOTO 100
       ELSE
         IF(VOLT.GT.VOLTE-0.4) THEN
           VOLT=VOLTE-0.5
           OPEN(60,File='c:VOLT.BUF',STATUS='NEW')
           WRITE(60,*) VOLT
           CLOSE(60)
           GOTO 100
         ENDIF
         GOTO 101
       ENDIF
 169   OPEN(70,File='c:STOP.RUN',STATUS='NEW')
       CLOSE(70)
       CLOSE(20)
```

```
      Call scan(F,IG)
      Call tempset(0.0)
      STOP
      END
c
c
c
      Subroutine scan(F,IG)
      CHARACTER*2 SWEEP
      Character*3 name
      Character*8 fname
      Sweep='60'
c       SWEEP='15'
      OPEN(80,FILE='INDEX.BUF',STATUS='OLD')
      READ(80,*) INDEX
      CLOSE(80)
      INDEX=INDEX+1
      OPEN(80,FILE='INDEX.BUF',STATUS='NEW')
      WRITE(80,*) INDEX
      CLOSE(80)
      WRITE(NAME,'(I3)') INDEX
      Write (fname,'(A1, A3, A4)') 'F',NAME,'.DAT'
      Open (50,file=fname,status='new')
      WIDTH = 100.0
      IF (IG.LT.24) IG=IG+1
      CALL GAINSET(IG)
      WRITE(50,*) IG,F
c    the following line is for avoiding too much signal
c    at the end of the run.
      f=f+200
      SF = F-WIDTH/2.0
      SPF = F+WIDTH/2.0
C       XMAX=SPF
C       XMIN=SF
C       YMAX=-1.0E32
C       YMIN=-YMAX
      IXT=3
C       IXT=1
      NA=15/IXT
      NP=2790/NA/IXT
      SLOPE=WIDTH/FLOAT(NP)
      CALL HP(SF,SPF,SWEEP)
      IDELY = 14
      DO 42 ID = 1,IDELY
       CALL KEITH(MV)
  42  CONTINUE
      DO 40 J=1,NP
           AVG=0.0
           DO 41 JA=1,NA
  300         CALL KEITH(MV)
              IF(MV.GT.20000.OR.MV.LT.100) GOTO 300
              AVG=AVG+FLOAT(MV)
  41         CONTINUE
             AMP=AVG/FLOAT(NA)
             DY=AMP
             DX=SLOPE*FLOAT(J)+SF
             WRITE(50,*) DX,DY
C             IF(AMP.GT.YMAX) THEN
C                YMAX=AMP
C                IMAX=J
C             ENDIF
C             IF (AMP.LT.YMIN) YMIN=AMP
  40    CONTINUE
C       CALL PLOT(NP,DX,DY,XMAX,XMIN,YMAX,YMIN)
       CALL KEITHA(T)
       CALL PRES(P)
       WRITE(50,*) T,P
       IG=IG-1
       CLOSE(50)
       return
       End
```

PROGRAM GETSPG

```
$LARGE
        IMPLICIT REAL*8 (A-H,O-Z)
        REAL*8 PA(10000),TA(10000),FR(10000),CA,DSQRT
        REAL*8 B(100),B1(100),B2(100),T(100)
        REAL*8 C(100),C1(100),C2(100),BD(100),N
        INTEGER TIM
        ZERO=0.0D 00
        ONE=1.0D 00
        TWO=2.0D 00
        EPK=119.8D 00
        B0=49.80D-03
        CON=6.8046D-02
        KEL=273.15
        OPEN (10,FILE='ARGON.DAT',STATUS='OLD')
        I=1
 200    READ(10,*,END=100) T1,T2,P1,P2,AMP,FR(I),TIM,IN
        IF(P1.EQ.0.0D0) GOTO 200
        IF(P2.EQ.0.0D0) GOTO 200
        IF(T1.EQ.0.0D0) GOTO 200
        IF(T2.EQ.0.0D0) GOTO 200
        TA(I)=(T1+T2)/TWO
        PA(I)=(P1+P2)*CON/TWO
        I=I+1
        GOTO 200
 100    CLOSE(10)
        M=I-1
        OPEN (10,FILE='TVC.DAT',STATUS='OLD')
        DO 25 I=1,74
        READ(10,*) T(I),B(I),B1(I),B2(I),
     CBD(I),C(I),C1(I),C2(I)
  25  CONTINUE
      CLOSE (10)
      OPEN (30,FILE='NAT.GAS',STATUS='OLD')
      OPEN (40,FILE='SPEED.GAS',STATUS='NEW')
c      open (50,file='a.gas',status='new')
c      open (60,file='b.gas',status='new')
c      open (70,file='c.gas',status='new')
      N=ZERO
  500 READ(30,*,END=300) T1,T2,P1,P2,AMP,FREQ,TIM,IN
c      write (60,*) amp,in
c      write (50,*) freq
      N=N+ONE
      IF(P1.EQ.0.0.OR.P2.EQ.0.0) GOTO 500
      TEMP=(T1+T2)/TWO
      P=(P1+P2)/TWO
      DT=T2-T1
      DP=P2-P1
      IF(TA(1).LT.TEMP) GOTO 500
      IF(TA(M).GT.TEMP) GOTO 500
      IF(AMP.GT.19000.0D0) IN=IN-1
      IF(AMP.LT.7000.0D0) IN=IN+1
c      write (60,*) freq
      CALL AMPGET(AMP,IN)
c      write (70,*) freq
      DO 20 I=1,M
         ISTOP=0
         IF (TA(I).LT.TEMP) GOTO 400
         ISTOP=1
  20  CONTINUE
 400  IF (ISTOP.EQ.1) GOTO 500
      FAR=(FR(I)-FR(I-1))/(TA(I)-TA(I-1))*
     C(TEMP-TA(I-1))+FR(I-1)
      PAR=(PA(I)-PA(I-1))/(TA(I)-TA(I-1))*
     C(TEMP-TA(I-1))+PA(I-1)
      TEMP=TEMP+KEL
      TS=TEMP/EPK
      CALL QAND(BS,BS1,BS2,BSD,CS,CS1,
     CCS2,TS,T,B,B1,B2,BD,C,C1,C2)
C     WRITE(*,*) ' QAND'
      BV=BS*B0
      CV=CS*B0*B0
      CALL VERVOL(PAR,V,TEMP,BV,CV)
C      WRITE(*,*) ' VERVOL'
      VS=V/B0
      CALL SPEED(CAR,TEMP,BS,BS1,BS2,BSD,CS,CS1,CS2,VS)
C      WRITE(*,*) ' SPEED'
      CG=FREQ*CAR/FAR
      TEMP=TEMP-KEL
      WRITE(40,*) N,DP,DT,P,TEMP,AMP,FREQ,CG,TIM,CAR,FAR
      GOTO 500
      close(70)
```

```
         close(60)
         close(50)
  300    CLOSE(40)
         CLOSE(30)
         END

         SUBROUTINE QAND(BS,BS1,BS2,BSD,
     CCS,CS1,CS2,TS,T,B,B1,B2,BD,C,C1,C2)
        IMPLICIT REAL*8 (A-H,O-Z)
         REAL*8 B(1),B1(1),B2(1),T(1),C(1),C1(1),C2(1),BD(1)
         REAL*8 M
         DO 20 I=2,74
          IF (TS.GT.T(I-1).AND.TS.LT.T(I)) THEN
           M=(TS-T(I-1))/(T(I)-T(I-1))
           BS=B(I-1)+M*(B(I)-B(I-1))
           BS1=B1(I-1)+M*(B1(I)-B1(I-1))
           BS2=B2(I-1)+M*(B2(I)-B2(I-1))
           BSD=BD(I-1)+M*(BD(I)-BD(I-1))
           CS=C(I-1)+M*(C(I)-C(I-1))
           CS1=C1(I-1)+M*(C1(I)-C1(I-1))
           CS2=C2(I-1)+M*(C2(I)-C2(I-1))
           RETURN
          ENDIF
  20     CONTINUE
         WRITE(*,*)'TSTAR OUT OF RANGE'
         RETURN
         END
C
        SUBROUTINE VERVOL(P,V,T,B,CV)
        IMPLICIT REAL*8 (A-H,O-Z)
        R=8.20575D-02
        TOL=1.0D-16
C INPUT P IN ATM
C INPUT T IN KELVIN
        V=R*T/P
  10    VN=R*T/P*(1.0D 00 + B/V + CV/V/V)
        TEST=V/VN
        IF(TEST.GT.1.0) THEN
        TEST=1.0D 00 - 1.0D 00/TEST
        ELSE
        TEST=1.0D 00 -TEST
        ENDIF
        V=VN
        IF(TEST.GT.TOL)  GOTO 10
        RETURN
        END
C
         SUBROUTINE SPEED(C,T,BS,BS1,BS2,BSD,CS,CS1,CS2,VS)
         IMPLICIT REAL*8 (A-H,O-Z)
         REAL*8 M,DSQRT
         M=39.948D-03
         R=8.31441D 00
```

```
       GAMA=5.0D0/2.0D0-BS2/VS+
      C(BSD*BSD-CS+CS1-0.5D0*CS2)/VS/VS
       GAMA=GAMA/(3.0D0/2.0D0-(2.0D0*BS1+BS2)/VS-
      C(2.0D0*CS1+CS2)/2.0D0/VS/VS)
       C=GAMA*R*T/M*(1.0D 00+2.0D0*BS/VS+3.0D0*CS/VS/VS)
       C=DSQRT(C)
       RETURN
       END
```

PROGRAM TOTDAT

```
     IMPLICIT REAL*8 (A-H,O-Z)
     OPEN(10,FILE='SPEED.GAS',STATUS='OLD')
     OPEN(20,FILE='TOTDAT.OUT',STATUS='NEW')
100 READ(10,*,END=200) X,X1,X2,P,T,AMP,F,EXPC,IT,ARGC,ARGF
     CALL SPEEDZ(T,P,RHO,Z,X1,X2,X3,X4,THEOC,X5,X6)
     T=T/1.8D0-273.15
     WRITE(*,*) IT
     THEOC=THEOC/3.2808399D0
     WRITE(20,300) P,T,AMP,F,ARGF,IT,ARGC,EXPC,THEOC
300  FORMAT(1X,F7.1,F8.3,F9.1,2F9.2,I8,3F9.3)
     GOTO 100
200  CLOSE (10)
     CLOSE (20)
     END
```

**COMMON GROUP 1**

```
integer UNL, UNT, GTL, SDC, PPC, GET, TCT
integer LLO, DCL, PPU, SPE, SPD, PPE, PPD
integer  ERR, TIMO, END, SRQI, RQS,  CMPL, LOK
integer  REM, CIC,  ATN, TACS, LACS, DTAS, DCAS
integer  EDVR, ECIC, ENOL, EADR, EARG, ESAC, EABO
integer  ENEB, EOIP, ECAP, EFSO, EBUS, ESTB, ESRQ
integer  BIN, XEOS, REOS
integer TNONE,  T10us, T30us, T100us, T300us
integer T1ms,   T3ms,  T10ms, T30ms,  T100ms
integer T300ms, T1s,   T3s,   T10s,   T30s
integer T100s,  T300s, T1000s
integer  S,LF
```

**COMMON GROUP 2**

```
character*50 flname
integer*4      bd,dvm,v,cnt,mask
integer*4      spr,ppr
data UNL/63/,UNT/95/,GTL/01/,SDC/04/,PPC/05/
data GET/08/,TCT/09/,LLO/17/,DCL/20/,PPU/21/
data SPE/24/,SPD/25/,PPE/96/,PPD/112/
data TIMO/16384/,END/8192/,SRQI/4096/
data RQS/2048/,CMPL/256/,LOK/128/,REM/64/,CIC/32/
data ATN/16/,TACS/8/,LACS/4/,DTAS/2/,DCAS/1/
data EDVR/0/,ECIC/1/,ENOL/2/,EADR/3/,EARG/4/
data ESAC/5/,EABO/6/,ENEB/7/,EOIP/10/,ECAP/11/
data EFSO/12/,EBUS/14/,ESTB/15/,ESRQ/16/
data BIN/4096/,XEOS/2048/,REOS/1024/
data TNONE/0/,T10us/1/,T30us/2/,T100us/3/,T300us/4/
data T1ms/5/,T3ms/6/,T10ms/7/,T30ms/8/,T100ms/9/
data T300ms/10/,T1s/11/,T3s/12/T10s/13/,T30s/14/
data T100s/15/,T300s/16/,T1000s/17/
data S/08/,LF/10/
```

# REFERENCES

1. Atkins P. W., Physical Chemistry, 3rd. ed., W. H. Freeman and Company, New York, 1986.

2. Benedict M., Webb G. B., and L. C. Rubin, J. Chem. Phys., **8**, 334, 1940.

3. Redlich O. and J. N. S. Kwong, Chem. Reviews, **44**, 233, 1949.

4. Peng, D.-Y., and D. B. Robinson, Ind. Eng. Chem. Fund., **15**, 59, 1976.

5. Starling K. E. editor, AGA8 "Compressibility and supercompressibility for natural gas and other hydrocarbon gases", AGA Transmission measurement committee report number 8 (AGA8), American Gas Association, 1986.

6. Vimalchand P. and Marc D. Donohue, Ind. Eng. Chem. Fundam., **24**, 246, 1985.

7. Vidal J., Ber. Bunsenges. Phys. Chem., **88**, 784, 1984.

8. Vera J. H. and J. M. Prausnitz, Chem. Eng. J., **3**, 1, 1972.

9. Prausnitz J. M., Int. Chem. Eng., **19**, 3, 401, 1979.

10. Inomata H., Arai K., and Saito S., J. Chem. Eng. (Japan), **22**, 6, 695, 1989.

11. Kreglewski Aleksander, Equilibrium Properties of Fluids and Fluid Mixtures, Texas A&M University Press, College Station, 1984, chapter 6.

12. Albright P. C., Edwards T. J., Chen Z. Y., and J. V. Sengers, J. Chem. Phys., **87**, 3, 1717, 1987.

13. Olchowy G. A. and J. V. Sengers, Phys. Rev. Lett., **61**, 1, 15, 1988.

14. Chen Z. Y., Albright P. C., and J. V. Sengers, Phys. Rev. A, **41**, 6, 3161, 1990.

15. Chen Z. Y., Abbaci A., Tang S., and J. V. Sengers, Phys. Rev. A, **42**, 8, 1990.

16. Kumar Sanjay, Gas Production Engineering. Gulf Publishing Company, Houston, Texas, 1987, pp. 46, 51-52.

17. Brown G. G., Katz D. L., Oberfell G. B., and R. C. Alden, Natural Gasoline and Volatile Hydrocarbons NGAA, Tulsa, Oklahoma.

18. Thomas L. K., Hankinson, R. W., and K. A. Philips, J. Pet. Tech., **22**, 889, 1970.

19. White D., Freidman A., and H. Johnson, J. Am. Chem. Soc., **72**, 3565, 1950.

20. Sona C. F., An Acoustic Study of Gases and Vapors, Ph.D. Dissertation, The University of Florida, 1986.

21. Reed Kyle, Thermophysical Properties of Hydrocarbons Determined Using a Spherical Resonator., M.S. Thesis, The University of Florida, 1990.

22. Colgate S. O., Sivaraman A., and Reed K., Acoustic Determination of The Thermodynamic Reference State Heat Capacity of n-Heptane Vapor., Research Report RR-109, Project 831-83 thru 86, Gas Processors Association, Tulsa, Oklahoma, 1987.

23. Colgate S. O., Sivaraman A., and Reed K., Reference State Heat Capacities of Three c-8 Compounds, Research Report RR-123, Project 831, Gas Processors Association, Tulsa, Oklahoma, 1989.

24. Colgate S. O., Sona C. F., Reed K. R., and A. Sivaraman, J. Chem. Eng. Data, **35**, 1, 1990.

25. Colgate S. O., Sivaraman A., and K. R. Reed, J. Chem. Thermodynamics., **22**, 245, 1990.

26. Colgate S. O., Sivaraman A., and K. R. Reed, Fluid Phase Equilibria, **60**, 191, 1990.

27. Colclough A. R., Metrologia, **9**, 75, 1973.

28. Temkin Samuel, Elements of Acoustics, John Wiley & Sons company, New York, 1981.

29. Levine Ira N., Quantum Chemistry, 3rd. Ed., Allyn and Bacon Inc., Boston, Massachusette, 1983.

30. Lord Rayleigh, Proc. London Math. Soc., **1**, iv 93, 1872.

31. Ferris Horace G., J. Acoust. Soc. Am., **24**, 1, 57, 1952.

32. Royal Mathematical Society Tables, Volume 7: Bessel Functions, Part III: Zeros and Associated Values, Cambridge University Press, London, 1960.

33. Mehl James B., and Moldover R., J. Chem. Phys., **74**, 7, 4062, 1981.

34. Mehl James B., J. Acoust. Soc. Am., **71**, 5, 1109, 1982.

35. Ewing M. B., McGlashan M. L., and Trusler J. P. M., Molecular Physics, **60**, 3, 681-690, 1987.

36. Campbell I. D., Acoustica, **5**, 145, 1955.

37. de la Tour Cagnaid, Annales de Chimie, **3**, 21, 127, 1822; 22, 410, 1823.

38. Andrews T., Phil. Trans., **159**, 575, 1869.

39. Andrews T., Proc. Roy. Soc. (London), **18**, 42, 1869.

40. Kuenen J. P., Commun. Phys. Lab. Univ. Leiden, No. 4B, 7, 1892.

41. Kuenen J. P., Koninkl. Akad. Wetenschapp. Amsterdam, Versl. Van Vergrad., **1**, 15, 1892.

42. Scott R. L., and P. H. van Konynenburg, Discuss. Faraday Soc., **49**, 87, 1970.

43. Scott R. L., Ber. Bunsenges. Phys. Chem., **76**, 296, 1972.

44. Wichterle Ivan, Fluid Phase Equilibria, **1**, 161, 1977.

45. Hirschfelder Joseph O., Curtiss Charles F., and R. Byron Bird, Molecular Theory of Gases and Liquids, John Wiley & Sons, New York, 1954.

46. Michels A., Blaisse B., and C. Michels, Proc. Roy. Soc. (London), **A160**, 358, 1937.

47. Wentorf R. H. and C. A. Boyd, J. Chem. Phys., **24**, 607, 1956.

48. Cailletet L., and E. Mathias, Comptes Rendus De L'Academie Des Sciences, **104**, 563, 1887.

49. Ipatieff V. N., and G. S. Monroe, Ind. Eng. Chem. (Anal. Ed.), **14**, 171, 1942.

50. Bagatskii M. I., Voronel' A. V., and V. G. Guak, J. Exptl. Theoret. Phys. (U.S.S.R.), **43**, 728, 1962. English translation: Soviet Phys. JETP, **16**, 517, 1963.

51. Voronel' A. V., Chashkin Yu R., Popov V. A., and V. G. Simkin, J. Exptl. Theoret. Phys. (U.S.S.R.), **45**, 828, 1963.

52. Colgate S. O., Sivaraman A., Dejsupa C., and K. C. McGill, Rev. Sci. Instrum., **62**, 1, 198, 1990.

53. Colgate S. O., Sivaraman A., Dejsupa C., and K. C. McGill, J. Chem. Thermodynamics, **23**, 23, 1991.

54. Piezoelectric Technology - Data for Designers; Vernitron: Bedford, Ohio, p. 14.

55. Huang Feng-Hsin, Li Meng-Hui, Lee Lloyd L., and Kenneth E. Starling, J. Chem. Eng. (Japan), **18**, 6, 490, 1985.

56. Ely J., NBS Reference Database number 14, "DDMIX", National Institute for Science and Technology, Supercritical Fluid Properties Consortion, Boulder, Colorado, May 1988..

57. Holste J. C., Hall K. R., Eubank P. T., Esper G., Watson M. Q., Warowny W., Bailey D. M., Young J. G., and M. T. Bellomy, J. Chem. Thermodynamics, **19**, 1233, 1987.

58. Andrews J. W., Trans. Roy. Soc. (London), **159**, II, 575, 1869.

59. Hautefeuille L. and L. P. Cailletet, Compt. Rend., **92**, 840, 1881.

60. Dewar J., Phil. Mag., **18**, 210, 1884.

61. Amagat E. H., Compt. Rend., **114**, 1093, 1332, 1892.

62. Chappuis J., Compt. Rend., **118**, 976, 1894.

63. Villard P., J. Phys., **3**, 441, 1894.

64. Verschaffelt J. E., Verhandel Akad. Wetenschappen Amsterdam, **94**, 1896; Comm. Leiden, No. 28.

65. Kuenen J. P., Phil. Mag., **5**, 44, 179, 1897.

66. De Heen, Bull. Acad. Roy. Bilfique, **31**, 147, 379, 1896.

67. Von Wesendonck, Verhandel Deut. Physik. Ges., **5**, 238, 1903.

68. Keesom W. H., Verhandel Akad. Amst., **321**, 533, 616, 1903; Comm. Leiden, No. 88, 1903.

69. Quinn Elton L. and Jones Charles L., Carbon dioxide, Reinhold Publishing Corporation, New York, 1936, p. 59.

70. Kammerlingh-Onnes H. and G. H. Fabius, Verhandel Akad. Amst., **44**, 1907; Comm. Leiden, No. 98, 1907; Proc. kon. Akad. Amst., Vol. 10, 215, 1907.

71. Bradley W. P., Brown A. W., and C. F. Hale Phys. Rev., **26**, 470, 1908.

72. Meyers C. H. and M. S. Van Dusen, Bur. Standards J. Research, **10**, 381, 1933.

73. Cardoso E. and R. Bell, J. Chim. Phys., **10**, 500, 1912.

74. Hein Paul, Z. Physik. Chem., **86**, 385, 1913-1914.

75. Dieterici C., Ann. Physik., **62**, 75-94, 1920.

76. Pickering S. F., J. Phys. Chem., **28**, 97-124, 1924.

77. Meyers C. H. and M. S. Van Dusen, Refrigerating Eng., **13**, 180, 1926.

78. Kennedy H. T., Cyril H., and Meyer S., Bur. Standards. Refrigerating Eng., **15**, 125-30, 1928.

79. Kennedy H. T., J. Am. Chem. Soc., **51**, 1360, 1929.

80. Michael A., Blaisse S., and Michael C., Proc. Roy. Soc. (London), **160A**, 358, 1937.

81. Lorentzen and Han Ludvig, Acta Chem. Scand., **7**, 1335-1346, 1953.

82. Tielsch H., and Tanneverger H., Z. Physik., **137**, 256-264, 1954.

83. Ernst S., and Thomas W., Forsch. Gebiete Ingenierw., **20B**, 161-170, 1954.

84. Wentorf R. H., J. Chem. Phys., **24**, 607-615, 1956.

85. Ambrose D., Trans. Faraday Soc., **52**, 772-781, 1956.

86. Ernst S., and Traube K., Progr. Intern. Res. Thermodyn. Transport Properties Papers Symp. Thermophys. Properties, 2nd., Priceton, New Jersey, 193-205, 1962.

87. Matthews, J. F., Chem. Rev., **72**, 71-100, 1972.

88. Moldover, M. R., J. Chem. Phys., **61**, 5, 1766-1778, 1974.

89. Altunin, V. V., The Thermophysical Properties of $CO_2$ [in Russian], Moscow, 1975.

90. Krynicki K., Neragi A. L., and J. G. Powles, Ber. Bunsenges. Phys. Chem., **85**, 12, 1153-1154, 1981.

91. Lesnevskaya M. S., Domracheva T. I., and M. B. Nikiforova, Zh. Fiz. Khim., **55**, 2671-2672, 1981.

92. Sengers J. V., Basu K. S., and Sengers J. M. H. Levett, NASA Contractor Report 3424, NASA Scientific and technical Information Branch, p. 59, 1981.

93. Morrison G., J. Phys. Chem., **85**, 759, 1981.

94. Adamov Sh. P., Anisimov, M. A., and V. A. Smirnov, The Thermophysical Parameters of Substances and Materials [in Russian], Moscow, No. 18, pp. 7-73, 1983.

95. Shelomentsev A. M., Teplofiz. Svoistva Uglevo Dorodov Nefteprod., 139-154, 1983.

96. Morrison G., and J. M. Kincaid, AICHE., **30**, 2, 257-262, 1984.

97. Kuenen J. P., Phil. Mag., **44**, 174, 1897.

98. Kuenen J. P. and W. G. Robson, Phil. Mag., **4**, 116, 1902.

99. Khazanova N. E. and L. S. Lesnevskaya, Russ. J. Phys. Chem., **41**, 9, 1279, 1967.

100. Fredenslund A. and J. Mollerup, J. Chem. Soc. Faraday Trans. I, **70**, 1653, 1974.

101. Clark A. M. and F. Din, Disc. Faraday Soc., **15**, 202, 1953.

102. Jensen R. H. and F. Kurata, A. I. Ch. E. Journal., **17**, 357, 1971.

103. Gugnoni R. J., Eldridge J. W., Okay V. C., and T. J. Lee, A. I. Ch. E. Journal., **17**, 357, 1974.

104. Nagahoma Kunio, Konishi Hitoshi, Hoshino Daisuke, and Mitsuho Hirata, J. chem. Eng. (Japan), **7**, 323, 1974.

105. Davalos Juan, Anderson Wayne R., Phelps Robert E., and Arthur J. Kidnay, J. Chem. Eng. Data, **21**, 81, 1976.

106. Stead K. and J. M. Williams, J. Chem. Thermodynamics, **12**, 265, 1980.

107. Moldover M. R. and J. S. Gallagher, A. I. Ch. E. Journal, **24**, 2, 267, 1978.

108. Khazanova N. E. and E. E. Sominskaya, Russ. J. Phys. Chem., **51**, 4, 548, 1977.

109. Douslin D. R. and R. H. Harrison, J. Chem. Thermodynamics, **5**, 491, 1973.

110. Sychev V. V., Vasserman A. A., Kozlov A. D., Zagoruchenko V. A., Spiridonov G. A., and V. A. Tsymarny, Theodore B. Seloves Jr. English-Language edition editor, Thermodynamics Properties of Ethane, Hemisphere publishing corporation, Washington, 1987, p. 34.

111. Goodwin R. O., Roder H. M., and G. C. Stragy, Thermophysical Properties of Ethane from 90 to 600 K at pressure to 700 bar. NBS Technical Note Number 684, U. S., Department of Commerce, NBS 1976.

112. Wiebe R., Hubbard K. H., and M. J. Brevoort, J. Am. Chem. Soc., **52**, 611, 1930.

113. Sage B. H., Webster D. C., and W. N. Lacey, Ind. Eng. Chem., **29**, 658, 1937.

114. Kay W. B., Ind. Eng. Chem., **30**, 459, 1938.

115. Beattie J. A., Su G.-J., and G. L. Simard, J. Am. Chem. Soc., **61**, 924, 1939.

116. Lu H., Newitt D. M., and M. Rubemann, Proc. Roy. Soc. (London), **178A**, 506, 1941.

117. Kay W. B. and D. B. Brice, Ind. Eng. Chem., **45**, 615, 1953.

118. Whiteway S. G. and S. G. Mason, Can. J. Chem., **31**, 569, 1953.

119. Palmer H. B., J. Chem. Phys., **22**, 625, 1954.

120. Schmidt E. and W. Thomas, Forsch. Gebiete Inq., **20B**, 161, 1954.

121. Kudchadker A. P., Alani G. H., and B. J. Zwolinski, Chem. Rev., **68**, 659, 1968.

122. Sliwinski P., Z. Phys. Chem. (Frankfurt), **68**, 91, 1969.

123. Bulavin P. A., Ostanevich Yu. M., Simkina A. P., and A. V. Strelkov, Ukr. Fiz. Zh., **16**, 90, 1971.

124. Minivich V. M. and G. Sorina, Russ. J. Phys. Chem., **45**, 306, 1971.

125. Khazanova N. E. and E. E. Sominskaya, Russ. J. Phys. Chem., **45**, 88, 1971.

126. Veronel' A. I., Gorbunova B. G., and V. A. Smirnov et. al., Zh. Eksp. Teor. Fiz., **63**, 964, 1972.

127. Berestov A. G., Giterman M. Sh., and N. G. Shmakov, Zh. Eksp. Tekhn. Fiz., **64**, 2232, 1973.

128. Miniovich V. M. and G. A. Sorina, Teplofiz. Svoista Veshchestv. Mater., **6**, 134, 1973.

129. Shmakov N. G., Teplofiz. Svoistva Veshchestv Mater., **7**, 155, 1973.

130. Strumpf H. J., Collings, A. F., and C. J. Pings, J. Chem. Phys., **60**, 309, 1974.

131. Goodwin R. D., J. Res. NBS, **79A**, 71, 1975.

132. Berestov T. A. and S. B. Kiselev, Teplofiz. Vys. Temp., **17**, 1202, 1979.

133. Stell G. R. and S. Torquoto, Ind. Eng. Chem. Fundam., **21**, 202, 1982.

134. Sivaraman A., Magee J. W., and R. Kobayashi, Fluid Phase Equilibria, **16**, 1, 1984.

135. Sivaraman A., Kragas T., and R. Kobayashi, Fluid Phase Equilibria, **16**, 275, 1984.

136. Wegner F. J., Phys. Rev. B, **5**, 4529, 1972.

137. Ley-Koo M., and M. S. Green, Phys. Rev. A, **16**, 2483, 1977.

138. Ley-Koo M., and M. S. Green, Phys. Rev. A, **23**, 5, 2650, 1981.

139. McGill K. C., Fast Fourier Transformed Acoustic Resonance With Sonic Transform., Ph.D. Dissertation, The University of Florida, 1990.

140. Skoog Douglas A. and West Donald M., Fundamentals of Analytical Chemistry, 4th edition, Saunders College Publishing, New York, 1982.

141. Harris Daniel C., Quantitative Chemical Analysis, 2nd. ed., W. H. Freeman Company, New York, 1986.

142. Shoemaker David P., Garland Carl W., and Joseph W. Nibler, Experiments in Physical Chemistry, 5th ed., McGraw-Hill Publishing Company, New York, 1989.

143. Harland Philip W., Pressure Gauge Handbook, U. S. Gauge Division, Ametek Inc., Sellersville, Pennsylvania, 1985.

144. Stull Daniel R., Ind. Eng. Chem., **39**, 540, 1947.

145. Gilkey W. K., Gerald Frank W., and Milo E. Bixler, Ind. Eng. Chem., **23**, 4, 364, 1931.

## BIOGRAPHICAL SKETCH

Chadin Dejsupa was born in Bangkok, Thailand where he attended primary and secondary school. He received a B.Sc. degree in chemistry from Kasetsart University in 1981. He worked as a laboratory instructor in general and physical chemistry at kasetsart University for two years. In 1986 he completed a M.S. degree in physical chemistry specializing in X-ray crystallography from the University of Hawaii. He joined the department of chemistry at the University of Florida in 1986 in order to pursue a Ph.D. There he studied under the supervision of professor Samuel O. Colgate in the physical chemistry division. In 1989 he received the chemistry department's outstanding teaching assistant award.

I certify that I have read this study and that in my opinion it conforms to acceptable standards of scholarly presentation and is fully adequate, in scope and quality, as a dissertation for the degree of Doctor of Philosophy.

Samuel O. Colgate

Samuel O. Colgate, Chairman
Associate Professor of Chemistry

I certify that I have read this study and that in my opinion it conforms to acceptable standards of scholarly presentation and is fully adequate, in scope and quality, as a dissertation for the degree of Doctor of Philosophy.

Martin Vala

Martin Vala
Professor of Chemistry

I certify that I have read this study and that in my opinion it conforms to acceptable standards of scholarly presentation and is fully adequate, in scope and quality, as a dissertation for the degree of Doctor of Philosophy.

D A Micha

David A. Micha
Professor of Chemistry and Physics.

I certify that I have read this study and that in my opinion it conforms to acceptable standards of scholarly presentation and is fully adequate, in scope and quality, as a dissertation for the degree of Doctor of Philosophy.

Willis B. Person

Willis B. Person
Professor of Chemistry

I certify that I have read this study and that in my opinion it conforms to acceptable standards of scholarly presentation and is fully adequate, in scope and quality, as a dissertation for the degree of Doctor of Philosophy.

Timothy J Anderson
Timothy J. Anderson
Professor of Chemical
Engineering

This dissertation was submitted to the Graduate Faculty of the Department of Chemistry in the College of Liberal Arts and Sciences and to the Graduate School and was accepted as partial fulfillment of the requirements for the degree of Doctor of Philosophy.

December 1991

Dean, Graduate School

UNIVERSITY OF FLORIDA
3 1262 08556 6999